Groundwater Dynamics in the Left Bank Catchments of the Middle Blue Nile and the Upper Awash River Basins, Central Ethiopia

Tilahun Azagegn

A Thesis Submitted to

The School of Earth Sciences

Presented in Partial Fulfillment of the Requirement for the Degree of Doctor of Philosophy in Earth Sciences (Hydrogeology)

Addis Ababa University

Addis Ababa, Ethiopia

December, 2014

Addis Ababa University,

School of Graduate Studies

This is to certify that the thesis prepared by Tilahun Azagegn entitled: Groundwater Dynamics in the Left Bank Catchments of the Middle Blue Nile and the Upper Awash River Basins, Central Ethiopia and submitted in partial fulfillment of the degree of Doctor of Philosophy in Earth Sciences (Hydrogeology)complies with the regulations of the university and meet the accepted standard with respect to originality and quality.

Signed by the Examining Committee

Prof. Tenalem Ayenew ________________ ____________________
Principal advisor Signature Date

____________________________ _______________ ____________________
Examiner (Internal) Signature Date

____________________________ _______________ ____________________
Examiner (External) Signature Date

____________________________ _______________ ____________________
Chair of School or graduate Signature Date

program coordinator

Abstract

Groundwater Dynamics in the Left Bank Catchments of the Middle Blue Nile and the Upper Awash River Basins, Central Ethiopia

Tilahun Azagegn

Addis Ababa University, 2014

Integrated geological, geophysical, hydrodynamic, hydrogeochemical and environmental isotopic studies together with simple regional groundwater flow model help conceptualize aquifer distribution, groundwater dynamics and relationship between aquifer systems of the Middle Blue Nile and the Upper Awash basins. A distinctive aquifer geometry reconstructed from regional stratigraphy, regional fault systems and geophysical evidences controls the size of recharge area for aquifer systems and aquifer distributions in the groundwater sub-basins. The NW-SE trending horsts beneath thick volcanic layers and ridges control aquifer distribution in the Middle Blue Nile basin into Guder, Muger and Jema groundwater sub-basins.The E-Wtrending impermeable mudstone capped horst underlying the volcanic aquifers controls aquifer distribution and constitutes a groundwater divide between the Blue Nile and the Upper Awash basins, channeling recharged water in the former to the latter. Among various recharge estimation methods employed, results from base flow separation that utilizes records from adequate river gauges better represent recharge distribution in the area. The overlay analysis made between base flow amount, lineament density and geological materials indicated that rock units exposed along the Yerer Tulu Wolel Volcanic Lineament zone and the Main Ethiopian Rift marginpromote more recharge than the rock units exposed away from these zones.Groundwater contours generally follow surface topography for flows considered at a catchment or sub-basin level. However, unique groundwater flow pattern that indicates interbasin groundwater flow from the Blue Nile to the Upper Awash basin has been obtained at a regional scale, which is attributed to the interplay between regional faults. $\delta^{18}O$ and δD-depleted waters with high TDS, $NaHCO_3$water types, positive residual alkalinity and low ^{14}C activityobserved along the water divide between the Blue Nile and the Upper Awash together with horizontal annual groundwater inflow of 152$Mm^3$to the Upper Awash groundwater basin obtained from the regional groundwater flow model, substantiate the interbasin groundwater flow conceptualized from litho-structural and hydrodynamic characterization.

Keywords: Blue Nile, Upper Awash, Interbasin, sub-basins, groundwater dynamics

Acknowledgements

The author is thankful to the school of Earth Sciences, Addis Ababa University for the opportunity to pursue the study and for facilities. The greatest appreciation goes to Prof. Tenalem Ayenew (principal advisor), Dr. Asfawossen Asrat and Dr. Seifu Kebede(co-advisors) and Dr. Mulugeta Alene(graduate program coordinator)for their support throughout the study.Thanks also go to AtoDagmawi Shiferaw,a chemist in the Isotope Hydrology Laboratory and all school members.

The German Academic Exchange Service (DAAD) is acknowledged for funding part of this work.Field work and laboratory analyses have been done in collaboration with the Addis Ababa Water and Sewerage Authority. Thanks go to the drilling companies,government water works design and supervision enterprises,Ministry of Water, Irrigation and Energy andMeteorological Agencyfor providing relevant data.Many institutions, which supplied relevant data, deserve special appreciation.

The author is grateful to the useful comments of Dr. Dessei Nidaw, Dr. Wakgari Furi, Ato Engida Zemedagegnehu, Ato Kasahun Aberaand Ato Behailu Birhanu.All friends, who directly or indirectly supported the study, deserve special appreciation.

Gratitude and love goes to my wife Roman Abate, for her all-rounded support. I honor my LORD, Jesus Christ for everything.

Table of Contents

List of Figures

List of Tables

List of Acronyms

AAWSA	Addis Ababa Water and Sewerage Authority
AET	Actual Evapotranspiration
BFS	Base Flow Separation
Bq/m3	Becquerels per cubic meter
CMB	Chloride Mass Balance
DEM	Digital Elevation Model
DIC	Dissolved Inorganic carbon
EC	Electrical Conductivity
FAO	Food and Agriculture Organization
GHB	General head boundary
GMWL	Global Meteoric Water Line
GPS	Global Positioning System
GSE	Geological Surveys of Ethiopia
Hrs/d	Hours per day
l/s	liters per second
LMWL	Local Meteoric Water Line
m.a.s.l.	meters above sea level
m/s	meters per second
m^2/d	meter square per day
m^3/s	meter cubic per second
MA	Meteorological Agency
meq/l	Mili-equivalent per litre
MER	Main Ethiopian Rift
mg/l	Milligram per litre
Mm^3	Million meter cube
MoWIE	Ministry of Water, Irrigation and Energy
NWP	North Western Plateau
PET	Potential Evapotranspiration
R	Runoff
RAP	River Analysis Package
RH	Relative Humidity
SEP	South Eastern Plateau
SMD	Soil Moisture Deficit
SRTM	Shuttle Radar Topography Mission
SSH	Sun shine Hour
SWL	Static Water Level
TDS	Total Dissolved Substances
VES	Vertical Electrical Sounding
WS	Wind Speed
YTVL	Yerer Tulu Wolel Volcanic Lineament

Chapter One: Introduction

1.1. Background

The Ethiopian landmass is divided into three major physiographic regions widely known as the NWPand associated lowlands, the SEPand associated lowlands and the MER. The southern flank of the Middle Blue Nile basin and the Upper Awash basin fall partly in the NWP and partly in the MER.

The area is underlain by geologic units that are strongly affected by tectonic activities (Tsegaye Abebe, 1995, Tsegaye Abebe et al., 1998). Rocks ranging in age from the Precambrian basement to Tertiary and Quaternary volcanics with cover of alluvial sediments outcrop in the area. Precambrian basement rocks are covered in most parts by rare Paleozoic and dominantly Mesozoic sedimentary successions which in turn are overlain by thick Tertiary volcanic rocks.

Sedimentary rocks of the area are found in a rugged eroded terrain; beds are dislocated and highly affected by normal faults of big magnitude of displacement. Moreover, fine grained clastic terrigeneous beds are intercalated in sandstone and limestone rock units. Hence, sedimentary rocks in the area form less productiveaquifer compared to aquifers in similar geological terrains, notably the extensive karst and clastic sedimentary rock aquifers in China, Mexico, USA, Israel and Nubian sandstone aquifers of northern Africa (Dafny et al., 2010; Franscesco et al., 2013, Ma et al., 2013, Nasir et al, 2011).

Extensive and multiphase volcanic and tectonic activities led to the complexity of volcanic rocks in the NWP including the study area.Hence, volcanic rocks of the area form complex aquifers, compared to the relatively simpler volcanic and tectonic architecture of the vast trap series volcanic lava flows elsewhere in the world (e.g., horizontal to sub horizontal Deccan basalts of Western India (Kulkarni et al., 2000), Karoo basalts of South Africa (Bristow et al., 1983), slightly dipping Colombia River flood basalts of the USA (Kahle et al., 2009) and Parana basalts of Brazil (Foder, 1989).

1.2. Previous Works

Studies on geology, geomorphology and hydrogeology have been conducted in the NWP, MER and the surroundings. Related articles, maps and reports in the area and the surrounding region have been reviewed.

A number of studies have been conducted in relation to geological, structural and geomorpholical set up of the NWP and the MER including the study area (e.g., Zanettin et al., 1974, 1978; Kazmin, 1980; Getaneh Assefa, 1981, 1991; TsegayeAbebe, 1995; TsegayeAbebe et al., 1998; Boccaletti et al., 1998; Pik et al., 1998, 2003, 2008; Dereje Ayalew et al., 2002, 2009; Kieffer, 2004; Tesfaye Korme et al., 2004; Gani et al., 2006, 2007, 2009; Genene Mulugeta et al., 2007; Ahmed Wolela, 2008, 2009). Some of the studies showed that the basins have outcrops ranging from Precambrian metamorphic basement rocks, Mesozoic sedimentary successions, and multipleCenozoic volcanic successions to Quaternary volcanics and alluvial deposits.

The Blue Nile gorge exposes a total of 2 – 3km thick sedimentary rock succession (e.g., Kazmin, 1980; Getaneh Assefa, 1981, 1991; Ahimed Wolela, 2008, 2009).The litho-stratigraphic units from oldest to youngest are the Adigrat (or Lower) Sandstone, Gohatsion Formation, Antalo Limestone, Mugher Mudstone and Debrelibanos (or Upper) Sandstone.The sedimentary rock units thin and pinch out to the northwest direction and show slight dipping towards the south and southeast directions (Getaneh Assefa, 1981, 1991).

The studies conducted in the volcanic terrain showed that the Ethiopian flood basalts form up to 2km thick sequences of diverse volcanic products (Keiffer et al., 2004; Dereje Ayalew et al., 2002, 2009). Though various studies (e.g., Visentin et al., 1974; Zanettin et al., 1974, 1978; Kazmin, 1980; Pik et al., 2003; Gani et al., 2007) classified the volcanic sequences of the NWP differently, recent studies (e.g., Keiffer et al., 2004) reclassified the same volcanic sequence into two major units: the flood basalt volcanics and shield volcanics, with spatial variations in age and composition between the two units.

The geometry of the Mesozoic sedimentary succession, Tertiary trap series flood volcanics and the shield volcanics has been strongly modified by tectonic activities notably related to the regional uplift. Tectonic activities and regional uplift eventually led to the formation of the MER, and subsequent reactivation of the rift bounding faults. The structural and morphological frameworks of the area have been shaped by mantle upwelling and subsequent continental break up, magmatic eruption, faulting and rifting (e.g., Chorowicz et al., 1998; Pik, et al., 2008; Beccaluva et al., 2009).

Some of the studies conducted on tectonic and geomorphic set up of the NWP and MER including the study area verified two prominent structural zones: the YTVL system crossing the study area in the southern part, and MER bounding the study area from the east (Fig.1).Erosion and incision also play significant role in modifying the land escape of the region (Gani et al., 2007).

Some hydrogeological studies have been conducted in the NWP and MER including parts of the Middle Blue Nile and the Awash basins (e.g., Birhanu Melaku, 1982; Tesfaye Cherinet, 1993; BCEOM, 1997, 1998; Birhanu Gizaw, 2002; Seifu Kebede et al., 2005, 2007, 2012; WWDSE, 2008; Tenalem Ayenew et al., 2008; Molla Demlie, et al., 2008, Andarge Yitbarek, 2009;Andarge Yitbarek, et al., 2012;Sima, 2009; Tewodros Rango et al., 2010; Wakgari Furi, 2011, Bretzler et al., 2011and references therein).

Most of the previous hydrogeological studies characterize the aquifer systems at a catchment, sub-basin or river basinlevels. However, some studies have been dealing with interbasin groundwater transfer between the aquifer systems of the NWP and the MER (Seifu Kebede et al., 2007, WWDSE, 2008, Andarge Yitbarek, et al, 2009, Wakgari Furi, 2011). Among the works,Seifu Kebede et al. (2007), based on hydrochemical and environmental isotope evidence pointed out that tectonic structures formhydrologic window between NWP and the MER that control rift ward transfer of groundwater from NWP. On the other hand, regional dip of sedimentary strata controls rift-ward transfer of groundwater from the NWPvolcanic and sedimentary rock aquifers (WWDSE, 2008).

Though the hydraulic connection between aquifer systems of the Middle Blue Nile and the Upper Awash basin has been addressed, recharge boundary, aquifer distribution, and groundwater flux between adjacent river basinsare poorly understood. Factors that control themalso remain generally unexplained. Hence, detailed investigation of the lithostratigraphy, tectonicregime andgroundwater flow patternsbelieved to help systematically conceptualize hydrogeological system. Converging evidencesfrom hydraulic properties of rocks together with hydrochemicaldata and environmental isotopes supported with simpleregional numerical groundwater flow model also help conceptualize thesystem(Freeze and Cherry, 1979; Anderson and Woessner, 1992; Clark and Fritz, 1997; Singhal and Gupta, 1999; Fetter, 2001).

1.3. Site Description

The study area is located in central Ethiopia, surrounding the city of Addis Ababa. It includes the three central left-bank sub-basins of the Middle Blue Nile basin (Guder, Muger, Jema) and the Upper Awash basin. The area is approximately bounded within 8°45’14” to 10°54’50”N latitude and 37°11’11” to 39°44’40”E longitude. The total area is 38,000 square kilometers out of which Guder, Muger, Jema and Upper Awash sub-basins cover 7088, 8263, 6760 and 16111 square kilometers, respectively.

The nearly parallel Guder, Muger and Jema Rivers flownortheast and join the Blue Nile River that flows nearly in the southwest direction. The Upper Awash River flows towards the MER in a southeast direction draining the YTVL zone (Fig. 1).

Surface elevations in the study area range between1000 m.a.s.l. in the Blue Nile gorge to over 4000 m.a.s.l.at rift margins. The study area, controlled by the extreme physiographic variations, is characterized by contrasting climatic zones ranging from hot and humid lowlands to cold and dry highlands. Average annual precipitation varies between 800 and 1200mm. The extreme mean monthlyminimum is 2.1^{o}C and extreme mean monthly maximum temperature is 31.1°C(FAO, 2013; IWMI, 2009).

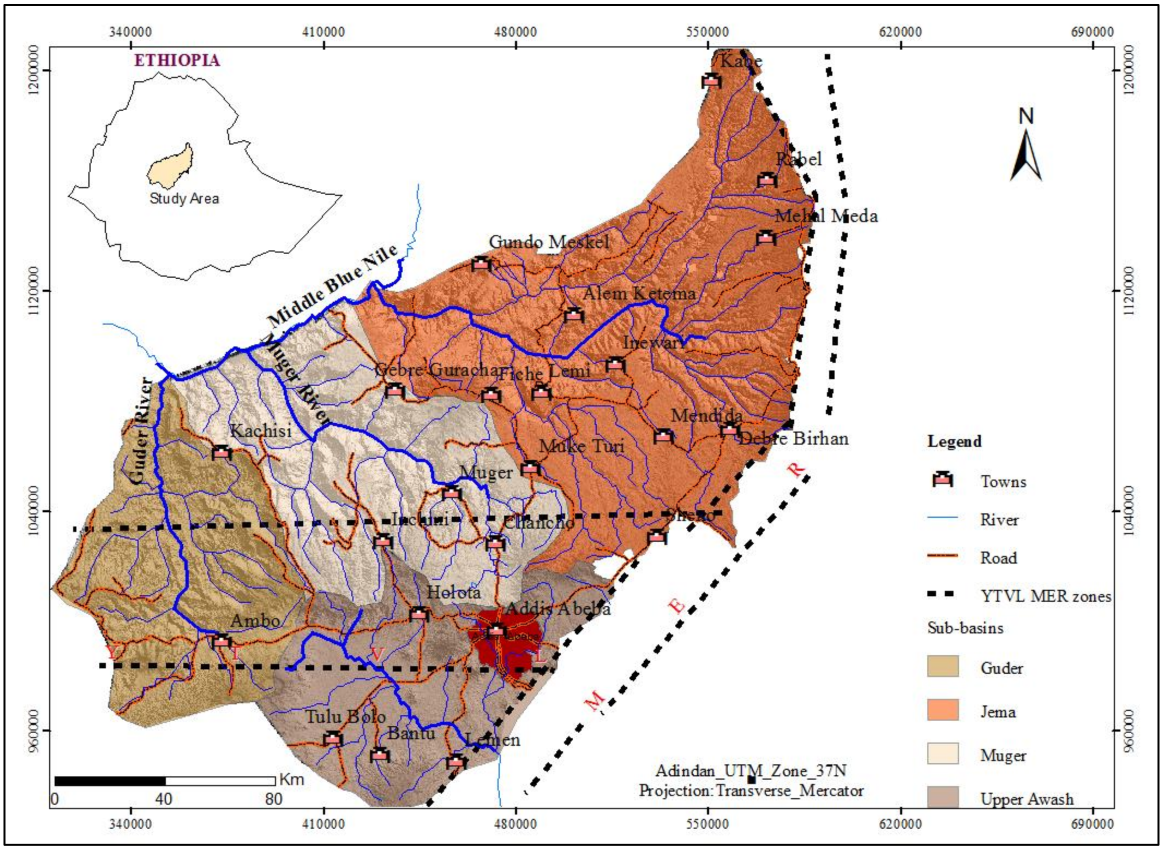

Figure 1. Location map

1.4. Objective

1.4.1. General objective

The general objective of the study is to characterize the barely known hydrogeological system of the area with emphasis given to amount of recharge, aquifer distribution, groundwater flow pattern, hydraulic connection and flux between aquifer systems of adjacent basins and the factors that control the groundwater dynamics.

1.4.2. Specific objectives

The specific objectives include:

- Characterization of litho-structural set up of the area from geological and structural studies, borehole lithologic logs and supplementary geophysicsso as to reconstruct sub-surface geometry that controls aquifer distribution, groundwater flow pattern and groundwater divides,

- Estimation of recharge to the aquifer systems of the sub-basins and quantify groundwater flux between the Blue Nile and the Upper Awash basins,
- Characterization of aquifer systems and groundwater flow patterns from litho-structural analysis, pumping test data and water level measurement in boreholes and dug wells and spring discharge survey,
- Characterization of the hydrochemical evolution of groundwater and major geochemical processes responsible for the changes so as to interpret flow patterns and aquifer distribution in the area,
- Identify recharge source for different aquifer systems and to characterize groundwater dynamics in the area from stable isotopes of water,
- Characterize groundwater dynamics in the area from groundwater age estimates made from radioactive carbon isotopes,
- Identifygroundwater discharge zones in the Upper Awash basin from measurements of on ^{222}Rnmade on Awash River and its tributary streams and
- Implement the conceptual model into simple regional numerical groundwater flow model and to help interpretation of the groundwater system.

1.5. Methods and Materials

To describe complex volcanic and underlying sedimentary rock aquifersin the area, the studyhas been conducted in an integrated approach using converging evidencesfrom geological, geophysical, structural, hydrodynamic, hydrochemical and environmental isotope studies Simpleregional groundwater flow modeling has been also conducted. Hydro-meteorological data has been usedto estimateresources annually added into the sub-basins and a groundwater flux between aquifer systems of the river basins.

Prior to the field work, existing water well drilling logs, pumping test data, water quality data, reports, maps, DEM from SRTM, images and scientific papersfrom the area and similar geologic terrains were reviewed. Problems and data gaps were identified. Meteorological and river discharge data were collected from MA and MoWIErespectively. Land use/land cover and soil information has been extracted and modified from FAO Land use land cover and soil maps of Ethiopia (FAO, 1984).

Geological study

The field work for geological characterization was conducted along selected traverses and where access is possible. Along these traverses: i) all important outcrops and contacts between lithologic units were geo-referenced and their elevations measured;ii) attitudes (strike and dip) of beds, joints, fractures, and faults were measured; and iii) lineament patterns extracted from DEM and images were verified where observable in the field. Rocks were characterized and named based on uniquenessof field observed properties.

Lineaments were extracted from DEM using Geomatica (version12)with some manual corrections. Different lineament density zones were mapped using kriging interpolation tools in ArcGIS10. Regional structures were identified from measurements of elevations of contacts between marker beds or geologic units in the field, observed from DEM and images and correlation with boreholelithologiclogs. Field measured data of attitudes were processed using Stereo32(version 1.0.2) to produce rose plots as indicative of regional structures. Some regional structures were also inferred from the trends of the observed regional structures.Geological map and cross sectionswere produced using ArcGIS10 and AutoCAD07 respectively. Schematic 3D models of sedimentary rock units underlying Tertiary volcanics were also produced using Surfur14.

Geophysical survey

Geophysical survey of electrical method wasconducted at some selected place along five profilesto supplement the litho-structural analysis and interpretation to verifyan E-W oriented impermeable mudstone caped horst. A total of 21 VES stations were selected for sounding survey with AB/2 separation between 1000m and 1500m. The survey was conducted using Terrameter SAS4000 and Syscal resistivity measuring deviceswith schlumberger electrode array. The raw geo-electric data were processed and interpreted by using, Win RESIST (Version 2004) and RESIX-IP (version 1990). Estimated resistivity and thickness of layers calibrated with borehole data were used as input parameters for starting model in the inverse modeling. True resistivity values and depths from the measured apparent resistivity data for all stations were obtained.Results were then presented in geo-electric cross sections and pseudo sections. Correlations made between geo-electric sections help schematize the general orientation of mudstone caped horst.

Hydro-meteorological study

Rechargeestimation to the aquifer systems of the four sub-basins have been conducted using meteorological data from 13 stations (P, RH, T, WS, SSH), river discharge data from 34 river gauge stations. Soil types, land use and land cover maps were also used from modified FAO Land use/land cover and soil maps of Ethiopia (FAO, 1984).

Prior to the recharge estimation, water balance variables (AET, runoff and withdrawal by pumping) were estimated using different estimation techniques. Recharge to the sub-basins has been estimated using water balance, chloride mass balance and base flow separation methods. Figures representative to the sub-basins from the methods were given in tables. A map showing different recharge zones has been produced from the result of base flow separation method using kriging tool in ArcMap.

Hydrodynamic Hydrochemical and isotopes studies

The field works for water point inventory for hydrogeological, hydrochemical and isotope studieswere conducted in all parts of the area where dug wells, springs andboreholes are available.During the field work, depth to the groundwater level was measuredwherever possible and spring discharges were estimated.Pumping test data obtained from drilling companies were processed using aquitest software, version 2.5to evaluate hydraulic parameters for aquifer materials. Hydrogeological map with groundwater contours and groundwater flow directions together with plots showing spring discharge and transmissivity was produced using tools in ArcGIS10.

During the field work, insitu measurement for EC, pH and water temperature have been conducted. Water samples were collected forchemical and isotope analysis in the laboratory. Hydrochemical resultshave been interpreted using diagrames version 3.1 and aquachem version 3.7 to calculate charge balance error and to identify water types.Different tools in ArcMap10 have been used for analysis spatial distribution and

Statistica 8.0 for statistical analysis of chemical data. Results were presented in maps graduated point plots.

Results for stable isotopes of water were plotted and interpreted on excel. Radiocarbon data has been also interpreted using the Pearson model. In situ counting for radon was conducted at different reaches of the Awash River and its tributary streams. Spatial variations in isotopic signature of the groundwater were plotted on maps.

Groundwater flow modeling

Prior to the numerical modeling, conceptual groundwater flow model has been produced and boundary condition has been established for the Upper Awash groundwater basin from the findings of other methods employed.Simple regional numerical groundwater flow model has been run using MODFLOW-2000. Results were presented in tables and maps.

1.6. Significance of the Research

The study significantly contributes to the understanding of the geometric set up of volcanic and sedimentary rocks that control groundwater dynamics and predominantly shed light on the hydraulic relationships and groundwater flux between the aquifer systems of the Middle Blue Nile and the Upper Awash basins. The new data generated in the course of the research will also enable further research at a larger scale in the area and the surrounding.

Since the research area is located in the central part of the country, surrounding the capital city of Addis Ababa, where groundwater is becoming a major source of water for domestic, industrial and agricultural purposes, it will play important role for sustainable utilization of the groundwater system in the area.

Chapter Two: Geology

2.1. Introduction

The geological mapping, structural measurements and lineament extraction approaches using GIS techniques helped characterize rock units, their spatial distribution and stratigraphic relationship. It also helped visualize and present sub-surface geometry of the geological units resulted from rock forming and palaeo-geodynamicprocesses.

In the study area, different lithostratigraphic units with distinctive stratigraphic set up in both sedimentary and volcanic terrains were identified (Figs. 2 and3). Zones with different lineament densities and regional structure with varying orientations and ages were also delineated (Figs. 4 and 5). Sub-surface geometry of volcanic and sedimentary rocksin the areahas been reconstructed and schematized in 3Dmodels (Fig. 6).

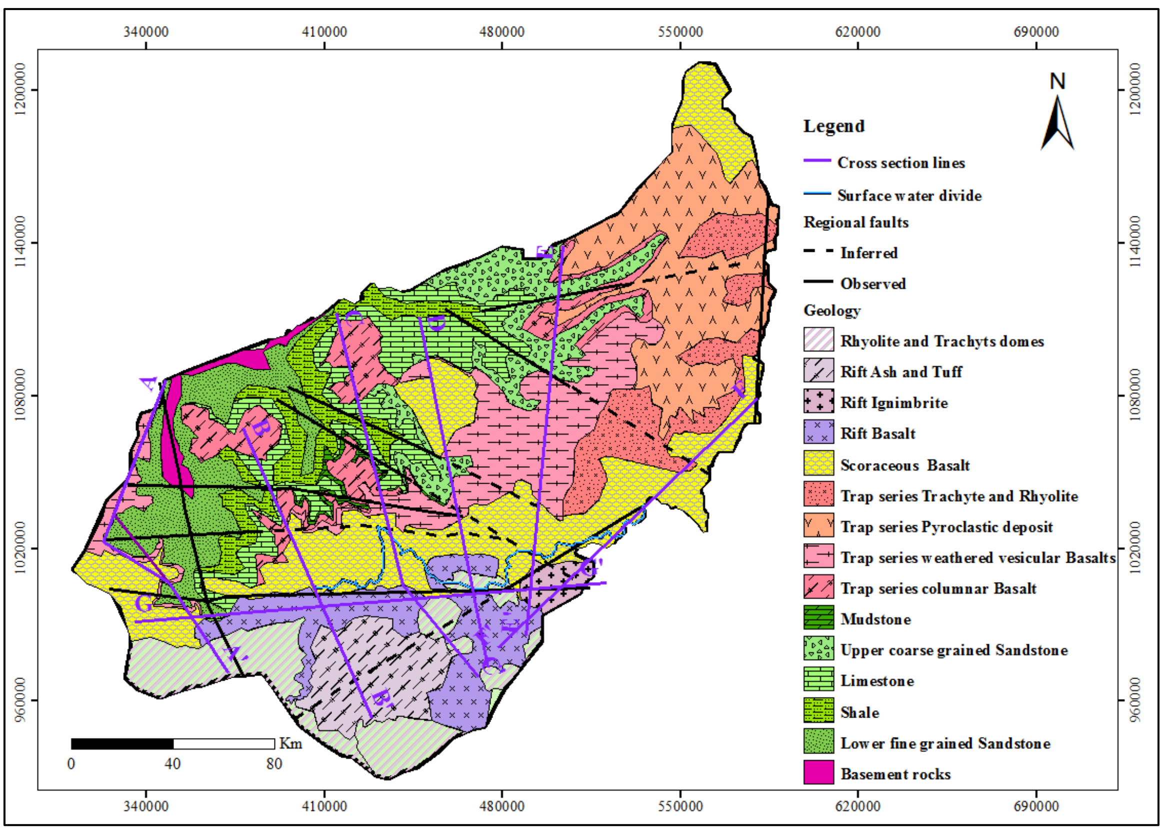

Figure 2. Simplified Geological map

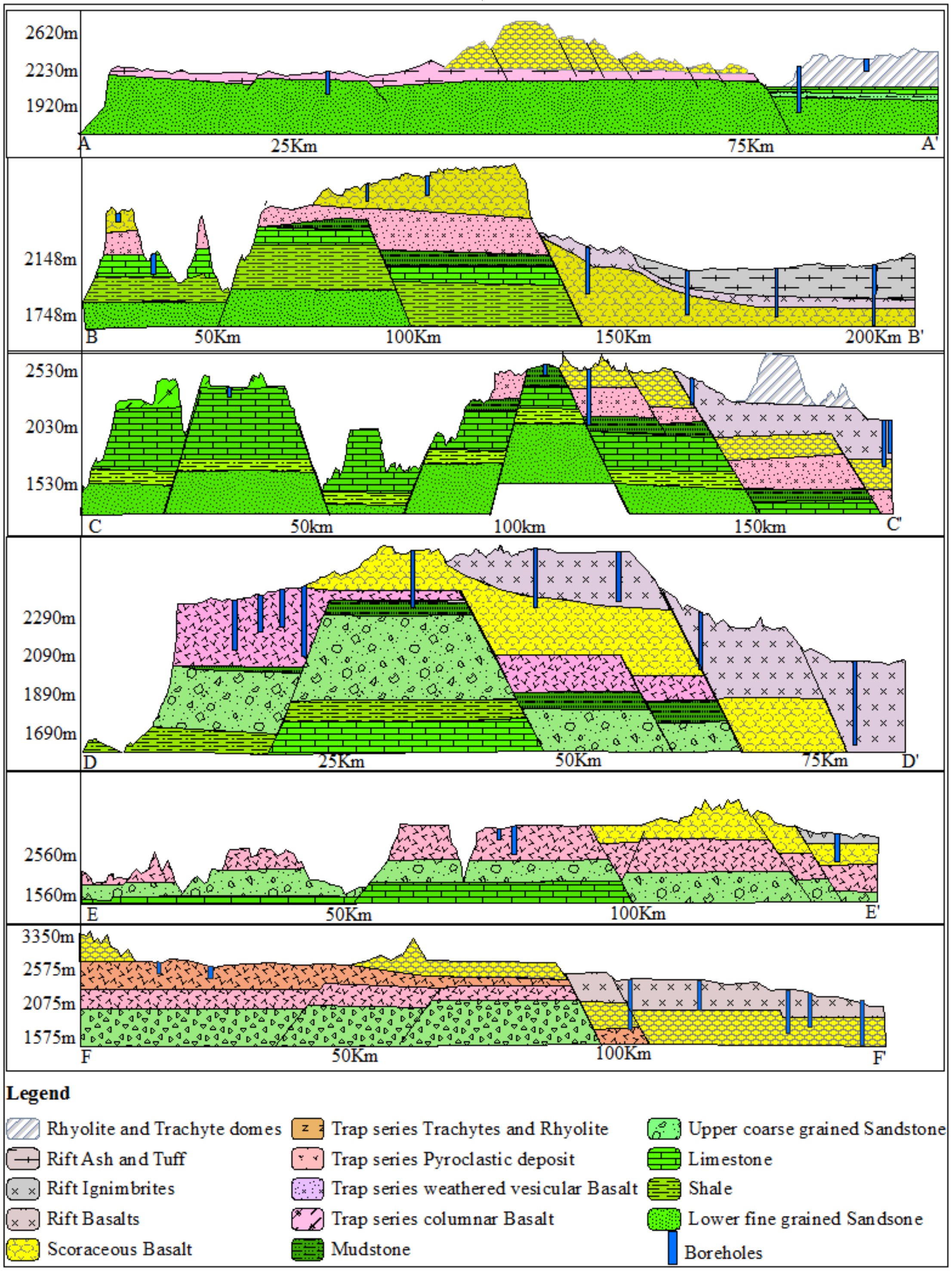

Figure 3. Geological cross-sections having hydrogeological significance

2.2.Lithostratigraphy

Five distinct sedimentary rock units and nine volcanic rock units are exposed in the study area (Fig. 2). The alluvial deposits in the area rarely exceed a few meters in thickness and are not mapped as a separate unit, while the basement rocks are rarely exposed.

2.2.1. Sedimentary rock units

The Mesozoic sedimentary rock units exposed in the area are the Lower fine grained Sandstone, Shale, Limestone, Upper coarse grained Sandstone and Mudstone from the oldest to the youngest.

The Lower fine grained Sandstone unit forming part of the Adigrat Sandstone (Mengesha Tefera et al., 1996) is composed of sandstone with thin lenses of siltstone and conglomerates. This unit outcrops in the deep gorges of the Blue Nile River where it is underlain by the basement and overlain by the Shale unit. It also outcrops on the vast plain of the Guder sub-basin. The maximum thickness of this unit as observed in the Blue Nile gorge is about 400m. The sandstone beds exposed in the Blue Nile River gorge show slight dip in a nearly southeast direction.

The Shale unit, composed dominantly of shale with intercalations of thin layers of gypsum, limestone and sandstone, forms part of the Gohatsion Formation (Mengesha Tefera et al., 1996). This unit outcrops in the gorges of the Blue Nile and its tributaries. The maximum thickness observed in the Blue Nile gorge is 580m. It thins and finally pinches out along the northwest direction towards the Guder sub-basin.

The Limestone unit which forms part of the Antalo Formation (Mengesha Tefera et al., 1996), is composed dominantly of slightly jointed and fractured limestone intercalated with thin beds of marl, shale and occasionally fine grained bands of sandstone. It outcrops overlying the Shale unit, in the gorges of the Blue Nile and its tributaries. The thickness of this unit is over 440m in the Blue Nile and Muger River gorges. This unit shows slight dipping in the southeast direction (1-2°).

The Upper coarse grained Sandstone unit is composed dominantly of sandstone with thick beds of conglomerates, thin beds of mudstone and shale, generally coarsening upward. Its thickness in the Muger River gorge reaches to over 400m and progressively thins to the northwest direction. The unit shows slight dip towards the south and southeast. In most parts of the basin, this unit outcrops below 2000m a. s. l. However, along the water divide between the Muger and Jema sub-basins north of Fiche town, this unit outcrops at relatively higher altitude (over 2400m a. s. l.), attributed to its uplift before the eruption of Miocene shield volcanic centers located in the proximity. Regional faults also strongly disrupted the original stratgraphic position of this unit.

The Mudstone unit is composed dominantly of mudstone with very thin beds of sandstone and shale. It outcrops in the Muger sub-basin underlying the volcanic rock units, and where it outcrops; its thickness reaches 110m, while a thickness of 216m is recorded from borehole lithologic logs.

2.1.2. Volcanic rockunits

The volcanic rock units exposed in the basin include Trap series columnar Basalt, Weathered vesicular Basalt, Pyroclastic deposits, Trachytes and Rhyolites, as well as Scoreaceous Basalts, Rhyolite and Trachyte domes, Rift Basalts, Ignimbrites and Ashes and Tuffs.

The Trap series columnar Basalt unit is characterized by conspicuous columnar blocks of varying diameter and lengths. It outcrops in the northern part of the Muger and Jema River gorges overlying the sedimentary rock units, representing the earliest flood basalt volcanism in the area. The lower part of inter-planar spaces among columns, are filled with secondary minerals (zeolites and clay).

The Trap series weathered vesicular Basalt unit consists dominantly of highly weathered and altered basalts. Vesicular spaces in its lower domain are completely filled with amygdales of zeolites and silica. It outcrops in the central parts of the area underlain by the Lower fine grained Sandstone in the Guder River gorge, and by the Trap series columnar basalts in the Muger and Jema sub-basins.

The Trap series Pyroclastic deposits consist dominantly of ash and tuff with minor ignimbrites, scoria and basalt layers. This unit outcrops in the Jema sub-basin overlying the Trap series columnar and weathered basalt units. It is overlain in some parts by fractured trachyte and rhyolite and in other parts by scoriaceous basalt units.

The Trap series Trachyte and Rhyolite unit consists dominantly of trachytes and rhyolites with thin layers of basalt. This unit outcrops in the Jema sub-basin overlying the Trap series weathered vesicular basalt and pyroclastic deposits, and overlain by scoriaceous basalts. The latter (scoriaceous Basalt unit) consists dominantly of fresh to slightly weathered scoria and scoriaceous basalts with thin intercalations of tuff. The unit outcrops along the rift margins and the YTVL zones. It directly overlies the Trap series volcanic rock units.

The Rift Basalt unit is composed of vesicular basalt with minor trachytes, exposed along stream banks and beds in the Upper Awash basin and southern part of the Muger sub-basin. The overall thickness of this unit is over 600m as observed from lithologic log of existing boreholes. The Rift Ignimbrite unit is composed of ignimbrites, with minor tuff and ash intercalations. It outcrops in the northeastern part of the Upper Awash basin forming extensive flat topography. The Rift Ash and Tuff unit is composed of tuff and ash forming a relatively undulating topography in the northeastern part and flat plains, dotted with small isolated rhyolite/pumice domes, in the northwestern part of the Upper Awash basin. The Rhyolite and Trachyte domes form isolated silicic domes and associated tuffs along rift margins and rift shoulders.

2.2. Geological Structures

The study area has a complex structural setting marked by extensional tectonics (fractures, joints and normal faults) related to the evolution of the active MER and the older YTVL zones (TsegayeAbebe, 1995; TsegayeAbebe et al., 1998). Fractures, joints with varying density and normal regional faults with varying orientations were identified in the area (Figs. 4 and 5).

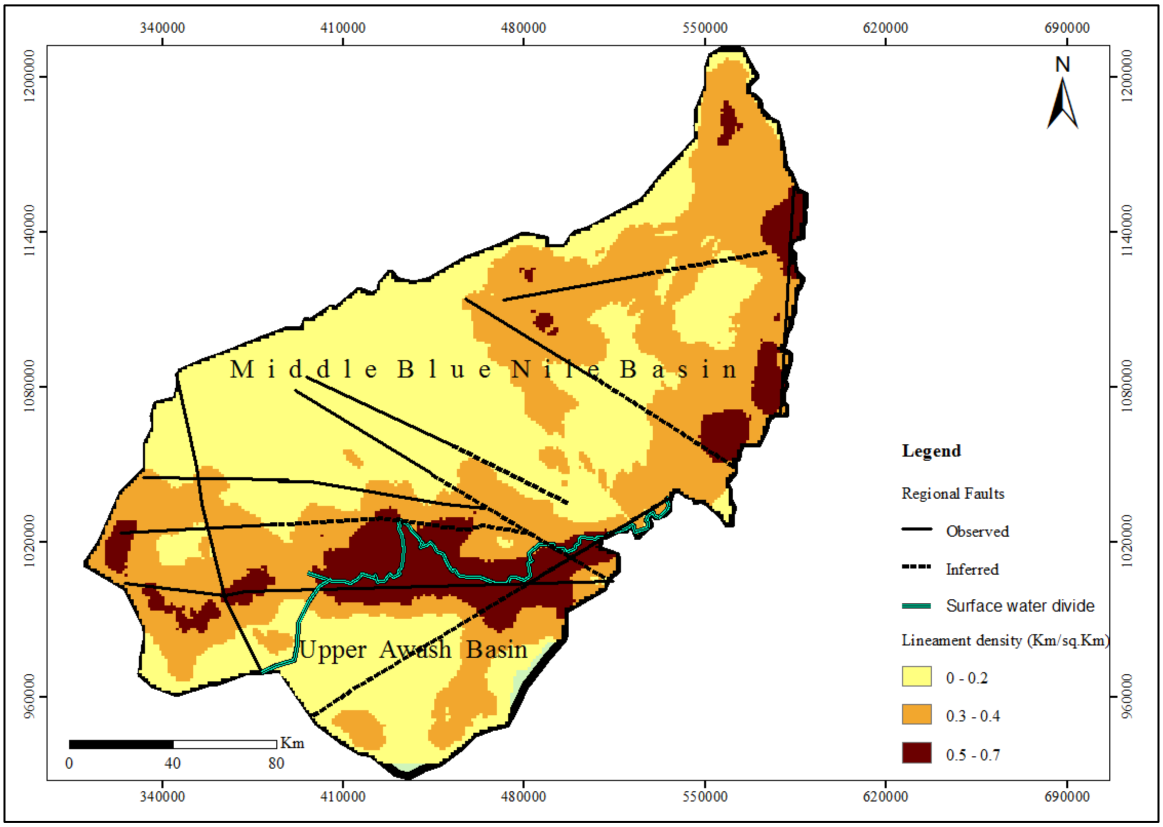

Figure 4.Lineament density distribution map.

2.2.1. Fractures and joints

Lineament (fracture and joint) density is high on lithologic units outcropping close to the margin of the MER and along the reactivated older tectonic zone of the YTVL (Fig. 4). The older units, notably the Lower fine grained Sandstone, Shale, Limestone, and the Upper coarse grained Sandstone units, as well as the Trap series columnar and weathered Basalt units are affected by lineaments dominantly oriented NW-SE. The younger volcanic rock units overlying the Trap series volcanics are highly fractured and jointed as they are mostly exposed along the MER margin and YTVL zones, with major lineament orientations along N-S, E-W and NE-SW directions.

The Lower fine grained Sandstone is slightly to moderately fractured with low lineament density (Fig. 4). The unit is affected by sparsely distributed, slightly penetrative to non-penetrative, dominantly non-extensive, variously oriented joint sets. The dominant joint set is oriented in a nearly E-W direction (strike of 105°) parallel to the orientation of the YTVL. To a lesser extent joints oriented in a NE-SW direction (strike of 75°) are observed (Fig. 5a). Similarly, the major fault systems that cause significant disruption of the structural blocks are NW-SE and E-W running (Fig. 3).

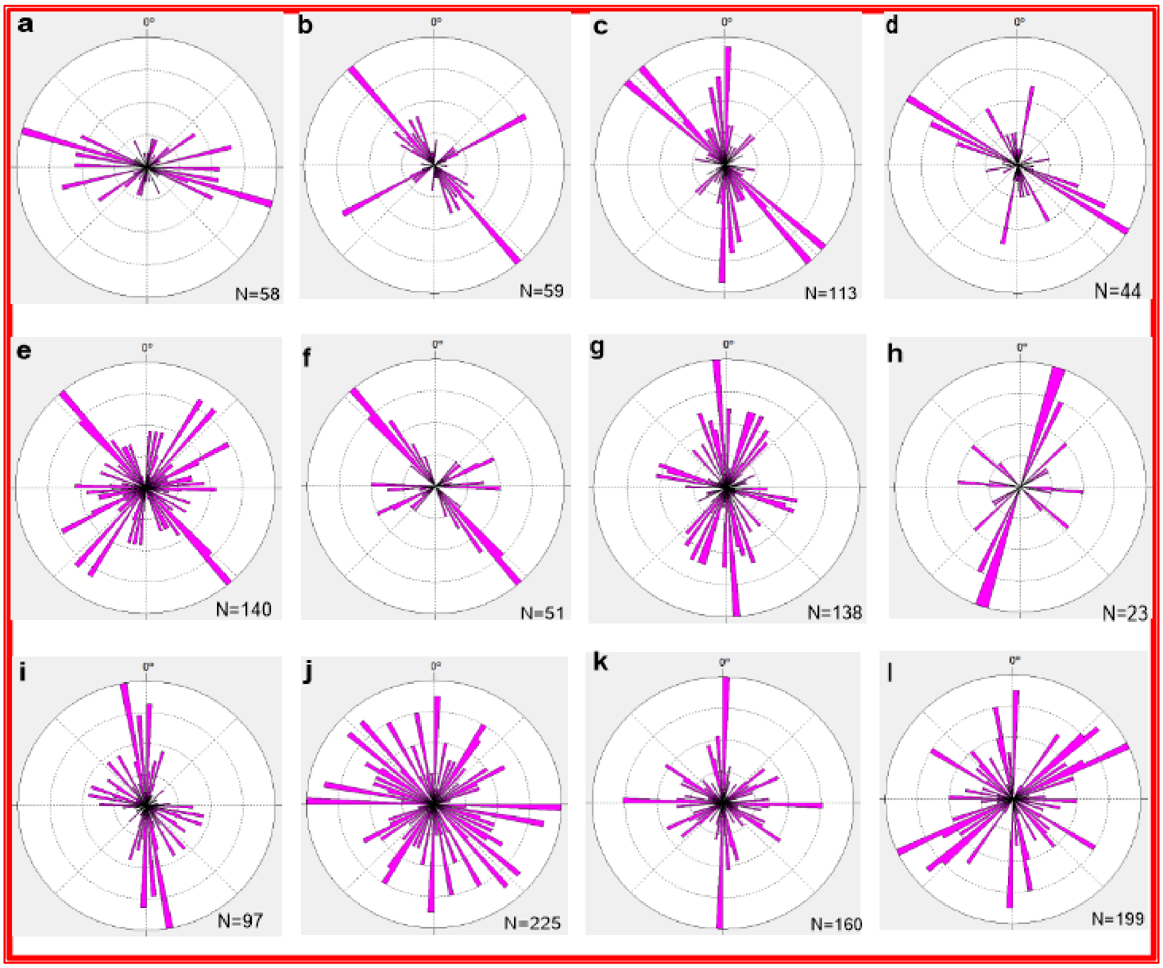

Figure 5. Rose diagrams of joint orientations

(a) Lower fine grained Sandstone, (b) Shale, (c) Limestone, (d) Upper coarse grained Sandstone, (e) Trap Series columnar Basalt, (f) Trap Series weathered vesicular Basalt, (g) Trap Series Pyroclastic Deposits, (h) Trap Series Trachyte and Rhyolites, (i) Scoriaceous Basalts along the rift, (j) Scoriaceous Basalt along YTVL, (k) Rhyolites and Trachytes domes and (l) Rift Ignimbrites and Basalts.

Lineament density in the Shale unit is very low (Fig. 4). The unit is affected by sparsely distributed, slightly penetrative to non-pentrative, non-extensive, variously oriented joints. The dominant joint set orientation is nearly NW-SE (strike of 140°) and to a lesser extent NE-SW (strike of 65°; Fig. 5b). Similarly, the Limestone and intercalated marl unit is affected by variously oriented joint sets and fractures of different sizes. Penetrative joints with extensive strike length terminating in marl layers are common. The dominant joint set orientation is nearly N-S (strike of 5°). To a lesser extent, joints oriented in a NW-SE direction (strike of 130° and 140°) also exist in the unit (Fig. 5c). The major fault systems that cause significant disruption of the limestone blocks are E-W, NW-SE and N-S running (Fig. 3).

Highly penetrative joints with extensive strike length are common in the Upper coarse grained Sandstone. The dominant joint set orientation is nearly NW-SE (strike of 125°), and to a lesser extent joints oriented in a N-S direction exist (Fig. 5d). On the other hand, the fault systems and sparsely distributed lineaments affecting the Mudstone unit are oriented in NW-SE and E-W directions (Fig. 3).

The Trap Series columnar Basalt unit is slightly jointed with dominant joint set orientation of nearly NW-SE (strike of 145°) and to a lesser extent SW-NE (Fig. 5e), while fractures in the Trap Series weathered vesicular Basalt are generally masked by weathering effect and where observed they are densely distributed with increasing trend towards the MER and YTVL zones. The dominant joint set orientation is nearly NW-SE with strike of 140° (Fig. 5f).

The Trap series Pyroclastic deposits are characterized by densely distributed fractures. However, highly penetrative joints with extensive strike length are rare, as most of the fractures are truncated by the overlying ash and weathered tuff layers. The dominant joint set orientation is N-S (Fig. 5g). Regional fault systems oriented NE-SW and N-S affected the unit (Fig. 3). Similarly the Trap series Trachyte and Rhyolite unit is affected by variously oriented, densely distributed, highly penetrative joint sets and fractures of variable sizes, commonly with extensive strike length. The dominant joint set orientation is nearly N-S with strike of 20° (Fig. 5h).

The Scoriaceous Basalt unit is moderately to highly jointed and fractured in some localities. Though joint orientations in this unit vary depending on its geographic location relative to the MER and YTVL systems, the dominant joint orientations are N-S and SW-NE along the MER and E-W along the YTVL zones (Figs. 5i and j).

The Rift Basalt and Rift Ignimbrite units are commonly affected by variously oriented, densely distributed, highly penetrative joints of variable sizes with extensive strike lengths are common. The dominant joint set orientation is SW-NE with a strike of 65° and to a lesser extent N-S (Fig. 5l). Joints and fractures are hardly observed on the Rift Ash and Tuff unit. On the other hand, densely distributed, variously oriented joint sets and fractures of variable size with dominant joint orientations of N-S, and E-W are observed on the Trachyte and Rhyolite domes (Fig. 5k).

2.2.2. Regional fault systems

Four principal fault systems have been identified in the area by previous workers (e.g., Tsegaye Abebe, 1995;TsegayeAbebe et al., 1998) and confirmed by the current analysis: the Red sea (NW-SE), the Gulf of Aden (E-W), the MER (NE-SW), and the reactivated Precambrian basement system (N-S).

The NW-SE oriented fault system affects mostly the Mesozoic sediments and older units of the Trap series volcanics, suggesting their Pre-Tertiary to early Tertiary age. These normal faults significantly displacethe affected blocks of these units exposed along Guder, Muger and Jema River gorges (Figs. 2 and 3). The faulted blocks are downthrown towards the NE in most cases, although SW dipping is not uncommon, resulting in the formation of some graben and horst structures generally oriented NW-SE.

Detailed geological maps, borehole lithologic logs and structural analysis show that normal block faulting associated with the older E–W oriented structural regime and partly with the Main Ethiopian Rift occurred leading to disruption and disaggregation of the sedimentary units, eventually forming typical horst and graben structures.The E-Woriented fault system affects the Mesozoic sediments and the overlying volcanic rock units along the reactivated YTVL zone. The faulted blocks are downthrown towards the south in most cases, although North dipping is also observed, resulting in the formation of a horst structure oriented E-W. A horst of Mudstone formed by these faults is covered by early episodes of the Tertiary volcanic units in the eastern part and outcrops on the surface in the westcentral part of the Muger sub-basin. This tectonic element together with the NW-SE oriented graben and horst structures likely controlled the geometric setting of the Mesozoic sediments underlying the Tertiary volcanics. This fault system has also been later reactivated, as its trace is clearly marked as a prominent lineament along the water divide between the Blue Nile and the Upper Awash, affecting the Tertiary and younger rock units.

The NE-SW fault system is common along the MER margin and field relationships confirm that this system is younger than the NW-SE and E-W fault systems. The faults are mostly dipping to the SE, throwing the Mesozoic sedimentary and Tertiary volcanic rock units to lower levels and later overlain by rift volcanic rock units.

The N-S fault system, which is mostly with short strike length and small magnitude of displacement, represents reactivated older Precambrian structures with clear surface manifestation.

Mode of emplacement, thickness and the geometric architecture of volcanic rock units depend on the geometry of the underlying Mesozoic sedimentary rock units; magnitude of displacement of fault systems; erosion and locations of eruption centers. The conceptual schematic illustrations constructed from geometric relationships between regional fault systems shows surfaces of Mesozoic sedimentary rock units before the emplacement of Tertiary volcanic rocks which help to systematically schematize the geometry of the overlying volcanic rock units (Fig. 6).

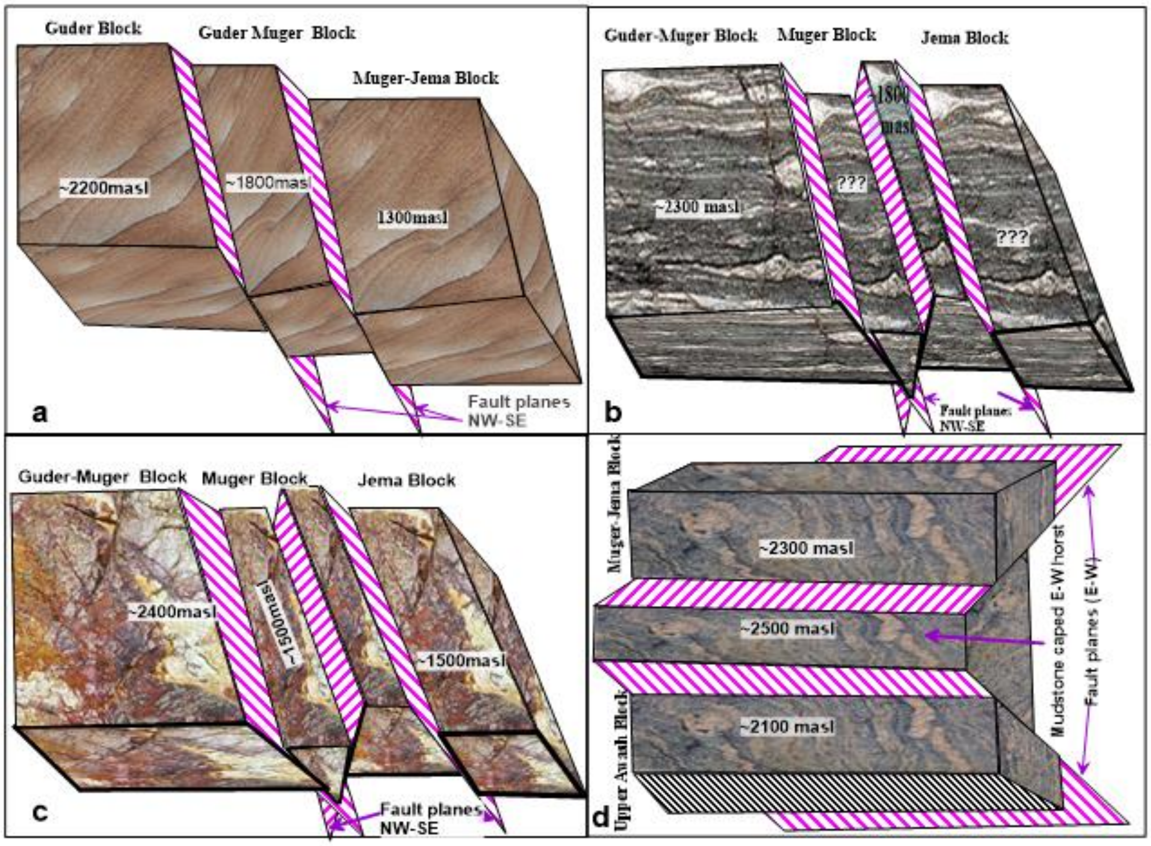
Guder Block
Guder Muger Block
Muger-Jema Block
~2200masl
~1800masl
1300masl
Fault planes
NW-SE
a
Guder-Muger Block
Muger Block
Jema Block
1800 masl
~2300 masl
???
???
Fault planes
NW-SE
b
Guder-Muger Block
Muger Block
Jema Block
~2400masl
~1500masl
~1500masl
Fault planes
NW-SE
c
Muger-Jema Block
~2300 masl
~2500 masl
~2100 masl
Upper Awash Block
Mudstone caped E-W horst
Fault planes (E-W)
d

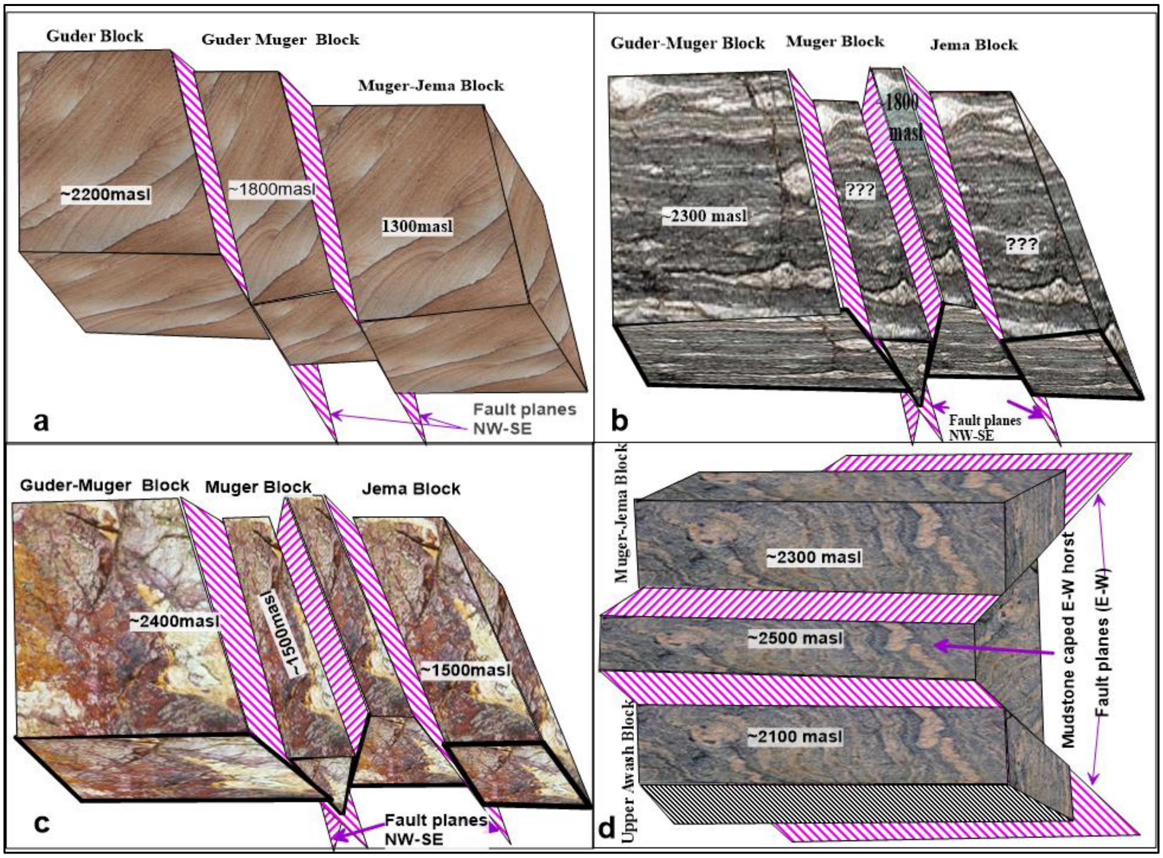

Figure 6.Schematic Illustrations ofsedimentary rock units

a) Lower fine grained Sandstone,b) Shale, c) Limestone, d) Mudstone and adjacent coarse grained Sandstone

Chapter Three: Geophysics

3.1. Introduction

The electrical resistivity method provides sufficient information about deep subsurface hydraulic condition as the method takes into account the conductance of the geological materials as an indicator of stratification of zones with different hydraulic properties (Kirsch, 2008).Sites for geophysical data acquisition were selected taking the orientation of mudstone caped horst observed from litho-structural analysis into account so as to better track its lateral extent and thickness of the overlying volcanic rocks (Fig. 7).

For calibration of VES data, lithologic logs of nine deep boreholes, ranging in depth from 216m to 600m were used. Some of the boreholes penetrated into volcanic rock units. One borehole drilled totally into sedimentary rock units. Some boreholes penetrated into the volcanic rock units and the underlying sedimentary rock units (Table 1).

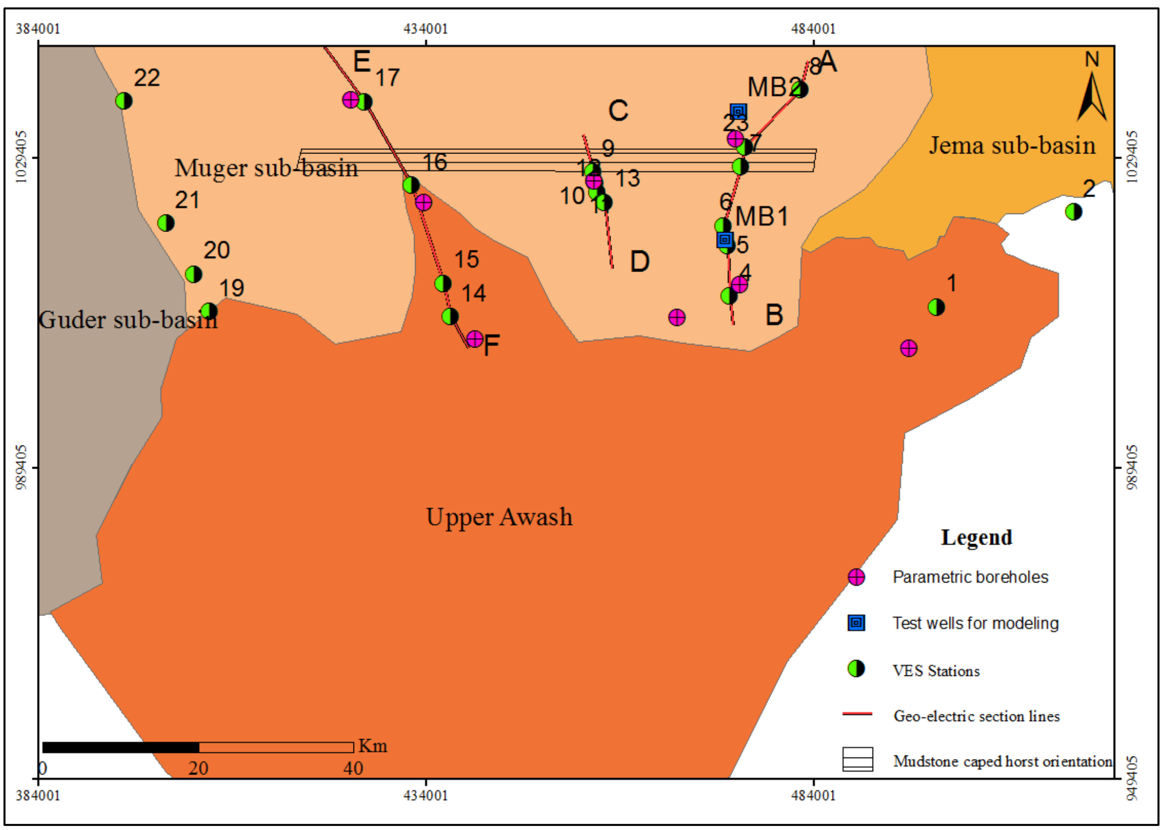

Figure 7.Geophysical survey stations

Based on the correlation between the VES results and the lithologic log information from the boreholes (Table 1) and geological contacts, different resistivity layers were recognized.Thesurvey mainly focuses to identifycontacts between the top most sedimentary unit and the overlying volcanic rocks. Very high and very low resistivity values that could likely be responses of sandstone and mudstone respectively, were obtained along three profile lines from the five. Along the remaining two profile lines, moderate resistivity that could represent volcanic rocks was recognized throughout the investigated depth. Hence, geo-electric cross-sections and pseudo sections were constructed along these three profile lines (AB, CD and EF) to schematize the lateral and vertical litho-structural variations in the area (Fig. 7).

The profiles are oriented in a nearly N-S direction. The spacing between VES, along profile AB and EF were made wide for regional observation but along profile CD, where there is a deep borehole that penetrated into sedimentary rock unit, the spacing between VES stations were made smaller for detail observation to definelateral extent of the mudstone caped horst structure (Figs. 8 and9). For each geo-electric section,VES data from 5 to 6 stations were used. See appendix 5,for the raw VES data.

Table 1.Lithologic logs of boreholes used for calibration of VES data

No	Locality	BH ID	UTME	UTMN	Depth, m	Summarized lithologic description
1	Chancho	BHT207	473911	1031930	0-324	Fractured and scoriaceous basalts
2	Holota	BHT113	440303	1006061	0-300	Massive, fractured and scoriaceous basalts
3	Legadadi	BHT121	496269	1004908	0-88	Ash/Ignimbrite
					88-268	Fractured basalt
					268-296	Ignimbrite
					296-336	Massive basalt
					336-600	Scoraceous basalt
4	Muger	BHT1378	433672	1023691	0-530	Massive, fractured and scor basalts
					530-602	Silty mudstone
6	Segno Gebeya	BHT206	455620	1026514	0-250	Massive, fractured and scoriaceous basalts
					250-273	Clayey mudstone
7	Sululta	BHT214	474421	1013070	0-110	Rhyolite/Trachyte
					110-304	Massive, fractured and scoriaceous basalts
8	Wosberi	BHT139 7	466306	1008828	0-220	Rhyolite
					220-460	Ignimbrite
9	Inchini	BHT1377	424332	1036895	0-54	Sand/weathered sandstone
					54-216	Silty mudstone

3.2. Electrical Signatures along the Profiles

Geo-electric section AB

This geo-electric section profile covers about 35 km. Along the profile at VESstations 7 and 23, the interpreted apparent resistivity value is very high below222m depth (925 ohm-m). This high resistive layer (Figs. 8 and 9) observed below depth 222m, is interpreted assandstoneor sand layer intercalated in the mudstone unitas explained by Getaneh Assefa (1981, 1991).This high resistive geophysical signature was not observed in the north and south of the VES stations mentioned, along the profile line. Overlying the high resistivity layer at the VES points mentioned and throughout the investigated depths at the remaining stations along the profile, apparent resistivity of layers are generally less than 470 ohm-m. These layers were interpreted as volcanic rock units with varied degree of fracturing, weathering and saturation with water. Boreholes used for calibration of the VES data located along this profile are BHT1397, BHT214and BHT207(Table 1).

Geo-electric section CD

This geo-electric section covers about 5km distanceand used for detailed observation of the mudstone caped horst. Along thisprofileat VES stations9 and 10,the interpreted apparent resistivity values are very low below a depth of 234m, less than 20 ohm-m.On the contrary; along the same profile in the southern side at VESstations 11 and 12, the interpreted apparent resistivity values are very high belowa depth of 213m, over 1000 ohm-m as it is clearly observed from the abrupt change of resistivity at the pseudo-section (Fig. 8). The very low resistivity is attributed to the mudstone but the very high resistive layer at the same depth is interpreted as sandstone both intercalated in the Mudstone unit. Overlying the very low and very high resistive layers at the points mentioned and throughout the investigated depths at the remaining stations along the profile, apparent resistivity of layers are generally less than 472 ohm-m. These layers were interpreted as volcanic rock units with varied degree of fracturing, weathering and saturation with water. A borehole used for calibration along this profile is BHT206.

Geo-electric Section EF

This geo-electric section extends for40 km distance. Along the profile at VESstation16, the interpreted apparent resistivity value is very low below500m depth (11-17 ohm-m). Along the same section in the northern side at VES station 17, the interpreted apparent resistivity values are also generally low where the survey was conducted on the exposed part of the mudstone.The Mudstone unit is the upper most layer in this area (Getaneh Assefa, 1991). Except at VES station 18 where the mudstone is overlain by thin volcanic rock, the electrical signature is nearly similaralong the profile, where very low resistivity is observed starting from the surface and extends to a depth of 200m with observed resistivity variationsattributed to intercalation of different layers in the Mudstone unit. Underlying the mudstone, high resistivity value is attributed tolimestone unit (124-322 ohm-m) and low value toshale (43-52 ohm-m). Similar to the other profiles, overlying the sedimentary rock units, there are geo-electric layers with moderate resistivity values (less than 454 ohm-m), which are attributed to volcanic rock units with varied degree of fracturing, weathering and saturation with water. Boreholes used for calibration along this profile are BHT113, BHT1378 and BHT1377.

3.3. Correlation between Geo-electric Sections

The correlations made between the three geo-electric sectionstogether with the geological evidences from borehole logs give a general E-W trend of the mudstone caped horstin the central part of the Muger sub-basin extending to the southern tip of Jema sub-basin. The mudstone capped horst exposedin the Muger sub-basin may gradually grade into sandstone caped horst to the east towards Jema sub-basin.

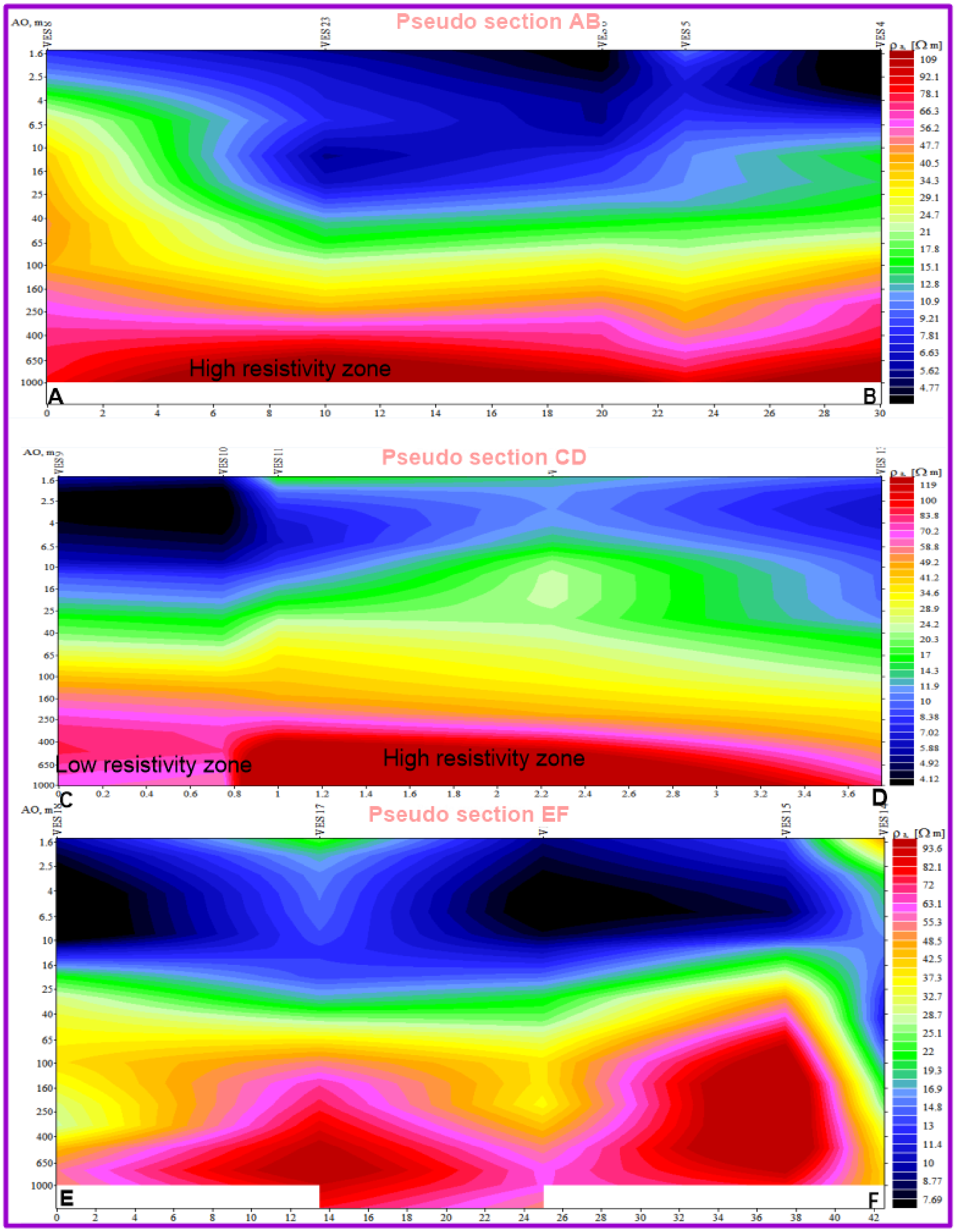

Figure 8. Pseudo-sections.

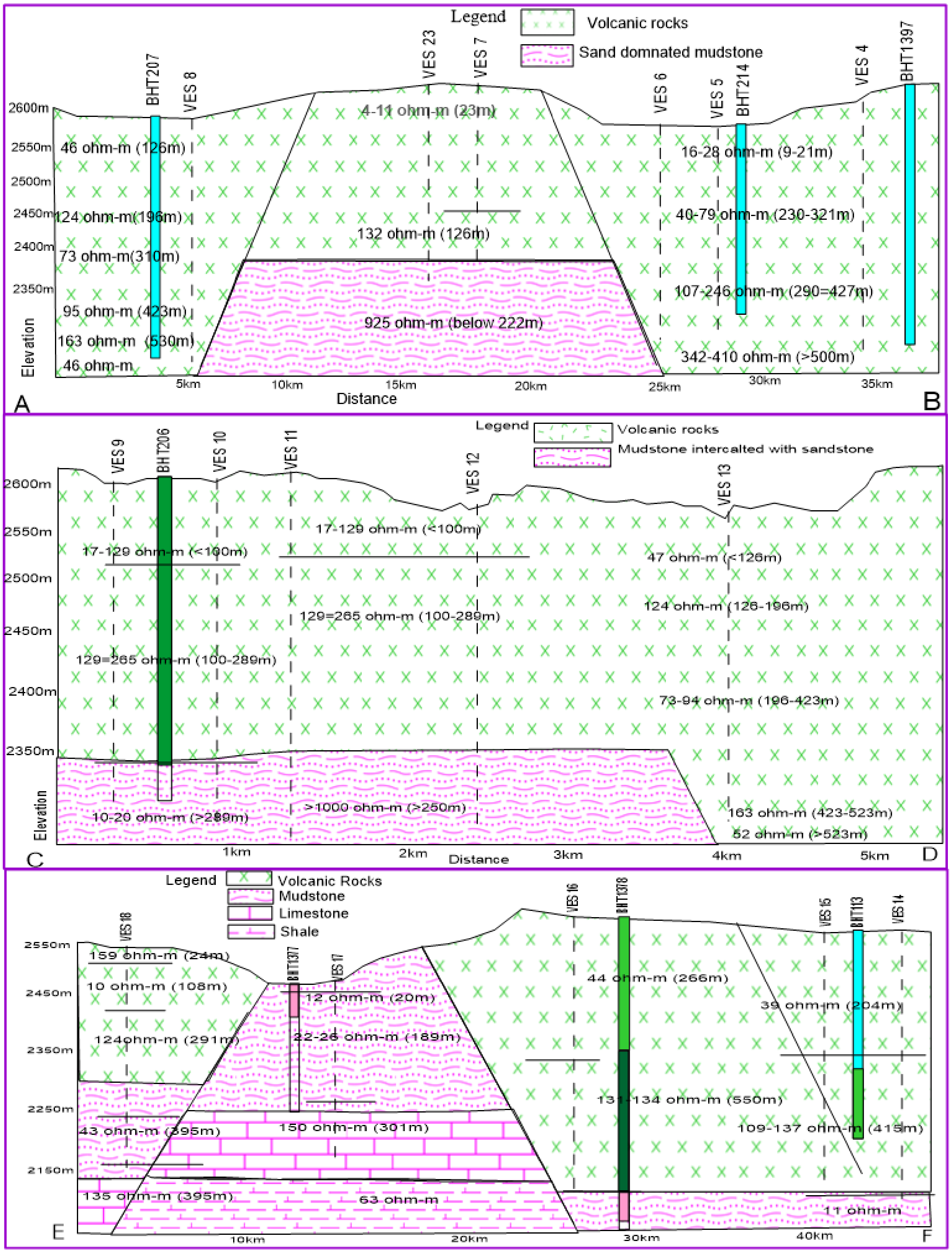

Figure 9.Geo-electric sections.

Chapter Four: Groundwater Recharge

4.1. Introduction

Recharge is one of the components in the hydrologic cycle and an important issue for hydrogeological characterization of aquifer systems. Characterizing recharge is also one of the major objectives in hydro-meteorological studies (Shaw, 1994).

In the current study, data used for recharge estimation includemean monthly meteorological data up to 20 years and daily river discharge data of upto 15 years (Tables 2, 3). Before analysis and interpretation, allthe data from MA and from MoWIE were checked for their quality.Only records with complete measurements were considered for analysis. Soil and land use/land cover maps were also used from modified FAO Land use/land cover and soilmaps of Ethiopia (FAO, 1984).

One of the major challenges in the hydro-meteorological characterization was absence of river discharge data for the three sub-basins (Guder, Muger and Jema) at their outlet from the study area or at their confluence with the Blue Nile River.Water availability estimation made by BCEOM (2000) shows that very low flow is available for the Muger and Guder Rivers during the dry season, while it is high for Jema River during the dry season.

Awash River draining the upper Awash basin, on the other hand has river discharge measuring station at Melka Kunture at its outlet from the study area, where it has high flows during the dry season.This has been verified by the observations made in March (mid of dry season) at Guder, Muger and JemaRivers where the former two have little flow or flow limited to river bed sediments.

During the same period, Jema River has big flow. For the same period,Awash River hashigh flow,as observed and revealedfrom measurements(Fig. 11). Hence, significant amount of groundwater emerge as base flow into Jema and Awash Rivers at the downstream reaches of the rivers.However, groundwater that recharges Guder and Muger

Rivers as base flow at their downstream part especially in the gorges close to the confluences with the Blue Nile River is insignificant.

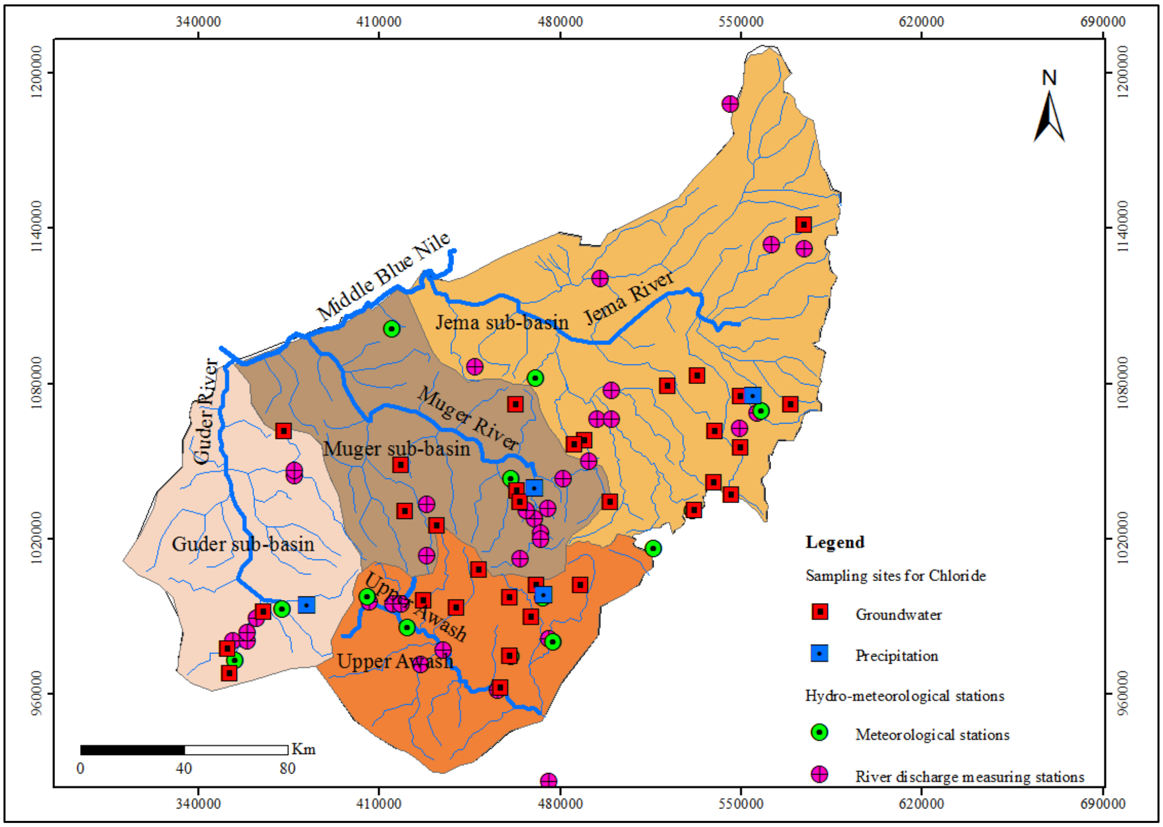

Figure 10. Hydro-meteorological stations.

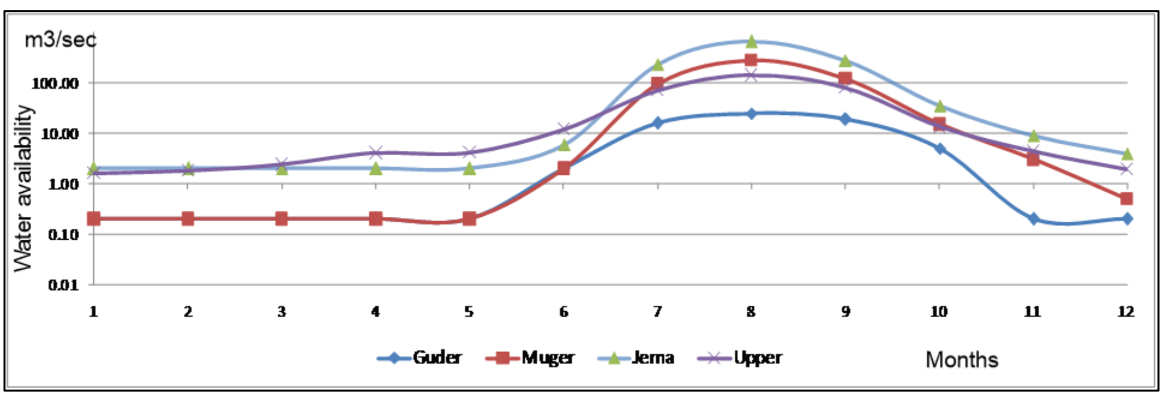

Figure 11.Long-term mean monthly flows (Modified from BCEOM, 2000).

Table 2. Meteorological stationsand measured variables.

Sub-basin	Stations	Year		Coordinate		P	T	RH	WS	SSH
		from	to	UTME	UTMN					
Guder	Ambo	1990	2010	372808	993137	√	√	√	√	√
	Tikur ichini	1990	2010	354551	973030	√	√			
Jema	Debre Berhan	1990	2010	558016	1069602	√	√	√	√	√
	Gohastsion	1990	2010	415187	1101284	√	√			
	Sheno	1990	2010	531558	1030973	√	√			
Muger	Fiche	1990	2010	470704	1082302	√	√	√	√	
	Aleltu	1990	2010	516212	1016421	√	√			
	Derba	1990	2010	461179	1043408	√				
Upper Awash	AAU observatory	1990	2010	473600	997565	√	√	√	√	√
	Akaki	1990	2010	477583	980437	√	√			
	Bonoya	1990	2010	461179	974616	√				
	Busa	1990	2010	420962	985993	√				
	Ginchi	1990	2010	405616	997900	√				

√ - symbol refers availability of data

Table 3.River gauge stations location, year of records and catchment areas.

Sub-basin	Station name	Coordinates		Year of record	
		UTME	UTMN	from	to
Guder	Bello at Guder	353747	980652	1959	2009
	Fato at Guder	359246	980633	1959	2009
	Guder at Guder	362576	989468	1959	2010
	Indris at Guder	359297	984114	1986	2010
	Tiliku Duber at Duber	377408	1044706	1997	2010
	Tinishu Duber at Duber	377414	1046549	1997	2010
Jema	Aleltu at Chancho	428623	1033519	1980	2010
	Aleltu at Muketuri	494514	1066619	1983	2008
	Beresa at Debre Berhan	556683	1068505	1963	2010
	Chacha at Debre Berhan	549376	1062967	1962	2010
	Robi Gumero at Lemi	500000	1077674	1983	2008
	Robi Jida at Muketuri	500000	1066619	1983	2008
	Selji at Kabe	545922	1188261	1979	2010
	Shy at Mehal Meda	561920	1133160	1980	2010
	Wenchi at Alem Ketema	475798	1114110	1996	2010
	Wizer at Mehal Mda	561523	1132366	1980	2010
Muger	Deneba at Chancho	475658	1031853	1981	2008
	Gerbi at Sululta	464842	1012465	1970	2010
	Gorfo at Gorfo	481337	1043408	1998	2010

Sub-basin	Station name	Coordinates		Year of record	
		UTME	UTMN	from	to
	Muger at Chancho	470347	1027938	1956	2010
	Roba at Chancho	472540	1022408	1980	2008
	Sibilu at Chancho	472538	1020197	1980	2010
Upper Awash	Awash at Belo	435120	977126	1986	2010
	Awash at Ginchi	406571	995976	1993	2010
	Awash at Melka Kuntre	455998	961621	1966	2008
	Berga at Addis Alem	434087	1000552	1975	2010
	Big Akaki at Akaki	468808	967255	1981	2009
	Holota at Holota	447365	1006556	1975	2008
	Jemjem at Wolonkomi	415362	994851	1998	2009
	Kela at Wolonkomi	418660	994844	1997	2009
	Kesem at Beke	507332	1012975	1986	2010
	Little Akaki at bridge	467055	1031257	1989	2004
	Mutinicha at Legadadi	490610	1000486	1989	2006
	Teji at Asgori	426313	971613	1975	2010

4.1. Data Analysis

Precipitation

A number of meteorological stations are available in the area. However, only few stations have complete set of precipitation records. To calculate aerial depth of precipitation of the sub-basins, point measurements with complete data found in each sub-basin were averaged by using arithmetic mean and Theissen polygonmethods (Table 4). Maximum monthly mean precipitations: 532mm, 607, 496mm and 428mm for Guder, Muger, Jema and the Upper Awash sub-basins respectively have been recorded during the period of the measurements.

Table 4.Depth of aerial precipitation (mm).

Sub-basin	Jan	Feb	Mar	Apr	May	Jun	Jul	Aug	Sep	Oct	Nov	Dec	Annual
Guder	31	37	63	103	118	225	286	284	186	62	18	13	1424
Jema	12	13	42	59	40	114	321	272	109	32	6	5	993
Muger	19	32	61	75	70	167	321	292	114	29	14	8	1201
Upper Awash	17	28	52	76	74	150	267	274	132	25	9	8	1112

Temperature

Since temperature is one of the most important parameters to consider in hydro-meteorological characterization and recharge estimation, monthly minimum, maximum and mean temperature records wereused for analysis.Temperature ranges between extreme mean monthly minimum (-2.1^{o}C) in Debre Berhan station to extreme mean monthly maximum (31.1^{o}C) at Ambo station have been recorded during the study period. To get representative monthly and annual means, point measurements with complete data found in each sub-basin were averaged (Table 5). Generally, November and December are the coldest months in all stations in the area, while April and March are the warmest months.

Table 5.Long-term mean monthly and annual temperature (^{o}C).

Sub-basin	Jan	Feb	Mar	Apr	May	Jun	Jul	Aug	Sep	Oct	Nov	Dec	Annual
Guder	17	17	18	18	17	16	15	15	15	16	15	16	16
Jema	13	13	13	14	14	14	13	13	13	12	12	12	13
Muger	18	18	19	19	19	18	16	16	16	17	17	17	17
Upper Awash	18	19	20	20	20	19	18	18	18	18	17	17	18

Relative Humidity

At any given temperature, air can hold a maximum amount of moisture; the saturation humidity and this is directly proportional to the air temperature. Relative humidity is the ratio between the amount of water the ambient air actually holds and the amount it could hold at the same temperature (Shaw, 1995). It is a dimensionless quantityand is commonly given as a percentage. The relative humidity expresses the degree of saturation of the air.Monthly and annual means of humidity inthe sub-basins were taken from available point data(Table 6)

Table 6. Mean monthly relative humidity (%).

Sub-basin	Jan	Feb	Mar	Apr	May	Jun	Jul	Aug	Sep	Oct	Nov	Dec	Annual
Guder	39	40	41	44	44	67	74	76	72	51	44	40	53
Jema	66	59	59	60	53	51	75	78	70	63	59	62	63
Muger	51	43	52	52	47	55	80	82	74	61	55	49	59
Upper Awash	41	41	43	50	48	61	75	76	69	49	43	43	53

Wind Speed

Rate of evaporation and evapotranspiration has a direct relation to and is strongly affected by wind speed. As water vaporizes into the atmosphere, the boundary layer between earth and air becomes increasingly more saturated so that the water vapor has to be removed and replaced with drier air continuously. This movement of the air and moisture transfer is directly proportional to wind speed and turbulence (Shaw, 2005).Monthly and annual means of wind speed in the sub-basins were taken from available point data (Table 7).

Table 7.Mean monthly and annual wind speed (m/s).

Sub-basin	Jan	Feb	Mar	Apr	May	Jun	Jul	Aug	Sep	Oct	Nov	Dec	Annual
Guder	2.1	2.5	2.1	2.1	1.7	1.3	1.0	0.9	0.9	1.6	2.1	2.4	1.7
Jema	2.4	2.7	2.6	2.3	2.6	2.2	1.6	1.5	1.7	1.8	2.1	2.4	2.2
Muger	2.3	2.6	2.5	2.2	2.5	2.1	1.5	1.4	1.6	1.7	2.0	2.3	2.1
Upper Awash	1.6	1.8	1.8	1.8	2.0	1.8	1.5	1.5	1.4	1.4	1.4	1.5	1.6

Sunshine hours

Although evaporation takes place almost without interruption during the day light and the night, the process is most active under direct radiation from the sun. Therefore variation in sunshine hour is important factor for evapotranspiration. Monthly and annual means of ET in the sub-basins were considered from available point data (Table 8).

Table 8. Mean monthly sun shine hours (hrs/d).

Sub-basin	Jan	Feb	Mar	Apr	May	Jun	Jul	Aug	Sep	Oct	Nov	Dec	Annual
Guder	9.2	8.3	7.5	6.8	8.1	7.5	5.4	5.4	6.1	8.3	9.0	9.2	7.6
Jema	8.8	7.8	7.7	6.9	7.4	4.9	4	3.8	4.8	8.9	9.1	9.5	6.9
Muger	8.5	7.7	7.6	7	8.8	7.6	5	5.1	7	9.1	9.3	9.1	7.7
Upper Awash	8.5	8.4	7.5	6.5	6.9	5	3	3.4	5.1	8.2	9.2	9.4	6.8

Land use land cover, soils and topography

The land cover of an area is controlled by its geographic, climatic, ecological and anthropogenic factors. Flat topography dominates Guder and the Upper Awash sub-basins while rolling topography dominates Jema and Muger sub-basins.Sandy soilsdominate the area. The dominant part of the area of the sub-basins is cultivated for cereal crops. Grass lands constitute some portions of the sub-basins area. Very small parts of the sub-basins area are covered with forests.

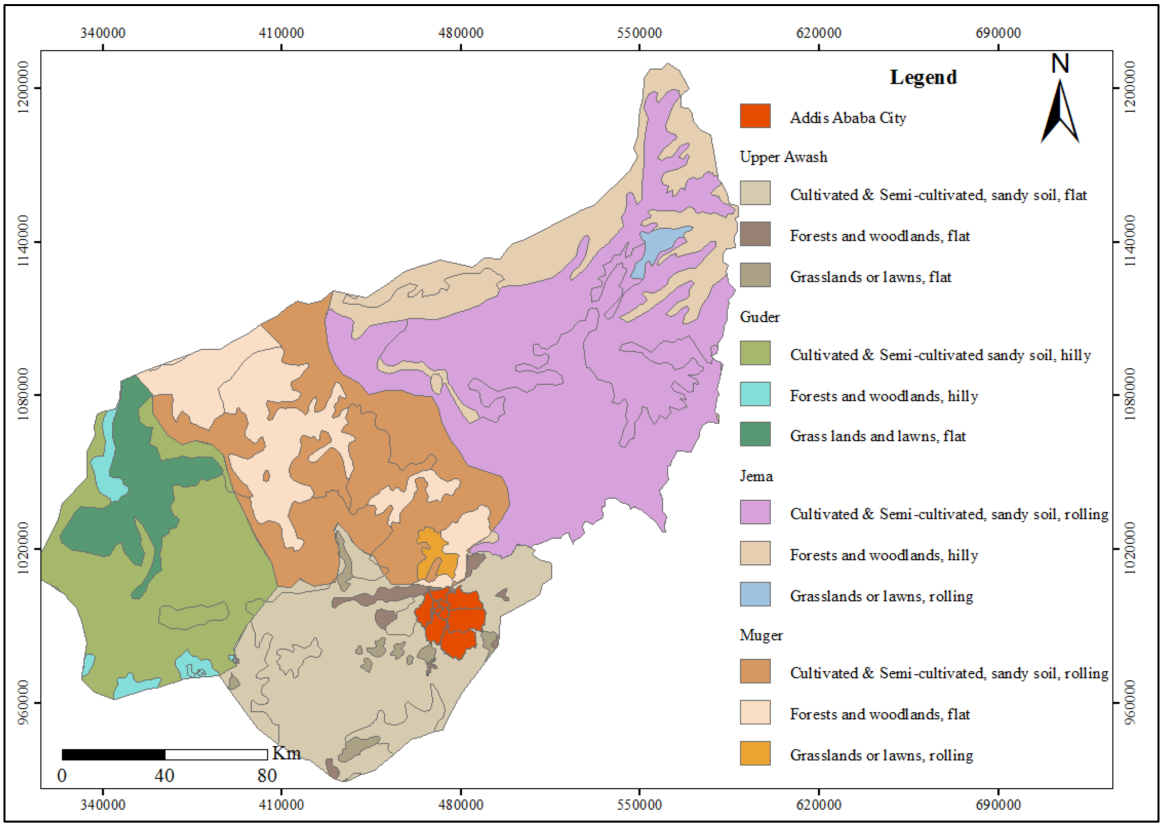

Figure 12.Land use/land cover and soils map(Modified from FAO, 1984).

Due to large size of the area occupied by the city of Addis Ababa, built physical features constitute significant portion of the Upper Awash but it is negligible for the other sub-basins. Proportions of soils and land use/land cover of the sub-basins were modified from FAO soil and Land use/land cover map of Ethiopia (FAO, 1984). (Fig. 12, Table 9).

Table 9.Proportions of land use land cover, soils and topography.

Sub-basin	Precipitation, mm	Land use land cover, soils and slopes	Proportion of area, %
Guder	1425	Cultivated & Semi-cultivated, sandy soil, flat	69
		Grass lands and lawns, flat	27
		Forests and woodlands, hilly	4
Muger	1202	Cultivated & Semi-cultivated, sandy soil, rolling	60
		Grasslands or lawns, rolling	3

Sub-basin	Precipitation, mm	Land use land cover, soils and slopes	Proportion of area, %
		Forests and woodlands, flat	37
Jema	992	Cultivated & Semi-cultivated, sandy soil, rolling	74
		Grasslands or lawns, rolling	1
		Forests and woodlands, hilly	25
Awash	1112	Cultivated & Semi-cultivated, sandy soil, flat	82
		Grasslands or lawns, flat	5
		Forests and woodlands, flat	5
		Urban areas	8

4.2. Estimation of Hydro-meteorological Variables

Except surface runoff in a well-defined geometric boundary, variables included in a general water balanceequation cannot be directly evaluated but estimated using different approaches (Jr and Lewis, 2003).

Evapotranspiration is influenced by various physical and aerodynamic factors as well as the availability of water. Physical factors include land use/land cover, soils, topography and geological set up. Aerodynamic factors include input solar energy, vapor pressure, and movement of air. The common hydro-meteorological variablesrelated to evapotranspiration are: T, RH, WS and SSH.Runoff from precipitation is affected by land use/land cover, soils and topographic set up of the area.

In addition to surface process that determines magnitude of evapotranspiration and runoff from precipitation, recharge rate is affected by subsurface geological structures and depth to the groundwater. Once recharged water has infiltrated into the soil, its passage downwards to join the groundwater storage depends on the geological structure as well as the nature of geologic material.

Prior to recharge estimation, values for PET, AET and runoff were quantified.Penman Combination method and Thornthwaite formula were employed to calculate PET of the four sub-basins. The methods take only aerodynamic factors into consideration. Turc empirical method and calculation made using SMD methods were applied to calculate representative AET values of the sub-basins. Runoff coefficient method has been employed to estimate runoff.

To minimize errors and for the sake of comparison, water balance, chloride mass balance and base flow separation methods have been employed for recharge estimation using the water balance variables. Base flow separation has been carried out using RAP software Version 3.0.3 and time plot program on excel sheet.

4.2.1. Potentialevapotranspiration

Employing the Penman Combination method using the meteorological elements such as T, RH, WS and SSH, mean monthly and annual PET values were calculated and results are given inTable 10.

Table 10. PET values obtained from PenmanCombination method (mm).

Sub-basin	Jan	Feb	Mar	Apr	May	Jun	Jul	Aug	Sep	Oct	Nov	Dec	Annual
Guder	94	100	106	101	99	69	56	53	59	86	87	93	1004
Muger	91	99	107	99	116	92	54	52	69	85	84	90	1038
Jema	68	83	88	82	91	79	49	48	59	72	72	68	859
Upper Awash	85	92	106	96	103	77	55	54	68	89	83	82	990

Thornthwaite formulahas been also employed to calculate PET values for the sub-basins from mean monthly temperature records, with an adjustment being made for the number of daylight hours (Shaw, 1994).The mean monthly and annual PET values calculated using the method are given in Table 11.

Table 11.PET values from Thornthwaiteformula (mm).

Sub-basin	Jan	Feb	Mar	Apr	May	Jun	Jul	Aug	Sep	Oct	Nov	Dec	Annual
Guder	73	81	89	88	92	75	69	67	67	71	64	65	901
Muger	76	82	86	93	105	89	67	65	68	70	72	72	945
Jema	61	67	68	71	79	73	69	69	65	58	55	54	790
Upper Awash	74	83	92	97	111	91	80	78	79	77	71	69	1003

Results from Penman Combination method and Thornthwaiteformulaare nearly close to each other. Hence, results from the two approacheswere averaged to get representative PET values for the sub-basins (Table 12).

Table 12.Summary of PET from Penman Combination and Thorthwaiteformula(mm).

Sub-basin	Jan	Feb	Mar	Apr	May	Jun	Jul	Aug	Sep	Oct	Nov	Dec	Annual
Guder	83	90	97	95	96	72	62	60	63	78	75	79	952
Muger	83	90	97	96	110	90	61	58	69	77	78	81	991
Jema	64	75	78	76	85	76	59	58	62	65	63	61	824
Upper Awash	80	87	99	97	107	84	68	66	73	83	77	75	997

4.2.2.Actual evapotranspiration

The Turc method uses empirical relations for calculating the annual AET from mean annual values of precipitation and temperature. The results obtained using themethod aregivenin Table 13.

Table 13.Annual AET values from Turc formula (mm).

Sub basin	Mean annual Precipitation, (mm)	Mean annual temperature, (0C)	AET
Guder	1424	16.3	786
Muger	1201	17.3	780
Jema	993	12.9	598
Upper Awash	1112	18.5	792

A soil moisture budget calculation has been carried out to evaluate AET values of the sub-basins. The values of soil moisture deficit and AET vary with soil type and vegetation (Shaw, 1994). Accordingly, the sub-basins have been classified into three land use/land cover units and vegetation with varying root depths (Fig. 12). The combination of land use/land cover and soilswith proportion of area coverage has been recognizedfrom FAO land use/land cover and soil maps of Ethiopia and given in Table 9. Cultivated lands with cereals, grass and forest were characterized with root constants: 75 mm, 150 mm and 250 mm respectively (Shaw, 1994). Hence soil moisture budget has been made on a monthly basis for these classes of land use/land cover according to their root constants using monthly mean precipitation and mean monthly PET from the Thornthwaite formula. The AET values calculated for each land cover units (root constants) were weighted with the proportion of their aerial coverage to get mean AETvalues of the sub-basins from the SMD method (Table 14).

Table 14. AET values from SMB (mm).

Sub-basin	Jan	Feb	Mar	Apr	May	Jun	Jul	Aug	Sep	Oct	Nov	Dec	Annual
Guder	43	45	67	88	92	75	69	67	67	62	54	37	766
Muger	32	41	64	77	74	85	136	125	60	63	45	30	831
Jema	25	24	43	58	43	73	69	69	65	53	34	22	578
Upper Awash	23	31	54	76	75	91	80	78	79	59	34	20	700

Nearly similar results were obtained from Turc formula and SMD method to the sub-basins. Values from the Turc formula and SMD method were then averaged to get representative AET values for the sub-basins (Table15).

Table 15.Summary of annual AET from Turc formula and SMBmethod (mm).

Sub-basin	SMB method	Turc formula	Average
Guder	766	786	776
Muger	831	780	806
Jema	578	598	588
Upper Awash	700	792	746

4.2.3. Runoff

Estimating runoff (R_o) from precipitation measurement is very much dependent on the time scale being considered (Shaw, 1994). In this work, annual runoff for each sub-basin has been estimated. Due to absence of river discharge data in Guder, Muger and Jema sub-basins at their outlet or at the confluence with the Blue Nile River, the volume of runoff was determined by using runoff coefficients (ratio of runoff to precipitation).

Runoff coefficients that vary between 0.17 and 0.35 were used depending on the land use/land cover, nature of soil and slope(ODOT, 2005). Proportions of land use/land cover and soiltypes(Table 9)together with mean annual precipitation in the four sub-basins were used to calculate mean annual runoff.

Table 16.Runoff estimates (mm).

Sub-basin	Annual runoff
Guder	421
Muger	233
Jema	272
Upper Awash	274

4.2.4. Recharge

Precipitation is the principal source for replenishment of moisture in the soil water system to recharge groundwater.The amount of moisture that will eventually reach the water table is going to recharge aquifer system in sub-surface. The amount of recharge to the aquifer system depends upon the rate and duration of precipitation, topography, soil texture and moisture conditions, depth to the water table and underlying litho-structural setting (Shaw, 1994). Due to many factors involved in affecting recharge, its estimation is subject to large errors.

Water balance method

The basic concept of water balance method is: Input to the system - outflow from the system = change in storage of the system (over a given period of time). Not only water balance computation but also computation of water balance variables always involveserrors, due to shortcomings inherent to the techniques used. Net change in soil moisture storage assumed to be zero on annual bases for water balance calculation.

In the study area, the inflow components include recharge from precipitation and groundwater inflow from other sub-basins. The outflow components include AET, runoff, groundwater outflow to other sub-basins and groundwater withdrawal by pumping.Considering the above inflow and outflow components, the general groundwaterbalance equation to estimaterecharge in the area for a given time period is given as:

$$R = P+G_i-E_T-R_o- Go-W \text{ ………….. } (1)$$

Where:R is annual recharge (mm)

P is mean annual precipitation (mm)

$E_T$ismean annual actual evapotranspiration (mm)

$R_o$ismean annual runoff (mm)

G_i is groundwater inflow (mm)

G_o is groundwater outflow (mm)

W is annual withdrawal of groundwater from the aquifer by pumping (mm)

Groundwater is being consumed by sparsely distributed settlements, villages and small towns, withdrawal of groundwater for consumptive purpose by pumping is negligible for Guder, Muger, and Jema sub-basins. On the other hand, significant amount of groundwater has been pumped from the Upper Awash basin for domestic, industrial and agricultural purposes.

It is difficult to quantify groundwater abstraction from the aquifer systems of the area for different reasons. Individuals, organizations, community and even towns except AAWSA don’t have a record for groundwater abstraction. Due to this limitation, amount of annual extraction of water from the groundwater source has been estimated based on daily groundwater abstractioninformation from AAWSA and rough estimation made using the following assumption for other groundwater users.

- For dug wells fitted with hand pump discharge rate of 0.5 l/s for 8 hrs/d,
- For shallow wells fitted with hand pump discharge rate of 1 l/s for 8 hrs/d,
- For deep private wells used for households fitted with submersible pump, discharge rate of 1.5 l/s for 8 hrs/d,
- For deep private wells used for hotels, small farms and water consuming factories, fitted with submersible pump, discharge rate of 5 l/s for 8 hrs/d.

The above assumptions are based on communications and information from groundwater users in the area. In total, data from 551 wells were used to quantify daily and annual abstraction from the aquifer in the Upper Awash groundwater basin. Annually, about 64 Mm^3 water has been pumped out, which is equivalent to 9.5 mm/year.

Neglecting groundwater inflow and outflow, recharge to the sub-basins has been calculated from the hydrological variables using the following relation and the results are given in Table 17.

$$R = P - E_T - R_o - W \qquad (2)$$

Table 17.Hydrological variables and annual recharge to from the WBM (mm).

Sub-basin	P	AET	Ro	W	R
Guder	1424	776	421	Negligible	227
Muger	1201	806	233	Negligible	162
Jema	993	588	272	Negligible	133
Upper Awash	1112	746	274	9.4	82.6

The evidence based conceptual model from geological characterization confirms that significant portion of Muger sub-basin and some portion of Jema sub-basin contribute groundwater inflow to the Upper Awash groundwater basin. However, evidences from geological characterization show that surface watershed and groundwater basins match for the Guder sub-basin. Hence, groundwater outflow from and inflow to the sub-basin is negligible. Hence, recharge to the Guder sub-basin is equal to recharge to the Guder groundwater sub-basin.

Recharge to the Muger and Jema and the upper Awash sub-basins has been calculated from hydrological variables using equation 2 and the results are given in table 17. However; evidence based conceptual model from geological characterization confirms that recharge area of 1770km^2 and 304km^2 from Muger and Jema sub-basins respectively, are contributing groundwater flux to the Upper Awash groundwater basin.

Total volumetric recharge to the Muger and Jema groundwater sub-basins is therefore equal to the difference between total volumetric recharge into the respective sub-basins minus volumetric recharge in the contributing areas.This groundwater outflow from the Muger and Jema sub-basins has been calculated using the size of recharge areas of the two sub-basins contributing groundwater flux to the Upper Awash groundwater basin as a factor of the mean annual recharge in the respective sub-basins. Hence, annual recharge to the Muger and Jema groundwater sub-basins get smaller with the amount equal to the groundwater flux to the Upper Awash groundwater basin (Table 18).

Table 18.Annual inflow to the Upper Awash groundwater basin from WBM (mm).

Sub-basin	Recharge (mm)	Contributing area (km^2)	Total groundwater inflow to Upper Awash (Mm^3)
Muger	162	1770	286.7
Jema	133	304	40.3

Sub-basin	Recharge (mm)	Contributing area (km^2)	Total groundwater inflow to Upper Awash (Mm^3)
Total			327

Due to groundwater flux from the Muger and Jema sub-basins, the water balance equation for the Upper Awash groundwater basinhas a form:

$$R = (P - E_T - R_o - W) + G_i \text{ ………………… (3)}$$

Using the hydrologic variables estimated to the Upper Awash basin and, inflow from muger and Jema sub-basins, volumetric recharge to the Upper Awash groundwater basin has been calculated (Table 19).

Table 19.Hydrologic variables and annual recharge to the Upper Awash from WBM.

Sub-basin	P	AET	Ro	W	R (mm)	Area (km^2)	Total (Mm^3)
Upper Awash basin	1112	746	274	9.4	82.6	6760	558
Groundwater out flow from Muger and Jema sub-basins equal to inflow to the Upper Awash basin							327
Upper Awash groundwater basin							885

Chloride mass balance

The CMB method assumes that the flux of tracer (Cl^-) input at the surface equals the flux of tracer reaching the groundwater table. This conservative nature of chloride ion made it to be chemically retained in solutions (Hem, 1985). The technique regards chloride as an inert element, and compared with other inorganic ions, it is not added or removed by water rock interaction. The element is considered as an inert in the hydrological cycle having its source from the atmosphere. It has the advantage over tracers involving water molecules in a sense that atmospheric inputs are conserved during recharge processes allowing a mass balance approach to be used.

As described bySomaratne and Smettem(2014), the basic equation applicable for the estimation of recharge using chloride mass balance method is:

$$R = (P.Cl_p)/Cl_g$$

Where: R is the annual recharge (mm),

P is the mean annual precipitation (mm),

$Cl_p$is chloride concentrations of the precipitation (mg/ l),

$Cl_g$is chloride concentrations of the groundwater (mg/ l).

Since chloride concentration becomes higher as the groundwater vertically percolates and crosses clay layers and fault gauges due to retardation and concentration of chloride ions, valuesfrom deep wells were excluded. Only average concentration of chloride in groundwater from shallow wells has been considered. Chloride concentrations of the precipitation samples collected from the four sub-basins at the same time were used as representative of chloride concentrations of the precipitations of the sub-basins.

The estimated recharge values using the CMB method vary with the chloride content in the groundwater and precipitation. Taking the mean values of chloride content in the groundwater into consideration, average annualrecharge values to the sub-basins were estimated (Table 20).

Table 20.Annual recharge from CMBmethod (mm).

Sub-basin	P (mm)	Chloride concentration (mg/l)				Groundwater data points	Recharge
		In precipitation	In groundwater minimum	In groundwater Maximum	In groundwateraverage		
Guder	1424	0.94	3.60	7.57	5.4	5	247
Muger	1201	0.88	2.20	10.60	7.1	7	148
Jema	992	0.97	2.00	13.10	7.9	11	122
Upper Awash	1112	0.84	3.90	13.80	6.9	11	135

Base flow separation

Base flow has been used as an approximation of recharge with the acknowledgement that it is probably less than the amount recharging the groundwater system (Daniel, 1996).The base flow separation method attempts to separate and quantify part of the streamflow hydrograph attributed to groundwater discharge. Daily river discharge records ofover ten years from 34stations were used for the analysis.

The separation of surface runoff and base flow has been made using a computer code RAP (version 3.0.3) and time plot.Base flow results from the two computer codes become similar for the attenuation coefficient of 0.93 for RAP instead of default value 0.975. Daily river discharge data from more than 6 stations for each sub-basin were used for the analysis.

The weighted meanbase flows, representative of the sub-basins, were obtained from the base flows of the gauged streams weighted with their respective catchment areas.Estimated mean annual recharge from base flow separation over the Guder, Muger, Jema and the Upper Awash are 272mm, 158mm, 86mm,103mm, respectively. Base flow results obtained for different gauged streams in the four sub-basins are given in Table 20.Sample base flow separation graphs using RAP and time plot for Awash River at Melka Kunture station is also given (Figs. 13 and 14).

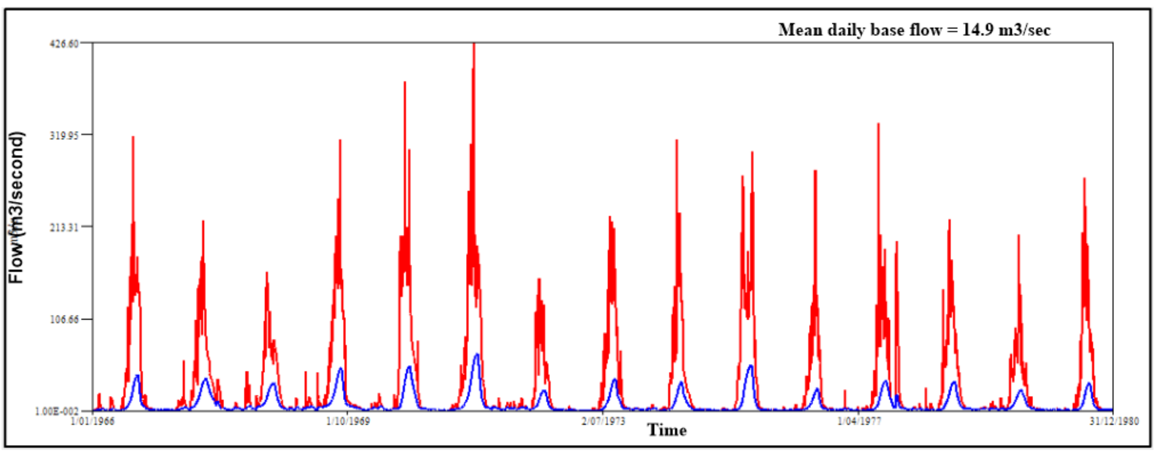

Figure 13.Hydrograph analysisfor Awash River at Melka Kunture using RAP.

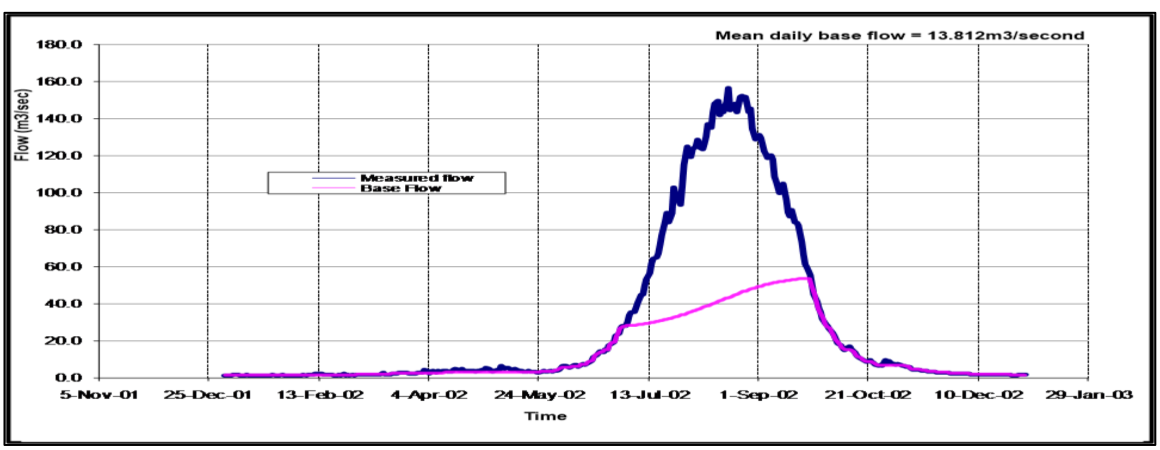

Figure 14.Hydrograph analysisfor Awash River at Melka Kunture using time plot.

Table 21. Mean annual base flow for gauged rivers.

Sub-basin	Station name	UTME	UTMN	Arrea (km2)	Base flow (Mm3)	Base flow (mm)	Weighted mean (mm)
Guder	Bello at Guder	353747	980000	350	60	354	69
	Fato at Guder	361000	979500	96	18	390	21
	Guder at Guder	363800	992600	741	120	347	143
	Indris at Guder	361000	984114	140	22	268	21
	Tiliku Duber at Duber	377408	1044706	387	12	68	15
	Tinishu Duber at Duber	377414	1052549	87	13	98	5
	Total			1801			272
Jema	Aleltu at Muketuri	494514	1066619	447	19	113	18
	Beresa at Debre Berhan	556683	1068505	135	15	209	10
	Chacha at Debre Berhan	543100	1062967	90	15	354	11
	Robi Gumero at Lemi	500000	1077674	887	25	70	22
	Robi Jida at Muketuri	500000	1066619	762	11	33	9
	Selji at Kabe	555922	1188261	30	2	138	1
	Shy at Mehal Meda	561920	1143160	68	9	239	6
	Wenchi at Alem Ketema	475798	1114110	286	13	57	6
	Wizer at Mehal Mda	561523	1132366	150	7	82	4
	Total			2855			86
Muger	Aleltu at Chancho	468623	1030200	29	2	152	4
	Deneba at Chancho	475658	1031853	86	8	203	16
	Gerbi at Sululta	464842	1012465	65	6	217	13
	Gorfo at Gorfo	480100	1039000	49	5	236	10
	Muger at Chancho	470347	1027938	480	38	107	46
	Roba at Chancho	472540	1022408	30	3	194	5
	Sibilu at Chancho	472538	1020197	375	29	191	64
	Total			1114			158
Upper Awash	Awash at Belo	435700	977126	2568	84	63	17
	Awash at Ginchi	406571	995976	76	7	116	1
	Awash at Melka Kuntre	457500	961621	4456	223	105	48
	Berga at Addis Alem	434087	1000552	248	18	142	4
	Big Akaki at Akaki	468808	967255	884	51	95	9
	Holota at Holota	445365	1006556	119	13	163	2
	Jemjem at Wolonkomi	415362	994851	148	14	194	3
	Kela at Wolonkomi	418660	994844	60	5	127	1

Sub-basin	Station name	UTME	UTMN	Arrea (km2)	Base flow (Mm3)	Base flow (mm)	Weighted mean (mm)
	Kesem at Beke	507332	1012975	50	3	150	1
	Little Akaki at bridge	471913	980522	131	5	114	2
	Mutinicha at Legadadi	490610	1000486	447	56	276	13
	Teji at Asgori	427000	971613	662	29	77	5
	Total			9849			103

Base flow relationship with geological structures

The boundary between surface runoff and base flow is difficult to define and strongly depends on the geological structure and nature of geologic materials. Permeable aquifers sustain high base flow contributions but impervious clays and built-up areas provide little or no base flow to a river (Shaw, 1994).

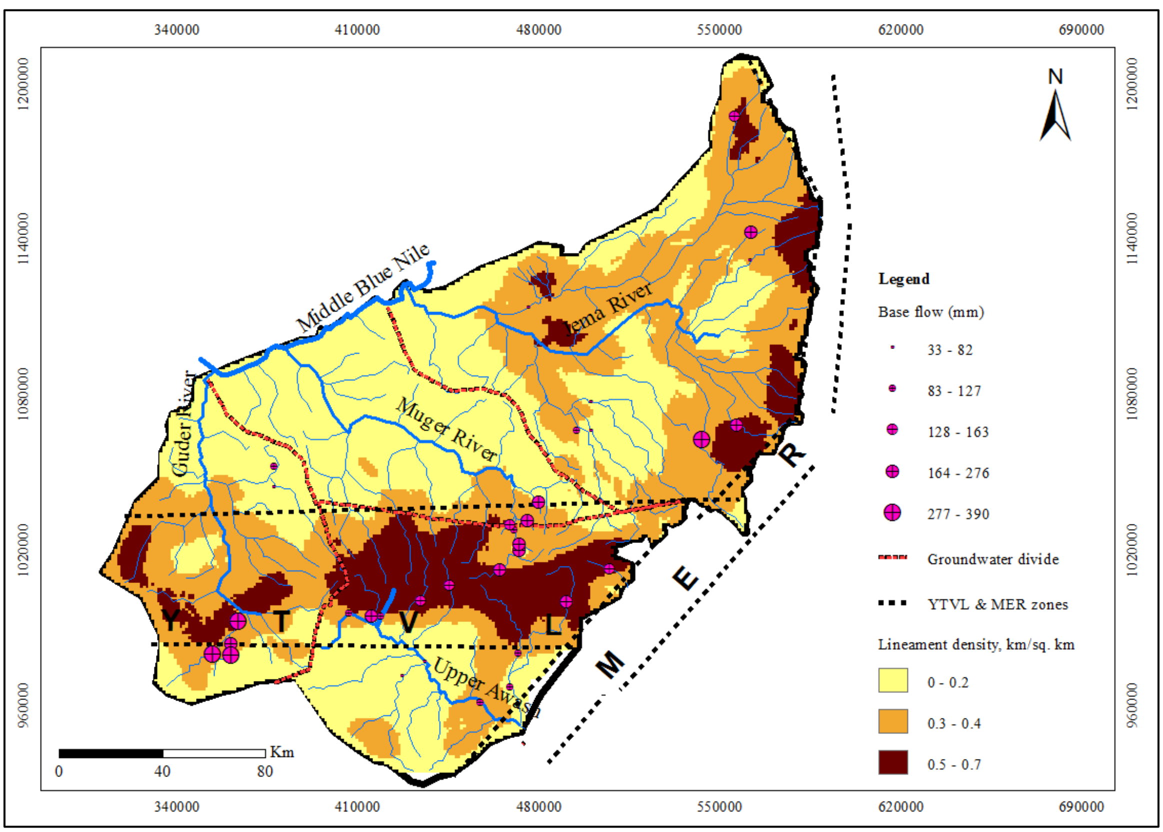

Figure 15.Relation of base flow with lineament density.

Base flows calculated for different catchments show wide range of values. Hence, the relationship between the amount of the base flow with the geologic material through which the dominant part of the river flows and lineament density were found to be important factors to look for.

The highest values of mean annual base flow have been observed for streams that flow through scoriaceous basalt unit along the highest lineament density zone. This zone is located along the water divide between the Blue Nile and the Upper Awash River basins and the rift margins. Likewise, streams that flow through the lower fine grained sandstone that outcrops along the highest lineament density zone also show very high base flow.

Moderate to high mean annual base flow is associated with moderate lineament density zone on the rift basalt and ignimbrite units. Streams dominantly draining the limestone (with marl intercalation), shale, ash, tuff and pyroclastic depositreceive very low base flow. Hence, recharge to the groundwater in these rock units is very low (Figs. 15, 16 and 17). Low base flow of the big and little Kaki Rivers could be associated to the built up physical features in Addis Ababa city.

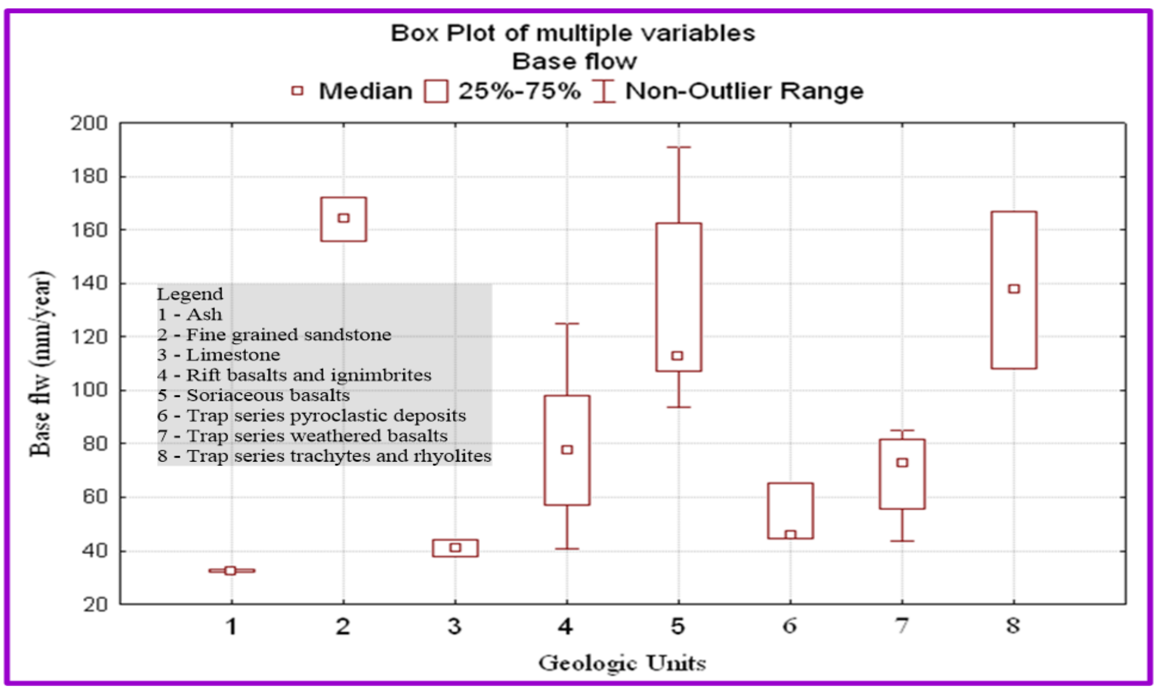

Figure 16.Relationship between amounts of base flow with different geologic units.

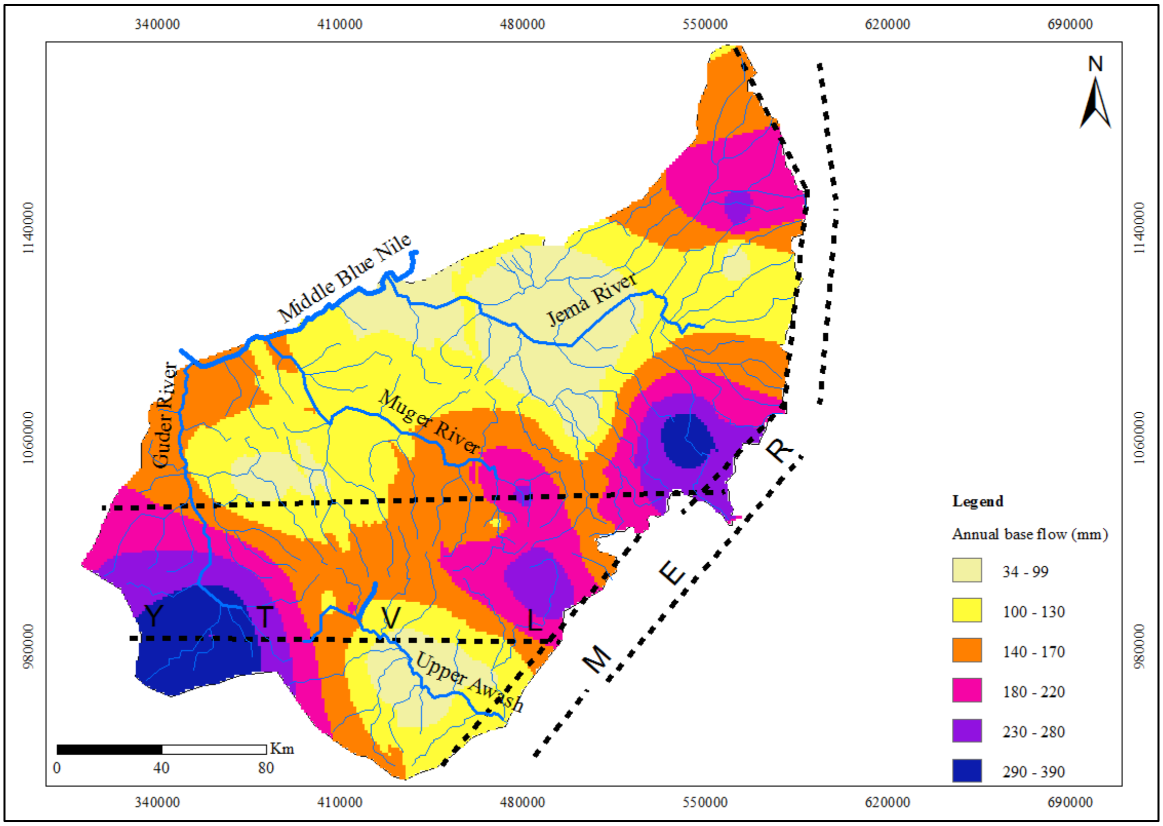

Figure 17.A raster map of base flow distribution.

Contrasts between recharge estimates from different methods

The three methods used to estimate recharge to the sub-basinsgave a wide range of values (Table 22). These methods produce estimates of recharge that reflect different spatial and temporal scales; have different data requirements, strengths, and limitations. In general, comparing the results may be difficult because of differences inherent in the methods.

The WBM is attractive because it can be applied almost anywhere meteorological data are available. A major drawback of the method is that recharge is estimated as the residual term in an equation where the other budget terms (P, AET, R and groundwater withdrawal) usually are estimated with considerable error, which can result in large errors in the recharge estimate. On top of that sparsely distributed data from 13 meteorological stations were used to calculate water balance variables and to estimate recharge to the sub-basins.The WBM method therefore gives a very rough estimation of rechargeas data from few stations were used for analysis to estimate representative values for very large areas.

Despite the fact that the CMB method is simple, there are a number of uncertainties associated with the method in estimating recharge. One of the uncertainties arises from using a onetime record of chloride concentration in precipitation as a representative. Another uncertainty source for the chloride mass balance approach is the sampling density of the groundwater.The biggest uncertainty is also associated with the analytical precision of the determination of chloride concentrationof precipitation and groundwater.The CMB method also gives a very rough estimation of recharge to the sub-basins.

River discharge data from gauged streams of varying catchment areas for streams flowing through different geologic units were used for the analysis of the base flow component. As the probability of a stream to drain different geologic units with varying hydraulic properties increases with increasing catchment area, leading toa noticeable differencein the estimate of mean annual base flow.However, when compared with the WBM and CMB, the BFS method is supported bysufficient data from 36 river gauge stations in the study area. Hence, recharge estimates from the BFS method are more reliable than the values from the other two as they were calculated from river discharge data representing small catchment areas, as well as nearly uniform geology and land uses/land cover features. Further hydrogeological characterization in this work considers recharge estimates from the BFS method.

Table 22.Summary of annual recharge estimates from different methods (mm)

Sub-basin	Recharge		
	WBM	CMB	BFS
Guder	227.0	247.0	272.0
Muger	125.0	148.0	158.0
Jema	130.0	122.0	86.0
Upper Awash	131.0	135.0	103.0

For Guder sub-basin, the three methods give nearly similar but very high values of recharge. The two available closely located meteorological stations used to calculate the mean have very high precipitation (Tables 3 and 4). Hence, the high value obtained from WB and CMB methods for the sub-basin is attributed to the exaggerated mean monthly and annual precipitation.River discharge records used in the sub-basin were obtained from streams draining the high lineament density zone, where the dominant geologic material is sandstone, basalt and scoriacious basalts along the YTVL zone. The high value obtained from the BFS method is therefore attributed to the high lineament density and more permeable rock units of the catchments the streams drain. The values obtained from the three methods, therefore over-estimate rechargefor the other part of the sub-basin further from the high lineament density zone.

For Muger sub-basin, the three methods give different values. Of all, the result from BFS method is the highest. River discharge records used in the sub-basin were obtained from streams draining the high lineament density zone, where the dominant geologic material is scoriacious basalts along the YTVL zone. The high value obtained from the BFS method is therefore attributed to the high lineament density and more permeable scoriaceous basalt rock units the streams drain. The value obtained from the BFS methods represent the sub-basin’s area closer to the YTVL zone but over-estimate recharge for the other part of the sub-basin further from the high lineament density zone.

For Jema and Upper Awash sub-basins, results from BFS method are generally low. The plausible explanation for these is that most of the river discharge records used for the Jema and the Upper Awash sub-basins were obtained from streams draining dominantly trap series pyroclastic deposit and rift ash rock units respectively both bearing low lineament density.Hence, the value obtained from the BFS method under-estimate recharge for the other part of the sub-basins where the geologic units are permeable and lineament density is high.

Chapter Five: Hydrogeology

5.1. Introduction

Aquifer properties and groundwater flow patterns have been characterized using hydraulic properties of rocks from geological studies and pumping test; chemical data, stable isotopes of water and radioactive isotopes.

Both primary and secondary porosities of rocks play significant role in groundwater occurrence, localization and flow, particularly in hard rock terrains(Todd, 1976). All aquifers contain some degree of heterogeneity and the fundamental characteristics of fractured rock aquifers are extreme spatial variability in hydraulic conductivity, and hence groundwater flow rate and pattern (Cook, 2003). Lthostratigraphic and structural framework of geologic units control aquifer hydrodynamic characteristics, aquifer productivity and boundary conditions (Singhal and Gupta, 1999).

In most cases, water table is a subdued replica of the land topography where groundwater divide matches with surface water divides. However, under certain circumstances, groundwater flows across surface water divides. The flow may continue through adjacent basins and to any intervening ranges, as long as the permeable rocks are continuous and sub-surface geometric architecture is favorable for groundwater movement (Fetter, 2001).

Starting fromthe precipitation source the chemical behaviour of groundwater would keep on changing with time. Major geochemical processes can be derived and hydrogeological system can also be conceptualizedfrom the changes groundwater underwent along flow paths in sub-surface (Hem, 1985).

In addition to conventional hydrogeological approaches, isotope hydrology was employed in the current study. As environmental isotopes are useful in tracing groundwater provenance evidences from stable isotopes of water (^{18}O and ^{2}H) are potential tools to complement groundwater flow characterization from water level, hydraulic properties of rocks and geochemical data. In addition, radioactive environmental isotopes (^{14}C and ^{3}H) are useful tools to estimate the groundwater age and groundwater circulation mechanisms. Evidences from radioisotope of radon (^{222}Rn) helps to systematically characterize the interactions between groundwater and surface water bodies (Clark and Fritz, 1997).

5.2. Aquifer Hydrodynamic Characteristics

Evaluation of the hydrodynamiccharacteristics of an arearequires understanding the hydraulic properties of rock units and their geometric set up and depth to the groundwater measurements.Depth to groundwater has been characterized from the groundwater level information from field measurements in boreholes and dug wells as well as available information from drilling results. Groundwater level contours were generated from depth to the groundwater measurements and groundwater flow patterns conceptualized. Finally groundwater flow boundaryas well as aquifer distribution into groundwater sub-basins has been conceptualized. Accordingly,geological units were further characterized for their hydraulic properties using information from pumping test data and spring discharges. Hydrogeologic units with varying hydraulic properties were then mapped.

5.2.1. Hydrodynamic data availability and quality

Data for hydrodynamic characterization have been generated from water point inventory in the field, from drilling companies, water works consulting organizations, and water supply organizations. The water point data includes dug wells, drilled wells and springs (Table 20).

Table 23.Hydrodynamic data.

No	Data type	Water points	Characteristics of water points	Remark
1	Dug wells	33	Depth range 5 – 20m SWL range 4 - 19m	Dug wells data were used only at places drilled wells are scarce
2	Boreholes	721	Depth range 20 – 602m SWL range 0 – 144.4m Transmissivity range 1.2 – 17,000 m2/d Discharge range 0.5– 140 l/s (pumping test) Artesian over flow up to 125 l/s Dry well up to 250m depth	Most of the drilled deep wells are found in the Upper Awash. They are few in Guder, Muger and Jema sub-basins.
3	Springs	280	Discharge range 0.5– 100 l/s	

No	Data type	Water points	Characteristics of water points	Remark
			Spring types – depression, contact, fault and thermal	

5.2.2. Hydrogeologic units

Regional extensive aquifers,aquicludes and barriers to the groundwater flow have been recognized from hydrogeological characterization.

5.2.2.1. Regional aquifers

Based on hydraulic characteristics of rock units, depth to the groundwater and mode of recharge and groundwater intake to their system, the following seven regional aquifer units were recognized (Fig. 18).

Lower fine grained Sandstone aquifer

This aquifer unit is constituted by sandstones which have low primary, as well as secondary porosity, except at places closer to the YTVL zone, where they are more fractured. In the Guder sub-basin, this unit forms a vast plain with gentle slope where it receives direct precipitation recharge through pore spaces, fractures and joint planes, and indirect recharge from runoff on the volcanic highlands. In the gorges of the Muger sub-basin and the steep gorges of the Blue Nile, this unit is overlain by impermeable shale. In the latter case, direct recharge from precipitation or groundwater inflow from the overlying units is negligible.

Transmissivity value of very few partially penetrating water wells into the unit ranges from13m^2/d to 56m^2/d (Fig. 18). Except along some regional faults and intersections of fault systems, discharge from few available springs emerging from the unit is very low. Depth to water in boreholes sunk into this unit varies from artesian condition to 52m. In general, a portion of this aquifer unit along the YTVL zone has good groundwater potential due to secondary porosity (Fig. 18).

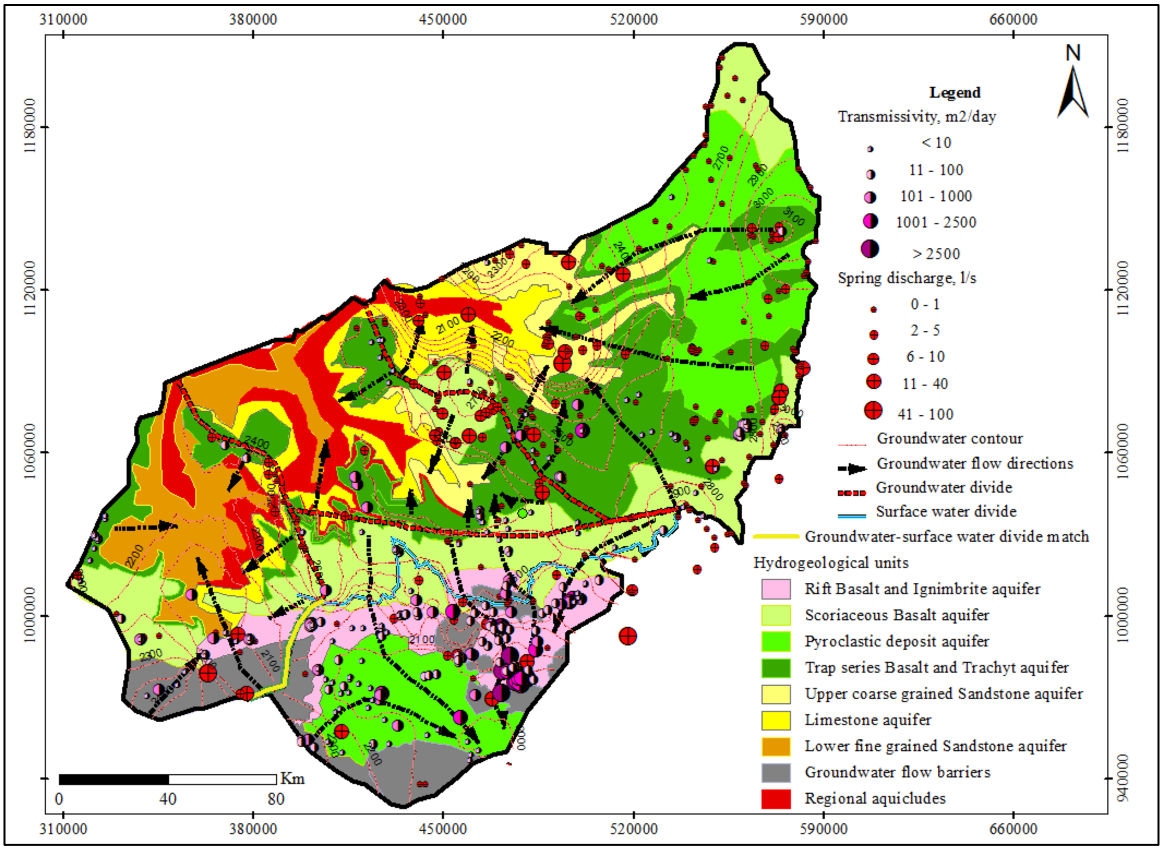

Figure 18.Hydrogeological map.

Limestone aquifer

The limestone aquifer is composed dominantly of jointed and fractured limestone intercalated with marl, with no signs of karstification. The thick intercalated marl, dominant in the lower levels of the unit, limits the hydraulic conductivity of this unit. Hence, only the upper part of the aquifer unit can receive recharge and store water provided that either it is exposed on the surface to direct recharge from precipitation, or the overlying unit is permeable to allow groundwater inflow. However, this unit forms cliffs and steep slopes in the gorges of the Blue Nile, limiting direct recharge from precipitation. In the northern part of the Jema sub-basin, this unit forms gentle slopes where it receives direct recharge from precipitation and recharge from flood water draining the surrounding volcanic highlands.

It also receives groundwater inflow from the overlying sandstone. On the other hand, in the Muger sub-basin, this unit is overlain by impermeable mudstone and associated palaeosol layers, which hinder groundwater transfer from the overlying volcanic rock aquifers. Moreover, away from the two major fault zones (MER and YTVL), lineament density on this unit is low leading to its low hydraulic conductivity. Transmissivity values range from 20 to 250 m^2/d. A few available springs have low discharge (0.5 to 10 l/s). The high transmmissivity value is obtained for a borehole located in the deep gorges of the Muger sub-basin along the NW-SErunning regional fault. Depth to groundwater in boreholes sunk into this aquifer unit varies from 10 to 41m.

Upper Coarse grained Sandstone aquifer

This aquifer unit is dominantly composed of cemented, coarse grained sand and layers of conglomerates, with thin lenses of mudstone and shale. The sandstones and conglomerates have high primary porosity. Where it outcrops on gentle slopes in the Jema sub-basin, this aquifer unit receives direct recharge from precipitation or from flood water drainingthe surrounding volcanic highlands. In the northern part of the Jema sub-basin, the moderate lineament density allows the unit to receive and store a good amount of groundwater. However, in the Muger sub-basin, the unit is overlain by impermeable mudstone, forms cliff wheredirect recharge to the aquifer systemis low.

Discharge from springs emerging from this unit is less than 1 l/s, though very high discharge springs ofup to 100 l/s have been observed from a spring emerging at intersections of regional faults. Depth to groundwater is shallow where the unit forms gentle slopes. Its hydraulic properties could not be quantified as pumping test data representative of the unit are not available. Similar to the underlying limestone aquifer, this unit shows slight dipping towards the south and SE. However, its general uplift during subsequent shield volcanism and disruption by NW-SE and E-W oriented regional faults complicated the geometry of the strata. The NW-SE oriented regional faults and associated fractures convey groundwater base flow to the Jema flow system as manifested by high discharge springs close to the Jema River bed.

Trap series Basalt and Trachyte aquifer

This unit comprises columnar basalts, weathered basalts, trachytes, ignimbrites and rhyolites. The aquifer unitoutcrops and forms flat to gentle topography and receive direct recharge from precipitation. However, in the Guder sub-basin, the unit is dominated by highly weathered basalt altered to clayand direct recharge from precipitation is low.

Part of this unit exposed adjacent to the MER and the YTVL zones has moderate to high lineament density and hence moderate hydraulic conductivity due to secondary porosity. Groundwater circulation is shallow along stream courses but relatively deep at ridges, and depth to the groundwater varies between 1m and 73m depending on the local geomorphologic setting. The locally varying aquifer lithology (basalt, trachyte, ignimbrite or rhyolite) as well as the frequency and degree of fracturing determine the aquifer productivity.

Transmissivity values rangewidely from 4 to 266 m^2/d due to strong variations in lineament density and geomorphic set up. Higher transmissivity is associated with the borehole sites located close to stream courses along high lineament density zone. A higher transmissivity value than observed is expected from this unit in the downthrown blocks within the rift and the Upper Awash basin due to reactivation of faults along theYTVL zone. Similarly spring discharges range from 0.5 to 20 l/s depending on the nature of emergence and associated tectonic structures. Springs that emerge along regional fault lines have high discharges but the depression springs emerging away from fault zones show low discharge.

Pyroclastic deposit aquifer

The pyroclastic deposit aquifer comprises the pyroclastic rocks within the Trap series volcanics from the plateau, and the volcanic ash and tuff deposits from the rift. Hydraulic conductivity of the unit is low, dominantly attributed to the low secondary porosity. The aquiferunit forms flatto gentle topography in the dominant part of the Upper Awash basin and northern part of the Jema sub-basin, where it receives direct recharge from precipitation but with very slow infiltration rate.

Transmissivityvalues arelow, in most cases less than 20 m^2/d. Spring discharges are also very low, usually less than 1 l/s. Generally, this aquifer unit is poorly productive.

Scoriaceous Basalt aquifer

The quifer unit is composed dominantly of scoria, scoriaceous basalt and boulders of basalt with very thin layers of trachytes, rhyolites, and palaeosols. This unit is characterized by high hydraulic conductivity attributed to its high primary porosity, and secondary porosity associated to the highest lineament density along the MER margin and the YTVL zone. Except at volcanic peaks, depth to groundwater is shallow, varying from a few meters to 96m.

Transmissivity values range from 3 to 60 m^2/day. Spring discharges are low except along the contact with the underlying Trap series volcanic rock units and at places where the unit is affected by regional faults. However, low transmissivity and low spring discharge may not represent the whole unit as the locations of the available wells and springs are in mountainous recharge areas.In most cases, the exposed part of this unit is a recharge area for the underlying aquifer systems or to the downthrown blocks of the same unit, in the Upper Awash basin.

Lithologic logs from deep wells on the downthrown block of this unit at the rift margin and close to the YTVL zone are used to verify the extent of this aquifer unit. Transmissivity values calculated from the pumping test data of these deep wells are very high, in most cases over 5000 m^2/d. The high transmissivity is attributed to the fact that the downthrown blocks are found in discharge area, receiving groundwater inflow via densely distributed lineaments along the rift margin and the YTVL zone.

Rift Basalt and Ignimbrite aquifer

The Rift Basalt and Ignimbrite aquifer unit is composed of vesicular basalts with high primary porosity and ignimbrites with lower primary porosity. Strongly fractured rocks forming flat to gentle topography, receive direct recharge from precipitation, or from flood water draining the mountains in the northeastern part of the Upper Awash basin.

The high lineament density along the MER and YTVL zones promotes fast recharge rate and increases the hydraulic conductivity of this unit. Groundwater circulation in this unit is generally shallow;depth to the groundwater varies between artesian flowing conditionsto 88m. Thermal groundwaters have also been struck by boreholes along some regional fault lines on this aquifer unit.

5.2.2.2. Regional aquicludes

The basement rocks,shale and mudstone constitute regional aquicludes in the area. Basement rock aquicludes are exposed in small portion of the gorges of the Blue Nile and Guder sub-basins at elevation below 1200m.a.s.l. Since shale rock unitis dominantly composed of thick shale, marl and gypsum intercalations, it forms regional aquiclude. Hydraulically, it separates the Lower fine-grainedSandstone and Limestone aquifer systems in Muger sub-basin and eastern part of the Guder sub-basin. It also serves confining unit for the underlying Lower finegrainedSandstone aquifer.Since mudstone rock unit is dominantly composed of thick mudstone and thin beds of sandstone intercalations, it forms regional aquiclude. Hydraulically, it separates the Limestone aquifer systems from the overlying volcanic rock aquifers

5.2.2.3. Groundwater flow barriers

Unless the trachyte and rhyolite domes are affected by fractures and faults, they form groundwater flow barriers.The N-S trending fault and associated fractures that affect the domes can transmit groundwater from the Blue Nile to the Upper Awash basin through the domes.

5.2.3.Groundwater movement

Shallow groundwater accessed through hand dug and shallow wells at higher elevations especially in mountainous areas represent localized flows and pass through some clay and palaeosol lenses. For this reason, water point information representing such localized flows in the volcanic units, and those from gorges within the Mesozoic sedimentary terrain were excluded from regional groundwater flow system characterization.In addition, water level measurements of a few flowing deep wells found in the Upper Awash basin were also excluded from analysis, since they are not sufficient to treat separately. Groundwater found in relatively flat topography and in lower elevations representing deeper zones of the aquifer forms part of the regional groundwater flow system. Information from such water points were used to characterize the regional groundwater flow.

Out of theboreholes and dug wells drilled into the volcanic aquifers 682 wells that havewater level measurement, have been used to produce groundwater contours and to characterize groundwater flow patterns. In addition, to characterize the hydraulic properties of the aquifers, 439boreholes data with transmissivity and 280 springs with discharge information were used (Fig. 18).

Groundwater flow directions were identified from the pattern of the water level contour map of the aquifers. Narrow contour spacing corresponding to high hydraulic gradients indicates rapid change in elevations of water level compared with those of wider spacing indicating presence of localized aquifers within the regional aquifer domain.

In the Guder and Jema sub-basins, groundwater flows following the general surface topography and finally converges into the respective river flow directions, where regional faults convey groundwater to low relief areas and rivers. In the Muger sub-basin, some irregularities in the flow-path pattern were observed where groundwater partly flows northward following the general surface topography and finally converges into the Muger River flow system; however, in the southern part, the groundwater flows southward together with the Upper Awash groundwater flow system and finally converges to the Upper Awash flow and the aquifer system in the rift (Fig. 19).

Moreover, local geomorphic setup and subsurface configuration of permeable and impermeable rock units control depth and pattern of groundwater circulation in the area. The E-W oriented horst of the impermeable mudstone underlying the Tertiary volcanics control aquifer distribution into Muger and Upper Awash groundwater sub-basins where surface water and groundwater divides do not coincide (Fig. 19).

The NW-SE horsts and local geomorphic setup of the areas are responsible for aquifer distribution among the Guder, Muger and Jema groundwater sub-basins. Based on geological and geophysical findings as well asgroundwater flow patterns observed, conceptual groundwater flow model has been developed for the volcanic aquifer of the Upper Awash groundwater basin (Fig. 20).

As evidences from lithologic logs of flowing boreholes in artesian condition in the area confirm, locally and/or regionally confined aquifers are available in the areas where intercalations of impermeable beds (clay, ash, weathered tuff and massive volcanic rocks) present. Degree of confinement depends on the thickness and the lateral extent of the confining beds.

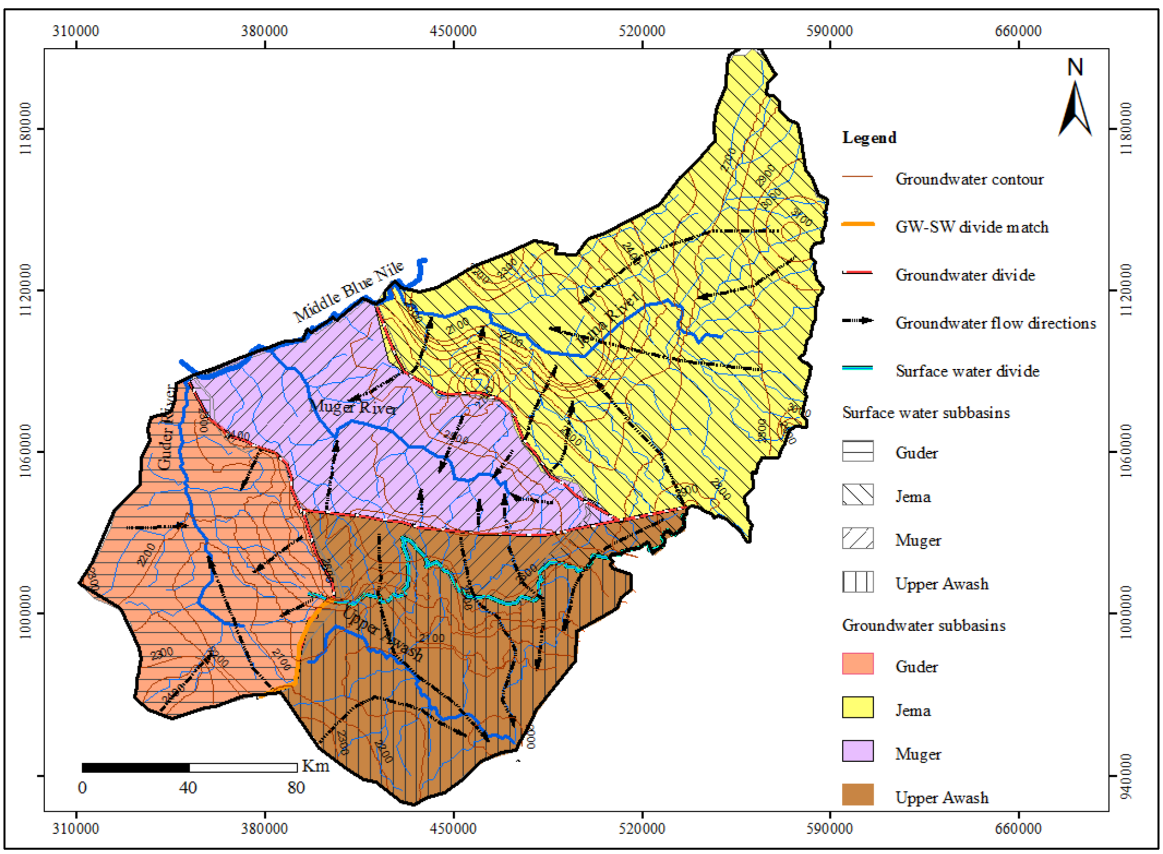

Figure 19.Relative distribution of surface water and groundwater basins.

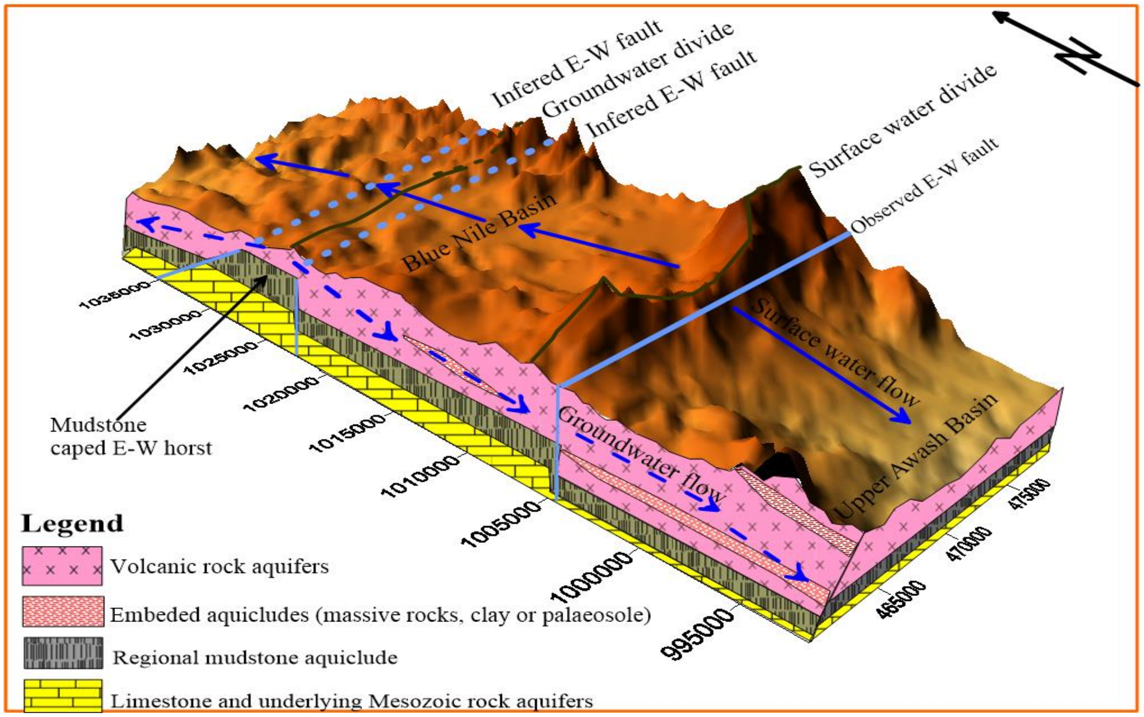

Figure 20.Conceptual groundwater flow model of the Upper Awash Groundwater basin.

5.3. Hydrogeochemistry

Due to the complex litho-structural set up of the area, hydrogeological characterization from analysis of hydraulic properties of aquifer material from pumping test and water level measurement are not sufficient to characterize flow dynamics. Therefore, chemical data have been used to provide more reliable information about the groundwater flow system.

Groundwater chemistry varies between rains to sea water chemistry (Appelo and Postma, 1993). There are several factors that control groundwater chemistry. The major ones include: mineralogy of the geologic units, structural set up, geomorphology, residence time, anthropogenic factors and interaction with surface water bodies (Freeze and Cherry, 1979). There are also several processes which are responsible for the changes that groundwater undergoes along the flow path. From the precipitation source, the chemical behaviour of groundwater would keep on changing with time. It is this change that help characterize groundwater dynamics in the aquifer system.

This section deals with the changes water undergoes along the flow paths, major geochemical processes, the factors that are responsible for the changes, and their implication on the hydrodynamic characteristics of aquifer systems.

5.3.1. Data availability and methods of analysis

Water samples were collected for chemical analysis during water point inventory. In addition, available chemical data have been collected from drilling companies and previous studies (Andarge Yitbarek, 2009). The following parameters were analyzed in the laboratory: TDS, EC, pH, $NH4^{+}$, Na^{+}, K^{+}, Ca^{+2}, Mg^{+2}, total Fe, Cl^{-}, F^{-}, NO_2^{-}, NO_3^{-}, CO_3^{-2}, HCO_3^{-}, SO_4^{-2}, PO_4^{-4}, total hardness and alkalinity. The following methods were used: titration method for Ca^{+2}, Mg^{+2}, Alkalinity, hardness, CO_3^{-2}, HCO_3^{-} and Cl^{-}; Flame bottom method for Na^{+} and K^{+}; gravimetric method for TDS; direct measurement for EC and pH; sulfamer method for SO_4^{-2}; Phosphobar method for PO_4^{-4}; Ferrobar method for total Fe; Standness method for F^{-}; Cadmium reduction method for NO_3^{-} and Deionization method for NO_2^{-} (NEERI, 2014).

According to the principle of electro neutrality, the sum of cations in meq/l should nearly be equal to the sum of anions in meq/l for the chemical data to be reliable for further geochemical characterization and interpretation (Freeze and Cherry, 1979). Therefore after charge balance calculation, chemical data with charge balance error not exceeding 5% were considered for the geochemical characterization. Out of the total, 328 chemical data with error percentage less than 5% were used (appendix 3). In addition to the electro neutrality test, error distribution has been evaluated using error distribution graph (Fig. 21).

The units of concentration used in the text unless specified differently are mg/l. The EC values are given in μS/cm and residual alkalinity values are given in meq/l. Different ratios mentioned in the text were calculated using meq/l unit.

The major challenge in hydrochemical characterization is uneven distribution of chemical data. Sufficient data from shallow and deep groundwater sources is available for the

Upper Awash. However, chemical data for the Guder, Muger and Jema sub-basins are sparsely distributed especially from the deep sources.

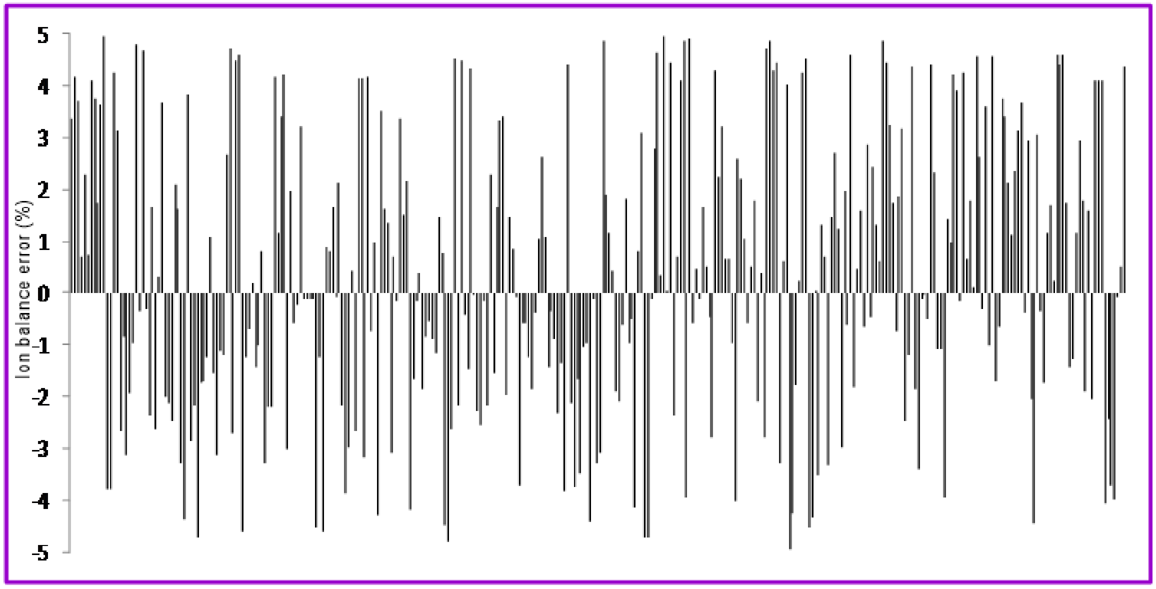

Figure 21.Ionic balance error distribution in the hydrochemicaldata.

5.3.2. Geochemical evidences for aquifer hydrodynamic condition

Ca^{+2}, Mg^{+2}, Na^{+} and K^{+} are the major cation constituents and HCO_3^{-} dominates the negatively charged species. The anion species, F^{-}, Cl^{-}, NO_3^{-} and SO_4^{-2} are not uncommon. TDS value ranges between 38 mg/l to 3220 mg/l. Cold to thermal waters with pH range between 6.27 and 8.68 are available. To seek geochemical evidences to interpret hydrodynamic condition in the area, variations in salinity, relations of ion ratio with TDS, groundwater type distribution, residual alkalinity, and chloride and fluoride distributions in the area have been evaluated.

Salinity

TDS in water is an important parameter to characterize the changes groundwater undergoes along the flow path. TDS value in the area ranges between 38 mg/l for cold water depression springs to 3220 mg/l for thermal deep wells along fault zones. The high TDS values, over 1000 mg/l are related either to thermal wells and springs along fault zones, very deep wells in discharge areas, and wells penetrated into and springs emerging from sedimentary strata (Fig. 22). Very high TDS waters are from the deep wells in the upstream part of Guder and the Upper Awash. Most of them are located along regional fault zones and surface water divides. A high discharge spring emerging from limestone along regional fault line also shows high TDS value.

The spatial distribution of TDS shows that the deep aquifers in the upstream part of Guder, Upper Awash close to the water divide with Blue Nile and downstream part of Jema are highly evolved waters with significant rock-water interaction, long sub-surface path length and residence time.

Presence of such highly evolved groundwater along the water divide between the Blue Nile basin (Guder and Muger sub-basins) and the Upper Awash basin marks clear incident of interbasin groundwater transfer along the water divide. However, the source of recharge (recharge area) for evolved groundwater in the southern upstream part of the Guder sub-basin surrounding Ambo town could be a subject of further study (Fig. 22).

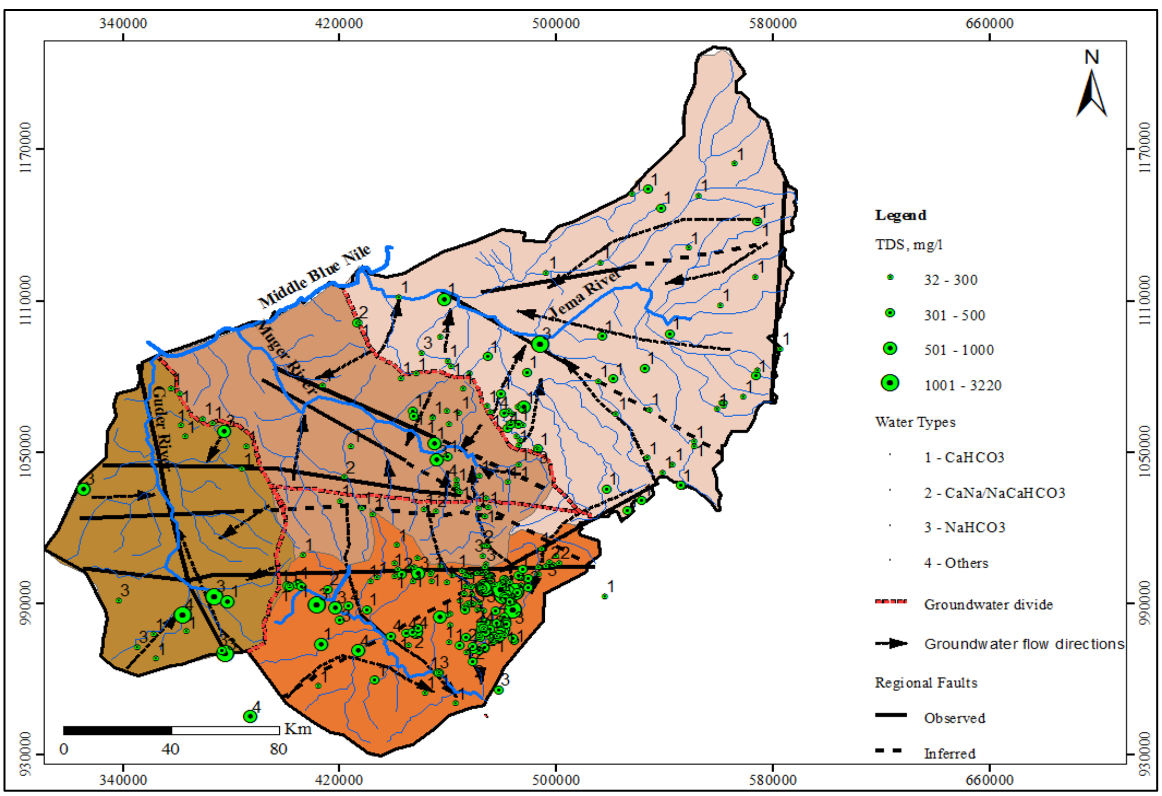

Figure 22.Groundwater types and TDS distribution.

__Ionic ratios__

Instead of characterizing individual ionic species, molar ratio of dissolved ionic species and their relationship with TDS helps trace the origin of solutes as well as the environment and major processes that generate the observed composition of groundwater (Hem, 1985). Accordingly, relationships of (Na^{+}+K^{+}),(Ca^{+2}+Mg^{+2})and (Na^{+}+K^{+})/(Ca^{+2}+Mg^{+2}) with TDS were used to characterize the sub-surface environment and the processes that cause observed changes in groundwater composition.

In general, along the groundwater flow paths, the concentration of the alkaline metals, Na^{+} and K^{+} increase with increasing TDS (Fig. 23a). On the contrary, the concentration of alkaline earth metals (Ca^{+2} and Mg^{+2}) gradually increases during early stage of geochemical evolution due to dissolution reactions from silicate weathering in volcanic aquifers and dissolution of calcite in sedimentary terrain but start to decline during later stage of geochemical evolution due to precipitation of calcite from solution when the groundwater becomes calcite saturated with saturation index greater than 1 (Fig. 23b).The (Ca^{+2}+Mg^{+2})/(Na+$^{+}K^{+}$) ratio is generally low for low TDS waters (Fig. 23c). However, some low TDS waters from sedimentary aquifers show slightly higher value of the ratio due to the dominant calcite and dolomite minerals constituting the rocks.

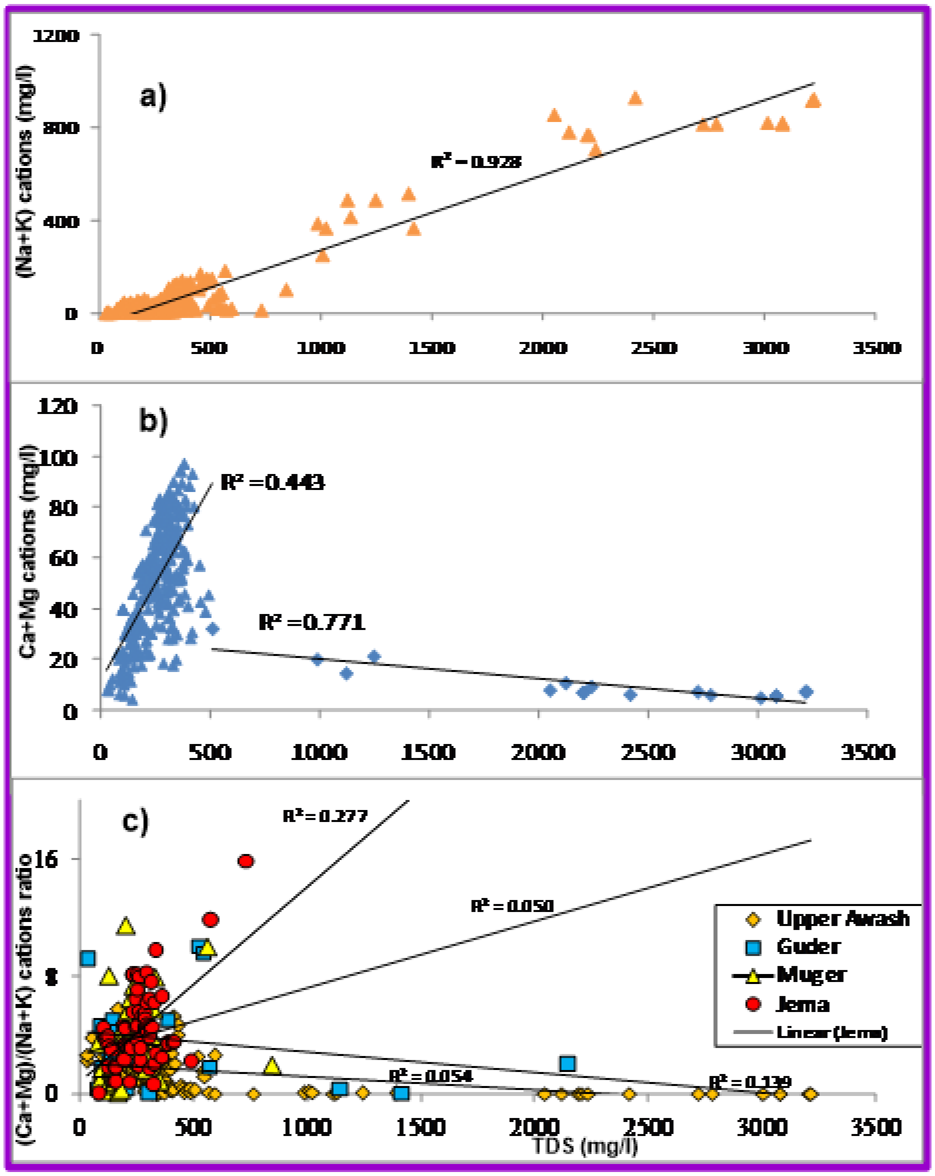

Figure 23. TDS versus $Na^{+}+K^{+}$(a), $Ca^{+2}+Mg^{+2}$(b) and $(Ca^{+2}+Mg^{+2})/(Na^{+}+K^{+})$(c).

Despite the fact that the correlation coefficient is poor, the variations in the trends of the $(Ca^{+2}+Mg^{+2})/(Na+^{+}K^{+})$ ratio versus TDS gives some geochemical evidences for aquifer hydrodynamic conditions in the area. Together with low TDS, increasing trend of $(Ca^{+2}+Mg^{+2})/(Na+^{+}K^{+})$ ratio in Jema and Muger sub-basins shows that all the waters in volcanic aquifers are at early stage of geochemical evolution with no sign of calcite precipitation where saturation index for calcite is less than 1. This in turn reveals that dominant portion of the two sub-basins constitutes recharge area for aquifer systems in their surroundings. However, for waters from Guder and the Upper Awash aquifer systems, the ratio generally decreases with increasing TDS, especially for thermal waters and for those from very deep sources. This signifies the fact that these waters are at their later stage of geochemical evolution where calcite starts to precipitate (Fig. 23c).

The high (Ca^{+2}+Mg^{+2})/(Na+$^{+}K^{+}$) ratio corresponding to the high TDS were obtained from deep and thermal wells located in the Upper Awash close to the water divide with Blue Nile and in the southern part of the Guder sub-basin. From this observation, recharge area for highly evolved groundwater in the southern deep aquifers of the upstream part of the Guder sub-basin and the Upper Awash is beyond the surface water divides. This suggests recharge area for highly evolved groundwater in the southern upstream part of the Guder sub-basin groundwater surrounding Ambo town may not be limited to the southern surrounding highlands within the sub-basin. Highly evolved groundwater found along the water divide between the Blue Nile to the Upper Awash basins substantiates interbasin groundwater transfer from the former to the latter.

Groundwater types

The piper plot of the chemical data helps to identify different water types (Fig. 24). Four major groups of water types ($CaHCO_{3,}$mixed $CaNaHCO_3$and $NaCaHCO_3$, $NaHCO_3$ and others) were identified in the area. The classification of the waters into group of groundwater types is based on major and minor cations and anions in the water samples. From the spatial distribution of groundwater types in the area, hydrogeological system characterization has been made and dominant hydrochemical processes were also defined (Fig. 24).

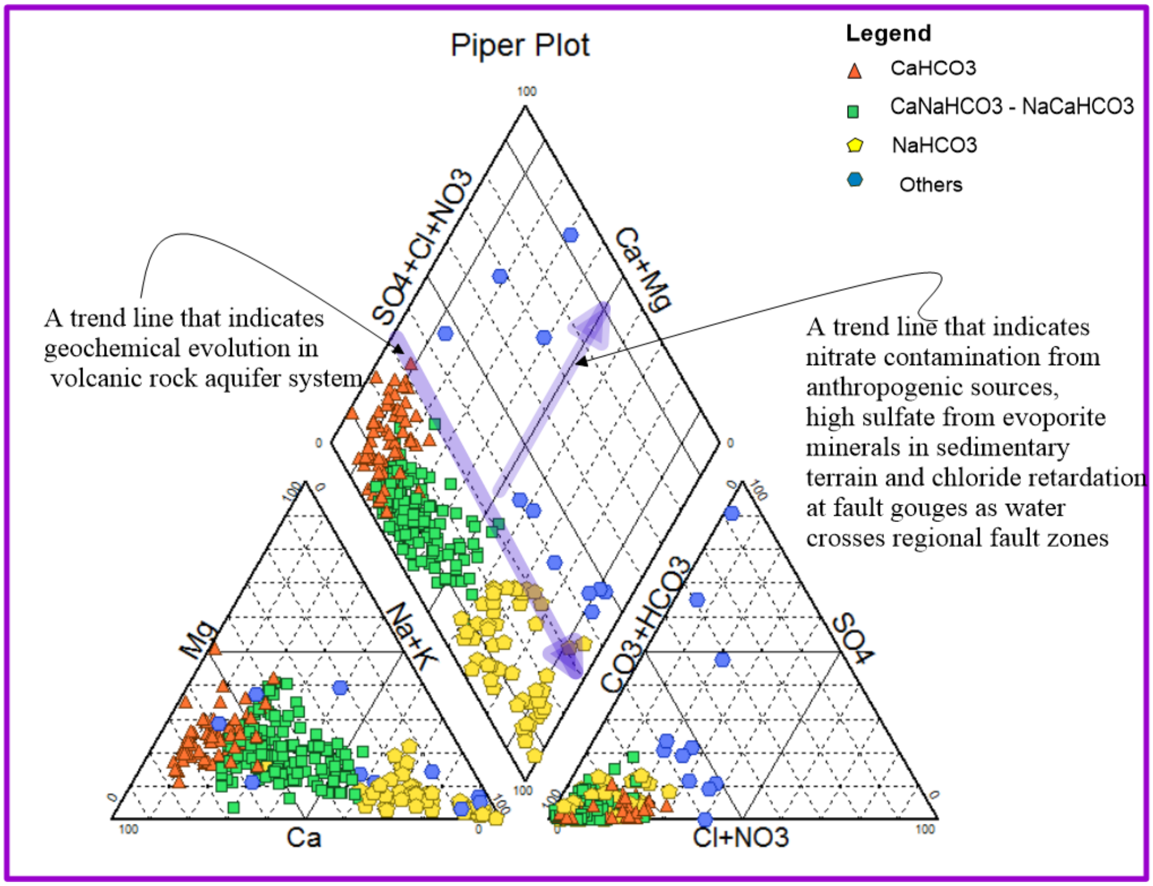

Figure 24.Piper plot applied to all water samples of the study area

The $CaHCO_3$water type that includes $CaHCO_3$, $CaMgHCO_3$ and $MgCaHCO_3$are observed in all the sub basins for water samples obtained dominantly from depression springs, dug wells and shallow drilled wells in parts of the study area. This groundwater type is characterized by very low TDS, often less than 500 mg/l, hence they represent early stage of geochemical evolution in recharge area and shallow depths of rapid circulation, relatively low residence time in sub surface, without significant water–rock interactions, corroborating similar observations earlier (Seifu Kebede et al., 2005, 2007). There are a few water samples from deep wells, which belong to this group. This could be possibly explained by mixing effect, where the sampled portion of the water is dominated by local recharges in the vicinity of the well. High TDS values were observed for waters of this type from limestone and sandstone aquifers. This is attributed to the higher solubility of minerals that constitute limestone. Mineralogy of the aquifer material is responsible for the distinction that can be made between $CaHCO_3$ and $CaMgHCO_3$ signature in this water type. The later is common in olivine rich rift basalt aquifers.

The second group of water type is mixed $CaNaHCO_3$ and $NaCaHCO_3$. This group represents groundwater circulating in intermediate zones (depth and travel distance from recharge areas). Water samples in this group were obtained from wells ranging in depth from 50 to 549m and springs emerging along fault lines. The waters in this group have TDS values ranging from 89 to 848 mg/l. For low TDS samples from some deep wells belonging to this group, the possible explanation is that the sample is dominated by local recharge; however, the high TDS values observed in this groupare attributed to groundwater from limestone (soluble). The water type in this group represents intermediate stage of geochemical evolution, with considerable travel distance from recharge area and/or at a relatively deeper part of the aquifer or mixing effect of local recharge with regional flow system. This in turn signifies that the groundwater belonging to this group is in the intermediate zone between the recharge and discharge areas.

The third water type group in the area is $NaHCO_3$. Water samples in this group were obtained from wells ranging in depth from 50 to 600m, cold and thermal fault springs. The group includes wide range of TDS values (107 – 3220 mg/l). Cation exchange at clay layer interfaces as water percolates to deeper zones could be a plausible explanation for few water samples from deep wells with low TDS belonging to this group from Muger and Jema sub-basins volcanic aquifer. Thus cation exchange is responsible for low TDS waters to attain $NaHCO_3$ water type in aquifers with clay intercalation and the particular sites of sampling belonging tothe group is recharge area. Waters with moderate TDS (500 - 1300mg/l)were obtained from limestone and sandstone aquifers in the northern part of the Muger sub basin and central part of Jema sub-basin. This shows higher level of geochemical evolution and particular sites of sampling are discharge zones for deep circulating waters.The high TDS waters from this group are thermal waters circulating along YTVL zone and south of it in the Upper Awash and in the Guder sub-basins. Silicate dissolutions are responsible for the high TDS, and the particular site of sampling is discharge area for regionally circulating waters. The presence of the high TDS

$NaHCO_3$ water types along the water divide between the Blue Nile and the Upper Awash again substantiates the interbasin groundwater flow from the former to the later.

The fourth group includes waters of mixed composition with high values of anion species (NO_3^-, Cl^-, SO_4^{-2}). Groundwater with a higher proportion of $NO_3^-$is possibly from anthropogenic sources like animal waste and fertilizer use in the area.The high concentration of NO_3^-ions together with low TDS and low pH in groundwater is indicative of the unconfined nature of the aquifer system and this also suggests that the groundwater is very young and the particular site of sampling is recharge area for the shallow aquifer system, observation similar with that of Seifu Kebede et al. (2005). The in this work include only few water samples from dug wells and unprotected springs in Jema sub-basin with high NO_3^-concentration over 50 mg/l.

There may be few cases where water samples from shallow unprotected wells show high Cl^-ion concentration from surface contamination. However, the remaining groundwaters with a higher proportion of Cl^- ion concentration are found in water samples from deep wells, thermal wells and springs. In volcanic rock aquifers, higher concentrations of Cl^- ion were observed along regional fault zones. In addition to acidic rocks like obsidian, and evaporates from sedimentary rocks, the high Cl^- ion contribution is attributed to waters circulating through deep seated sedimentary rocks or stagnation and retardation of the ion due to its large ionic size atfault gauges along regional faults.

Waters rich in $SO_4^{-2,}$ observed from limestone and fine-grained sandstone units in Jema, Muger and Guder sub-basins, resulted from dissolution of intercalated gypsum layers. However, high SO_4^{-2} observed in volcanic aquifers of the Upper Awash along fault zones close to the water divide with the Blue Nile are indicative of deep seated limestone and sandstone units with gypsum intercalation. The high SO_4^{-2}could also be due to water flowing through gypsum containing units as indicated in few geological logs of boreholes from the YTVL zone.

Though, petrographic analysis has not been done, silicate dissolution contributes the high concentration of Ca^{+2}, Mg^{+2}, Na^{+2} cation species and HCO_3^- from anion species in the volcanic terrain. Similarly dissolution of carbonate minerals contributes for the high SO_4^{-2} concentration in sedimentary terrain. Dissolution of silicate minerals of the olivine group (forsterite), plagioclase (anorthite), pyroxene group (enstatite) and other ferromagnesian minerals in volcanic terrains, and calcite dissolution in limestone and sandstone units were previously reported (Bretzler et al., 2012; Seifu Kebede et al., 2005).

The high TDS and $NaHCO_3$water typesfrom the deep wells located along surface water divide between the Blue Nile and the Upper Awash basins suggests interbasin groundwater flow from the former to the later. The higher proportion of Cl^- and SO_4^{-2} along the water divide between the mentionedbasinsalso corroborates the idea of interbasin groundwater transfer. Unlike the Upper Awash and Guder, absence of waters at highest stage of geochemical evolution even at deeper zones in the volcanic aquifers of Muger and Jema sub-basins also suggests the volcanic aquifer in the Blue Nile basin located adjacent to the Upper Awash are recharge areas (see Fig. 22).

Residual Alkalinity

Alkalinity can be defined as the capacity of a solution to neutralize acids (Hem, 1985). Residual alkalinity (RA), the difference between concentration of $HCO_3^-$and the sum of concentration of Ca^{+2} and Mg^{+2}, all in meq/l is used for understanding the changes affecting the chemical composition of the groundwater along the flow path. Together with TDS, it helps to identify recharge area from discharge area and inflow of meteoric water from precipitation along the groundwater flow paths.

Regardless of depth, waters from volcanic aquifers of Jema and Muger sub-basins and shallow groundwater from Guder and the Upper Awash are characterized by negative RA. Negative RA distributed all over the area indicates presence of active recharge. Some deep wells with negative RA values indicate interconnection of deep aquifers with shallow groundwater through fractures at high lineament density zone. For the waters leaching volcanic rocks of the rift in discharge zone, positive value of RA were obtained (Tesfaye Cherinet et al.,2001).Likewise, for the deep wells under artesian condition in the Upper Awash and southern part of Guder, RA is positive and increases with increasing

TDS (Fig. 25a,b). High discharge fault spring emerging from limestone aquifer also belongs to this group. The positive RA for deep wells, most of them in artesian condition signifies that mixing from meteoric water to the deep aquifers is negligible.

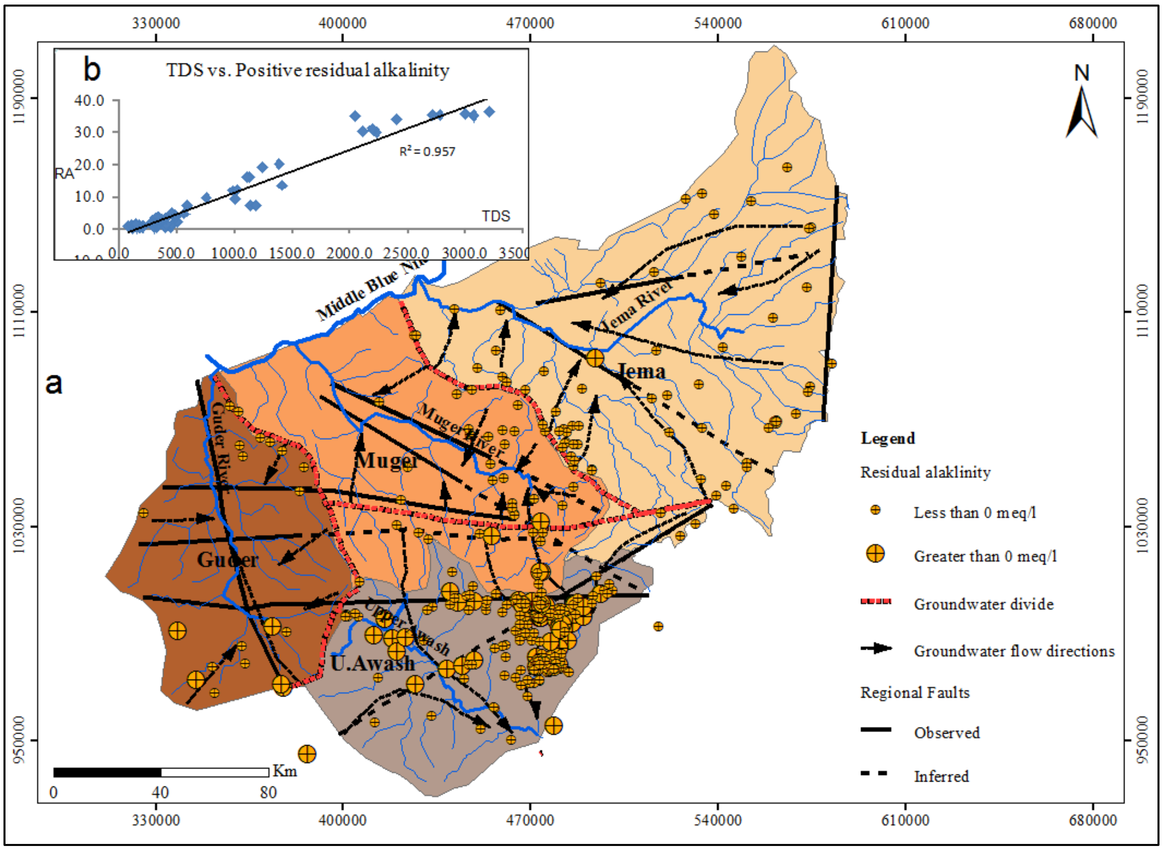

Figure 25. Residual Alkalinity (a) TDS versus positive residual alkalinity (b)

The high RA values from deep sources along the water divide between the Blue Nile, mainly Muger sub-basin and the Upper Awash basin substantiate the interbasin groundwater transfer which is in agreement with Seifu Kebede et al. (2007). The high residual alkalinity together with high TDS observed at a high discharge fault spring emerging along regional fault from limestone in Jema River gorge showspresence of regional aquifer discharging into this zone (Jemo River gorge). A high RA value together with high TDS along the water divide between the Upper Awash and the Blue Nile provespart of the Upper Awash along the divide and south of is a discharge zone for the regional deep aquifers

Fluoride and chloride distribution

Acidic rocks (obsidian, ash, tuff) exacerbated by heat anomaly generated along regional faults or from recent hot eruption centres favour high fluoride incorporation into the groundwater (Hem, 1994). Recent acidic volcanic centres in the area especially along the MER margin and the YTVL zones are responsible for the higher concentration of fluoride (Birhanu Gizaw, 2002). Recent studies categorize, the MER and adjacent highlands into 3 fluoride concentration zones: zones with low fluoride (<1.5 mg/l); intermediate fluoride zone along rift escarpment (1.55 – 5 mg/l); and high fluoride zone, along rift axis and rift floor calderas (> 5 mg/l)(MoWIE, 2013).

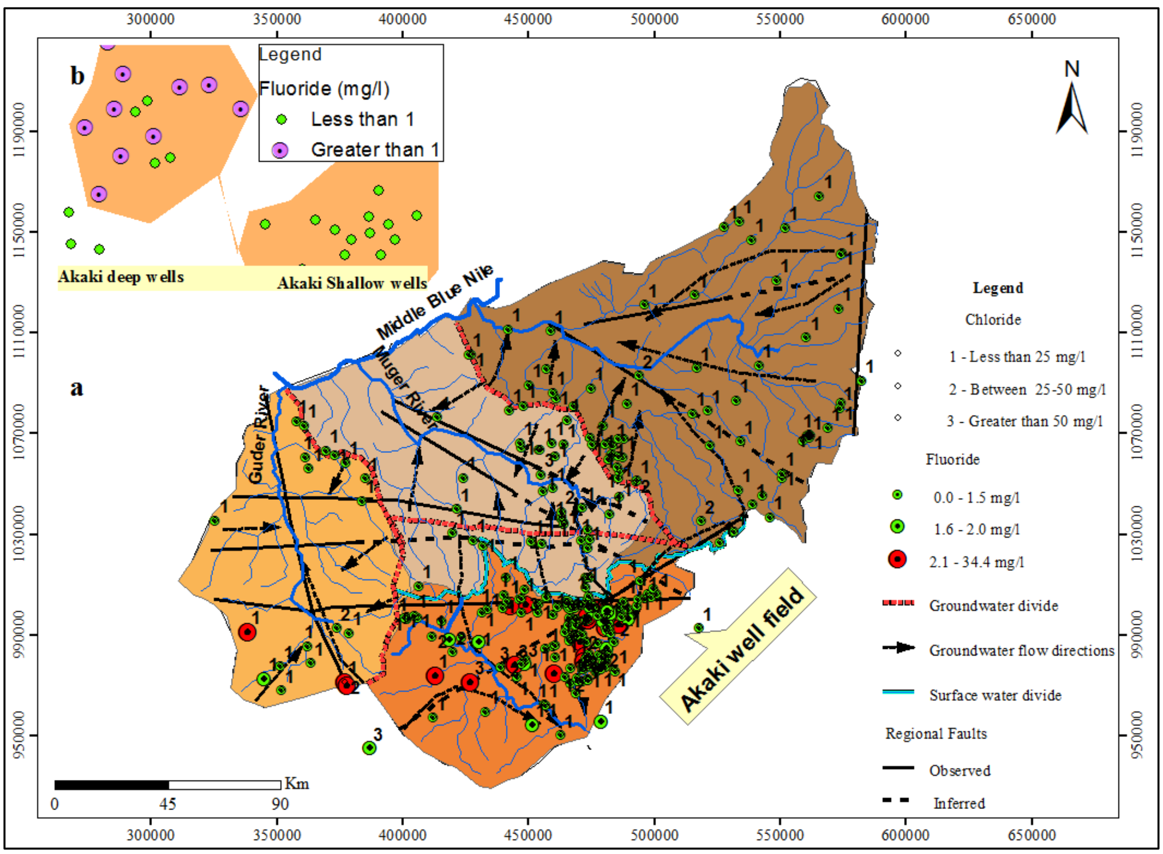

Figure 26.Chloride and fluoride ionsa) andfluoride in shallow and deep wells(b)

In this work, it has been verified that at rift margins in the Upper Awash, high fluoride concentration is associated with some regional fault systems provided that the fault systems favour deeper groundwater to emerge as thermal springs or the deep zone of the aquifer is penetrated by drilling along these fault zones.Fluoride concentrations are generally low in trap series volcanic rock aquifers (Fig 26a). Moreover, it is low in rift volcanic rock aquifers, provided that their locations are far from the regional faults and acidic volcanic centres and depth of penetration is shallow.

For deep wells located away from regional fault zones and acidic eruption centres in the Upper Awash basin, fluoride concentration is slightly higher than the concentration in shallow wells in the same area. The plausible justification for relatively high fluoride concentration in the deep wells of the Upper Awash is mixing effect of fluoride reach groundwater that crosses fault zones and acidic centres along the YTVL as the evidence is seen in the comparison made between shallow and deep wells in the southern part of Addis Ababa in Akaki Well field (Fig. 26b).As the case in the Upper Awash from Akaki well field, rift ward flowing groundwater from plateau may intensify the fluoride concentration in the aquifer systems of the rift and rift margins if the flowing groundwater encounters acidic rocks with heat anomaly along the flow path.

However, fluoride concentration or depletion scenarios could be complex and depending on the groundwater flow paths. During plateau-rift transfer of groundwater heat anomaly together with acidic rock media, are responsible for fluoride concentration changes in aquifers of the rift margins like the aquifers in the study area.

Volcanic rocks generally yield little concentration of chloride to normally circulating groundwater. However, sedimentary rocks like evaporates are more important sources (Hem, 1985). Few groundwater samples from the sandstone and limestone aquifers show relatively higher Cl^-concentration due to intercalated evaporates. In the volcanic rock aquifers, higher concentrations of Cl^-were observed alongregional fault zones. Deep seated sedimentary rocks or stagnation and retardation of the large size Cl^-ion while the groundwater is crossing clay gauges along regional faults could be possible explanation (Fig. 26a).

5.3.3. Water quality

Chemical quality of water from precipitation is altered before infiltration through evaporation if it stays for some time on surface water bodies, in vadose zone during infiltration and percolation and during movement as groundwater along flow path from recharge area to discharge areas, via several geochemical processes(Appelo and Postma, 1999). In addition, human activities, problems associated to well construction and well site locations have strong bearing on natural groundwater quality deterioration. Water quality problem in the study area is related to the high values of F^-, TDS, $NO3^-$, $SO4^{-2}$, and sodium hazards.

The average nitrate concentration in some of the well waters exceeding the WHO guideline was observed in Addis Ababa regions and surrounding highlands.In the study area, higher concentration of nitrate in the water samples as a result of contamination from agricultural runoff, refuse dump, human and animal waste(20.5mg/l)exceeding the threshold valuehas been reported (Andualem et al.,2014). The highly fractured bare rocks in Addis Ababa areaand its surrounding permit fast circulation of the pollutants over large distances and to a great depth. The widespread uncontrolled waste disposals promote pollution of groundwater resources as observed from the high level of nitrate and other contaminants in the shallow aquifers of Addis Ababa and its surrounding(Tamiru, 2001, Tamiru et al., 2005). NO_3^-concentrationis high in recharge areas where nitrogen fertilizers are commonly used. Some poorly constructed wells and wells fed by contaminated water bodies in urbanized areas such as Addis Ababa also suffer from NO_3^- contamination.

High TDS, F^-, $SO4^{-2}$ and sodium hazard are common problems of thermal waters from the deep sources as observed from wells located along regional faults. In addition, very high SO_4^{-2} concentrations up to 1383 mg/l were observed for water samples collected from aquifers insedimentary terrain.

5.4. Isotope Hydrology

Often, hydrogeological and hydrochemical studies are not sufficient to shed light on the groundwater hydrodynamics of complex volcano-sedimentary terrain. Since environmental isotopes can produce a more reliable conceptual model of a groundwater flow system and a useful tracer for groundwater recharge, stable and radioactive isotopes have been used to bridge information gapform other methods.

5.4.1. Water sample collection and analysis methods

Water samples were collected and analyzed for stable isotopes of water ($\delta^{18}O$ and δD)and ^{14}C. In total, analyses for 206 water samples for stable isotopes and 12 samples for ^{14}C have been conducted. In situ measurement was conducted for ^{222}Rn at10 different reaches of Awash River and its tributary streams. Samples for $\delta^{18}O$,and δDwere collected from all parts of the study area. However,sampling for $^{14}C$and ^{222}Rn measurement sites were restricted to the area surrounding of the water divide line between the Middle Blue Nile and the Upper Awash basins and the E-W mudstone caped horst structure identified from geological and geophysical studies(Fig. 27).

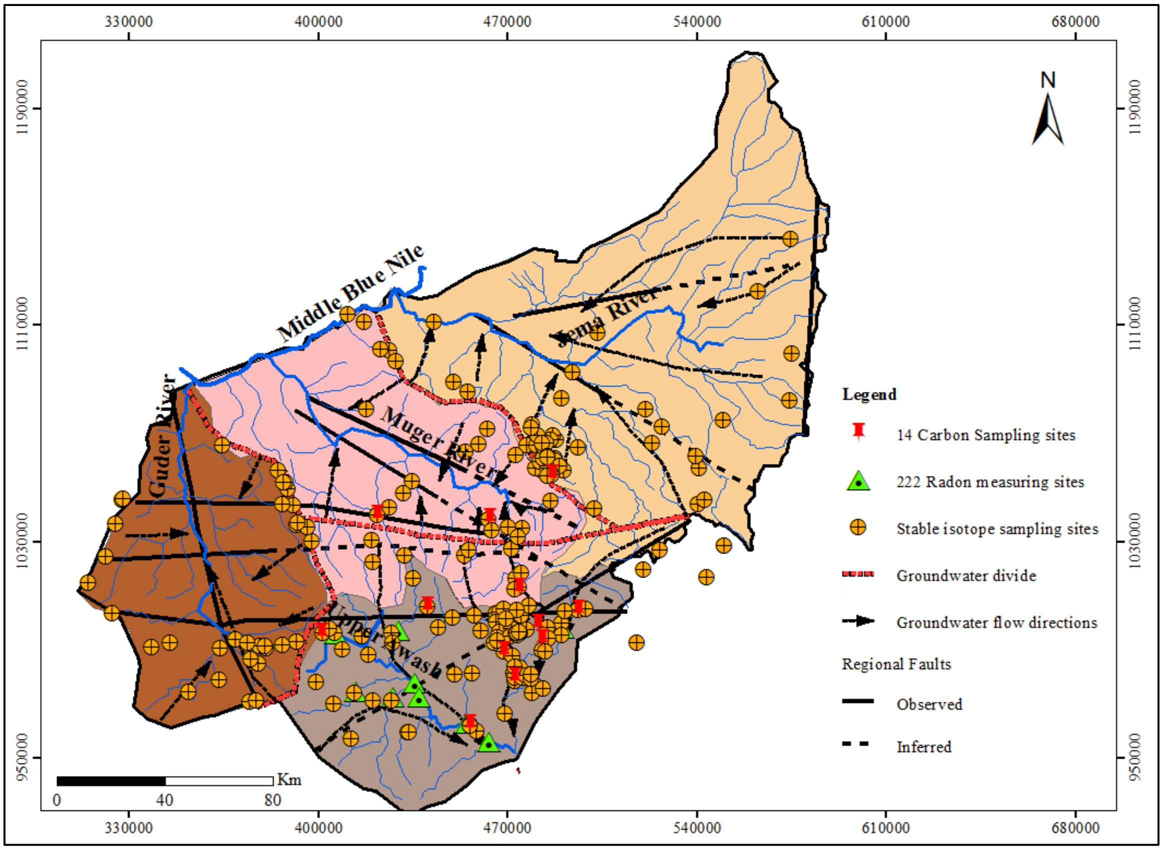

Figure 27. Sampling sites for isotope study

The following sampling, preparation and laboratory analysis methods were used for stable and radio isotopes (Clark and Fritz, 1997):

- After taking measurements of EC and pH in the field, samples of 1 liter volume were collected for $\delta^{18}O$ and δD analyses. Laboratory measurement for $\delta^{18}O$ and δDwere conducted by using an equipment called LOS Gatos Research DLT-100 leaser instrument configured with auto sampler together with standards at 5 sample interval, keeping one of the standards an intermediate isotope composition to the other two standards.

- After measuring EC, pH and titration for alkalinity, samples of volume between 50 and 60 liters were collected for ^{14}C analysis. The pH levels of the water sample were adjusted to 11 using NaOH salt, $BaCl_2$ salt of 100 to 115 gm has been added and the sampleswere shacked and left for a day for inorganic carbon to precipitate.

The precipitated inorganic dissolved carbon in the form of $BaCO_3$ was then kept in a plastic container of 1 liter size and sealed in order to avoid contamination with atmospheric CO_2. These samples were sent to the laboratory D'Avignon, France. The ^{14}C of the extracted DIC was measured using benzene analysis and liquid scintillation counting method with +0.1pmc and $\delta^{13}C$ were determined using mass spectrometry with uncertainty of +0.1%o.

- Counting for ^{222}Rn is straightforward, and a relatively simple counting device called Rad7 has been used to measure the radon activities in the field at some selected reaches of Awash River and its tributary streams. In total, radon activities were counted at 10 systematically selected points along the flow paths of the Awash River and its tributary streams. Each measurement was carried out for one hour including four cycles of 15 minutes duration. Three measurement points are located in Rift basalt and ignimbrite units where Awash River and its tributary streams emerge; four measurement points are located in the rift ash and tuff unit, two measurement sites are located at downstream part of the Awash River where the geologic unit is dominantly basalt and ignimbrite.

5.4.2. Stable isotopes of oxygen and hydrogen

Most cold groundwater resources are of meteoric origin (meteoric groundwater). There is a strong relationship between the $\delta^{18}O$ and δD values of precipitation reflected in the Meteoric Water Line (IAEA, 2000). The slope is 8 and deuterium excess is 10. In areas where the relative humidity immediately above the ocean is or was below the present mean value, d is greater than +10‰. The value of d is primarily a function of the mean relative humidity of the atmosphere above the ocean water. The coefficient d in groundwater study can therefore be regarded as an indicator of climatic condition during recharge. The higher d-excess is related to significant evaporation of local surface waters under low humidity, and the vapour mass mixes with atmospheric reservoirs and re-condenses (Clark and Fritz, 1997).

The monthly rains of Addis Ababa at IAEA station plot, gives a local meteoric line (LMWL) defined by: $\delta D = 7.2\ \delta^{18}O + 11.9$ with weighted mean summer precipitation for $\delta^{18}O$ and δD composition of -1.56 and +1.48, respectively and spring precipitations of +0.47 and +17.36, respectively(Seifu Kebede et al., 2012). The $\delta^{18}O$ and δD values of various water groups from the area (surface waters, shallow and deep groundwaters) were plotted against the GMWL and the LMWL adapted from Seifu Kebede et al. (2012).

Different ranges of values were observed for the water groups categorized into surface waters, shallow groundwater, and deep groundwater. Based on the observed value ranges, fractionation processes attributed to evaporation of meteoric water before recharge are highlighted and the effects of mixing from different sources within the hydrologic systemare also addressed.

Surface waters

Major theme of sampling surface waters for isotopic study is to characterize interaction between surface water and groundwater of the area.Precipitation on the Ethiopian highlands is generally a result of the clouds from oceans, which arrive after several rainout effects (Seifu Kebede et al., 2012). Evaporation from surface water causes enrichment in δD and $\delta^{18}O$ and the trend line of surface waters plots with slope less than slop of LMWL (Fig. 28).

In reference to summer rain of Addis Ababa at IAEA station, surface water bodies are enriched in both $\delta^{18}O$ and δD due to evaporative process. This is evident in the figure above for samples taken from surface water bodies, rivers and a lake. In this area, evaporation plays a significant role in modifying the isotopic signature of residual surface waters which are enriched both in $\delta^{18}O$ and δD. The evaporation effect which results in an enrichment of the heavy isotopes in the liquid phase with respect to the vapor phase allows to identify the admixture of superficial water like dam, lake and river waters to groundwater and to identify groundwater that has previously been subjected to evaporation before recharge.

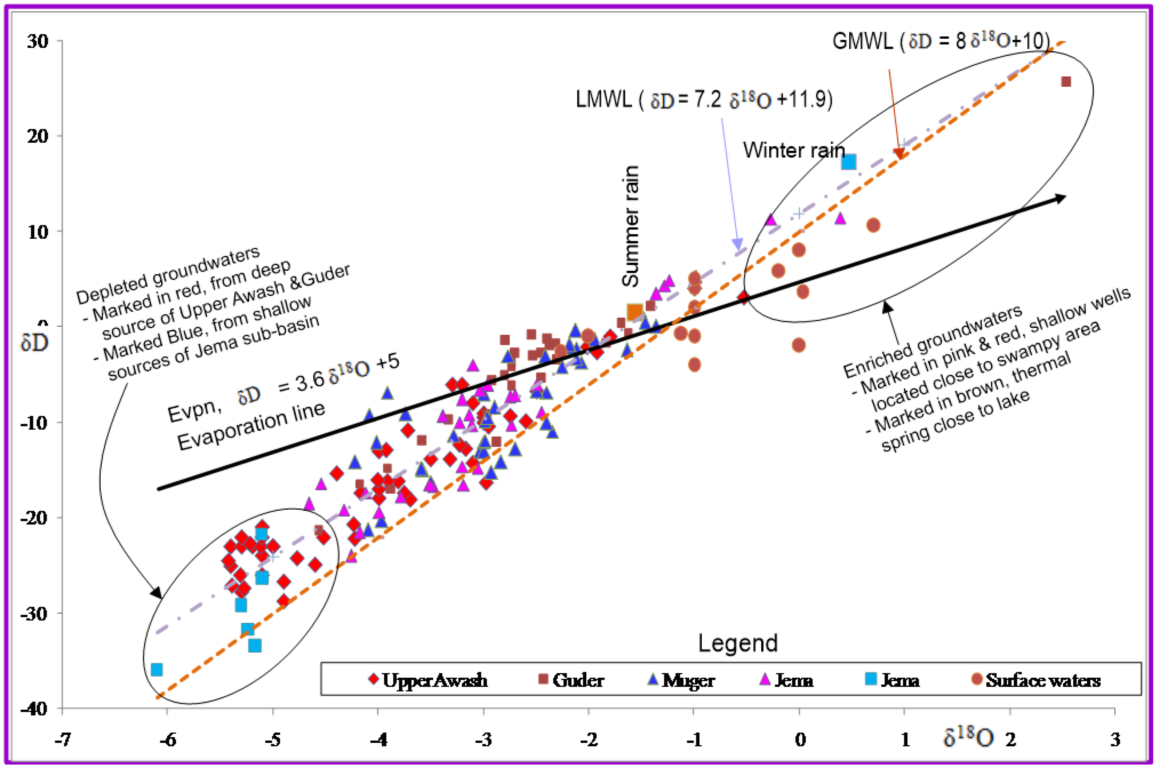

Figure 28.Distribution of stable isotopes of water.

Few samples collected from groundwaters that have some link with surface water bodies systematically diverge from GMWL/ LMWL and their slopes assume evaporation line.Thus, the isotopic signatures of few shallow groundwaters located close to rivers and thermal spring located very close to Lake Wonchi in Guder sub-basinshow deviation from the LMWL and fall nearly along the evaporative line. Signature from shallow groundwater suggests possibility of groundwater and surface water inter-connection where depth to the groundwater is shallow. The Wonchi thermal spring signature suggests possibility of deep groundwater and surface water inter-connection along regional faults.

Shallow groundwaters

The isotopic signatures of shallow groundwaters from Muger,Jema and the highland part of the Upper Awash and Guder range from -6.1 to +0.39 and -35.9 to +11.41, respectively for $\delta^{18}O$ and δD. Generally, the average values of $\delta^{18}O$ and δD are nearly similar with the average values of summer rainof the IAEA station at Addis Ababa, observation similar with Seifu Kebede et al. (2007). On the other hand, winter rains show little resemblance with the groundwaters (Fig. 29). Hence the aquifer system in the area gets recharge dominantly from summer rain. The range in $\delta^{18}O$and its resemblance with summer rain for shallow groundwaters suggests connection of shallow groundwater to local recharge from present day (modern) precipitations.

In addition to evaporative effect associated to surface water connected aquifers, wide range of values in $\delta^{18}O$ and δD are explained by amount effect for some highly depleted waters from shallow aquifer in Jema sub-basin (Figs. 28 and29). This is attributed to fractionation due to amount effect associated to intense rain fall events in the area where monthly mean precipitation sometimes exceeds 500mm at Fiche and DebreBirhan meteorological stations.

Generally, the isotopic signature of water samples from shallow aquifer system in all parts of the research area suggests the aquifer systems are connected to local recharge from modern precipitations.

Deep groundwaters

Non evaporated or slightly evaporated meteoric waters are generally recognized by their proximity to the meteoric water line whereas waters directly altered by evaporation or mixed with water enriched through evaporation, plot to the right of it (IAEA, 2000).

Results of the study also show that deep groundwaters from Guder and Upper Awash basin are characterized by lighter isotopic signature (depleted). The $\delta^{18}O$ and δD values generally range from -5.28 to -2.87 and -31.71 to -9.0, respectively. Almost all samples plot to the left of the GMWL and highly depleted compared to the summer rain of Addis Ababa IAEA station (Figs. 28 and 29). This suggest that the deep aquifer in the Upper Awash have some signature of records of a cold time recharge with low evaporative effect or it indicates recharge that might have occurred during wetter periods than the current period and/or that the precipitation altitude was higher which is in agreement with the observation of Seifu Kebede, 2007; Molla Demlie et al., 2008; Rango et al., 2008 and Bretzler et al., 2011.

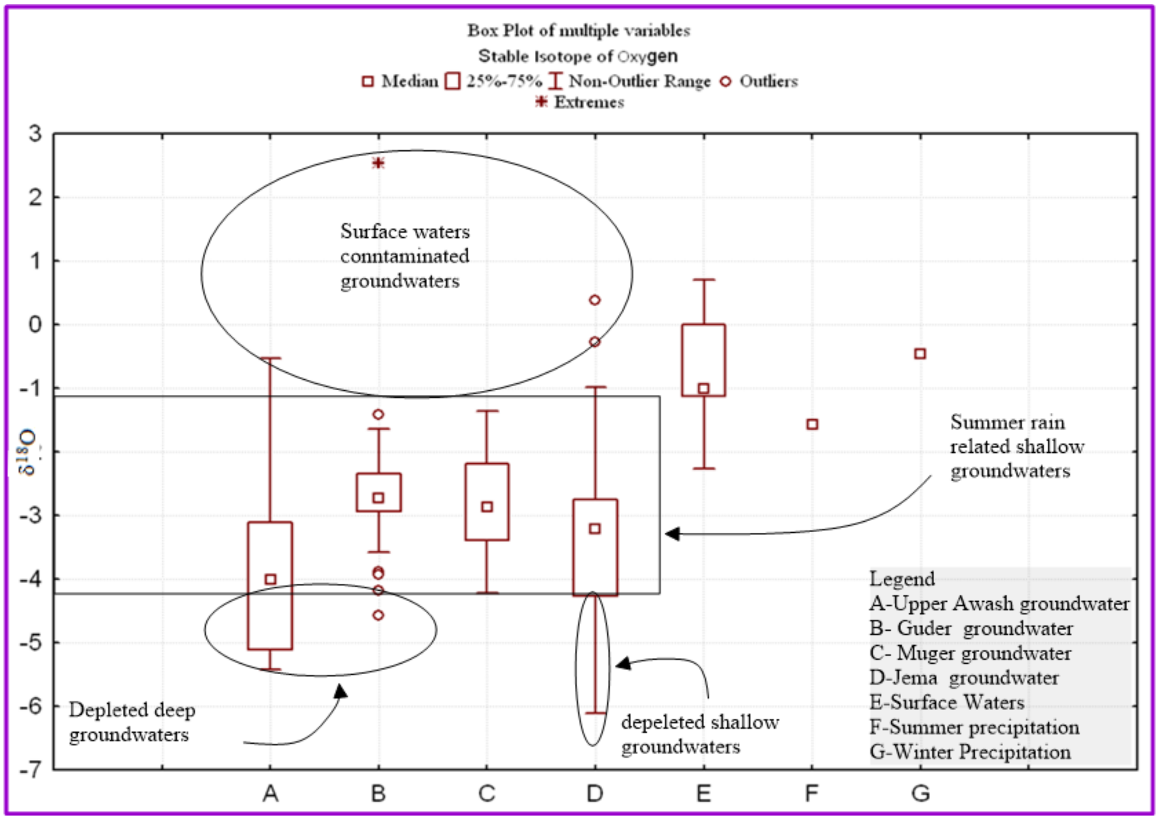

Figure 29. Variation in $\delta^{18}O$ in the sub-basins

Highly depleted waters from deep wells from the Upper Awash and Guder sub-basins including thoselocated very close to and along the water divide between the Blue Nile and the Upper Awash basin supports the conceptual model developed from other methods(evidence for interbasin groundwater transfer). In summary, recharge for the deeper part of the aquifers in the upper Awash is dominated by sources either relatively far or at a higher altitude in cold climate and not limited to the basin alone.

5.4.3. Radio isotopes

Determining groundwater residence times is critical to the understanding of hydrogeological systems and to characterize groundwater and surface water interactions.

Radioactive isotopes such as $^{14}C$and ^{3}H are produced by the interaction of atmospheric gases with cosmic radiation and are commonly used to determine groundwater residence times while ^{222}Rn is used to evaluate interaction between surface water and groundwater (Clark and Fritz, 1997; IAEA, 2000). In this work, to meet the objectives, the radiogenic isotopes:, ^{14}C, $^{222}Rn$and ^{3}H with half-lives 12.3 years, 5730 years, 3.8 days respectively have been used.

Radiocarbon

Groundwater ages are difficult to define because water flowing into a well may not travel with pure piston flow; rather, it is a mixture of waters, recharged at different locations and times. Hence, groundwater age can be considered a mean residence time in sub-surface. Because of its capacity to date old groundwater, up to 30,000years and due to its presence in dissolved inorganic carbon (DIC) in groundwater, ^{14}C is the most widely used radiogenic dating tool in regional aquifers (Clark and Fritz, 1997). The activity of ^{14}C is a measure of the abundance of ^{14}C relative to total carbon, and the reduction (decay) in ^{14}C with time along groundwater flow path is used to estimate groundwater residence times.

Conventional groundwater age, if the initial concentration of the parent is known and has been remained constant in the past and the system is closed, can be calculated using the relation:

$$t = -8267 \cdot \ln \left[\frac{a_t{}^{14}C}{a_{initial}{}^{14}C} \right]$$

However, dilution of ^{14}C due to addition of old ^{14}C-free carbonates from the aquifer matrix and diffusion of ^{14}C into the aquifer matrix may happen along the flow path. The dilution of ^{14}C through reaction is accounted for in the decay equation by the dilution factor, q and the equation then becomes:

$$t = -8267 \cdot \ln \left[\frac{a_t{}^{14}C}{q \cdot a_{initial}{}^{14}C} \right]$$

Hence, various schemes and spread sheet models to calculate q for correcting ^{14}C ages based on $\delta^{13}C$ values of DIC have been proposed (Clark and Fritz, 1997). For this study, Pearson correction model, that accounts interaction of groundwater with soil CO_2, has been used. The model considers processes that adds, removes or exchanges carbon from the DIC pool and which thereby alters ^{14}C concentrations will also affect the ^{13}C concentrations.

$$q = \frac{\delta^{13}C_{DIC} - \delta^{13}C_{carb}}{\delta^{13}C_{soil} - \delta^{13}C_{carb}}$$

Where: q is the dilution factor

$\delta^{13}C_{DIC}$ is a measured ^{13}C in groundwater

$\delta^{13}C_{carb}$isd^{13}C of the calcite being dissolved

$\delta^{13}C_{soil}$ isd^{13}C of the soil CO_2

The groundwaters from the escarpment, including the study area are characterized by low dissolved oxygen, no signs of H_2S and sulphate reduction and corresponding oxidation of organic matter. Hence it could not play a role in the dilution of the ^{14}C signature of sampled groundwater (Bretzler et al., 2011). Since the aboveclosed system relation precludes isotope exchange with the soil gas, the$\delta^{13}C_{soil}$ value is replaced withan initial value of recharge water ($\delta^{13}C_{rech}$) using the relation:

$$\delta^{13}C_{rech} = \delta^{13}C_{soil} + \text{enrichment factor}$$

The dilution factor then becomes:

$$q_{\delta^{13}C} = \frac{\delta^{13}C_{DIC} - \delta^{13}C_{carb}}{\delta^{13}C_{rech} - \delta^{13}C_{carb}}$$

Since, values for $\delta^{13}C_{soil}$, pH of recharge water and $\delta^{13}C_{carb}$ were not generated by this work, they were taken fromBretzler et al. (2011). The value for $\delta^{13}C_{soil}$ is -17 ‰ forpH 6.5 and for $\delta^{13}C_{carb}$is+2‰.Corresponding value of enrichment factor from graph is2‰.and $\delta^{13}C_{rech}$ becomes -14‰(Clark and Fritz, 1997). These values together with $\delta^{13}C_{DIC}$ results for the groundwater samples were used to estimate dilution factor for each sample so as to calculate ^{14}C age with Pearson model (Table 22).

Table 24.^{14}C activity and groundwater ages (years)

ID	Locality	T°C	pH	Alk	$a^{14}C$ (pmc)	$\delta^{13}C$ (‰)	Conv. age	Age from Pearson
BHT1001	Legadadi	28	8.10	225.46	15.80	-10.05	15505	12910
BHT1002	Muketure	19	7.30	188.44	90.20	-11.96	1072	Modern
BHT1003	Akaki	22	7.86	345.90	66.00	-8.79	3708	178
BHT1004	Jemo BH24	22	7.84	197.64	59.80	-9.57	4510	1571
BHT1005	Ginchi	21	8.23	384.30	66.60	-7.76	3650	Modern
BHT1006	Melkakuture	31	7.71	319.47	49.00	-10.10	6148	3588
BHT1007	CMC	22	7.98	209.80	74.90	-8.08	2674	Modern
BHT1008	Sululta	18	7.30	85.05	80.9	-9.65	2010	Modern
BHT1009	Derba	19	7.50	183.00	49.10	-9.06	6148	2828
BHT1010	Salayish	22	8.02	274.50	24.90	-9.21	11759	8552
BHT1011	Inchini	17	7.10	143.30	90.90	-12.00	1008	Modern

As shown above in the table, $\delta^{13}C$ and $\partial^{14}C$ values vary between -12.0%o to -8.0%o and 15.8pmc to 90.9pmc respectively.

The elevated $\partial^{14}C$ valuesof the groundwater over50 pmc (Fig. 30, Table 24)represents aquifers with very young ages in unconfined condition receiving modern recharge in Jema, Muger and the Upper Awashsub-basins.Samples in this category are also characterized by low pH and low alkalinity. This is attributed to mixing effect of modern recharge through fractures, joints and fault systems and availability of recharge in all parts of the area for shallow part of the aquifers.

Samples from artesian wells (aquifers in confined and semi-confined condition) in the Upper Awash basin with$\partial^{14}C$ value less than 50 show relatively older ages. These samples have relatively higher pH and alkalinity. Some of the samples in this category weretaken from wells located very close to the water divide between the Blue Nile and the Upper Awash. The old ages for deep wells (BHT1010 and BHT1001) located northeast and north of Addis Ababa, at distances of 5 to 10km from the surface water divide between the Blue Nile and the Upper Awash basins, suggests recharge source for deep circulating groundwater in the Upper Awash is beyond the water divide in Blue Nile. This also suggests the travel distance of the regional groundwater in a confined condition in the Upper Awash is beyond the water divideand hence attests the conceptual model developed from geological and geophysical methods and later supported with geochemical evidence and other environmental isotopes.

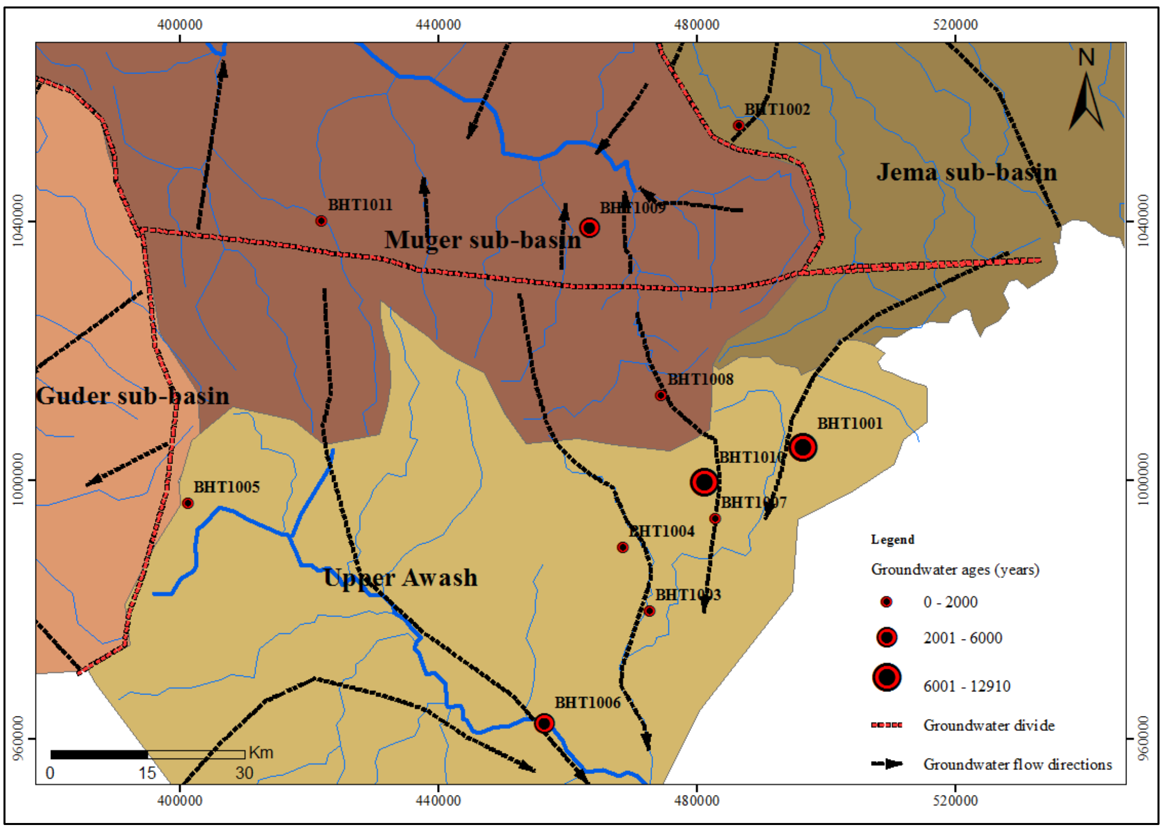

Figure 30.^{14}C age distribution

The quantitative dating information obtainedbefore correction for dilution varies between 1,008 to 15,505 years. It varies between modern and 12,910 years after ^{14}C age correction using Pearson model. The mean resident time of deep circulating waters from the volcanic aquifers in the area are dominated by pre-Holocene origin (between 11,000 and 12,000 years), which is in a general agreement with the observation of Bretzler et al., (2011) for escarpment deep aquifers in the area.High degree of closed system phenomenon is not expected in the study area since the rock units are highly affected by fractures, joints and faults through which water from modern recharge contaminate older waters.

Tritium

Since the mid-eighties, the tritium values in rain water have been about 10 TU in the northern hemisphere, except for some local anthropogenic releases of tritium from the nuclear industry and other uses of tritiated materials and helps date groundwaters younger than 150 years. (IAEA, 2000).

Regarding the tritium concentrations in the area, for Akaki catchment, (part of the Upper Awash) concentrations ranging from 0 TU for thermal wells to 20 TU for shallow aquifer has been reported (Birhanu, 2002). Molla et al. (2009) reported tritium values ranging from 0.4 TU for deep wells tapping lower basaltic aquifer to 5.7TU for shallow aquifers. Andarge (2009) reported tritium concentrations ranging from 0.4 TU for deep wells tapping lower basaltic aquifer to 2.8TU for shallow aquifers. Tritium concentration below detection limit for deep wells to 5.2 TU for shallow aquifer in the Upper Awash and rift floor have been reported (Brezler et al., 2011).

According to the observation of the authors, measurable tritium concentration from the shallow part of the aquifer in the area suggests mixed modern and submodern watersrecharged after atomic explosion of 1960s.However, highly evolved waters with very low tritium concentrations show typical pre-bomb tritium signature, signifies deep circulation, longer travel distance and residence time.

According to the authors, the groundwaterevolves from tritium-containing, low TDS-$CaHCO_3$ water type showing recently rechargeon the plateau and escarpments totritium-free groundwater,highly depleted in stable isotopes, high TDS-$NaHCO_3$ water type dominating deep circulating escarpment and rift floor aquifers.

The tritium-containing, low TDS-$CaHCO_3$ groundwater types, enriched in stable isotopes are observed in all parts of the study area, mostly from shallow part of the aquifer system. However, spatial distribution of tritium-freehighly depleted in stable isotopes and high TDS-$NaHCO_3$ groundwater type has been observed along the water divide between the Blue Nile and the upper Awash basins. The unique spatial variation in geochemical evolution together with pre-Holocene radiocarbon signature from wells drilled into the confined portion of the aquifer, located very close to the water divide between the basins helps realize the existence of deep circulating water with long residence time and travel distance as evidence of interbasin groundwater flow.

Radon

Radon (^{222}Rn), the daughter of ^{226}Ra, is a radioactive noble gas with a half-life of 3.8 days. Radium is easily soluble in water and is gained by dissolution from rocks. As a noble gas, it is not being absorbed by solids. Moreover, it is highly soluble in water; consequently, ^{222}Rn is likely to accumulate in groundwater. Because of its short half-life, when groundwater with ^{222}Rn discharges into surface water bodies like rivers and lakes, its activity decreases by radioactive decay. This feature of ^{222}Rn is a qualitative indicator for groundwater-surface water interaction (IAEA, 2000).

Radon degasses completely after it discharges to the surface water bodies, hence low radon count in the rivers shows that the water in the river is not the result of the base flow in the same area or nearby. On the contrary, the presence of the short-lived radon in surface water always means that the groundwater is feeding the river at its measured reach.

The Upper Awash groundwater basin is chosen for regional groundwater modeling among the groundwater basins. Knowledge of groundwater and surface water interactions are important for model input to set different boundary conditions. In the Upper Awash basin, poorly permeable ash covers very wide area where floodwater resides for long time after the rainy season. Moreover, streams that flow through the ash unit have base flow lowerthan the base flow of streams that flow through other geologic units with better permeability (scoriaceous basalts, vesicular basalts, ignimbrites).Hence, radon measurement has been conducted at different reaches of the Awash River and its tributary streams that flow through different geologic units to determine interactions of surface waters and groundwater and to characterize relationship between base flow of rivers and rock units with different permeability.To avoid contamination from precipitation, the measurement has been conducted in the month of May/2014.

With ^{222}Rn activity measurement mechanismof surface water of Awash River and its tributary streams interact with the groundwater has been schematized, and the effects of permeability of various geologic units on the interactions between surface water bodies and groundwater have been appraised.

The highest reading, 600 to 800 Bq/m^3 is from the downstream part of the Awash River where the geologic unit is dominated by rift basalts and ignimbrites and lineament density is high. This zone is identified as discharge zone for the regional groundwater into the Awash River flow system. From the highest values in this zone, it can be concluded that the groundwater that discharge into the Awash River flow system in areas at its outlet from the study area has relatively longer residence time flow path length.

Moderate reading, 100 to 200 Bq/m^3,is from the upstream part of the Awash River where the geologic unitsare dominantly composed of scoriaceous basalt, rift basalts and ignimbrites, with the highest lineament density. This zone is identified as discharge zone for local groundwater into the tributary streams of the Awash River flow system where the resident time of the groundwater is so small to dissolve and incorporate sufficient ^{222}Rn into the groundwater.

The lowest reading, less than 100 Bq/m^3 is observed in the mid way of the Awash River and its tributary streams, where the geologic unit is dominantly Rift ash(Fig. 31).

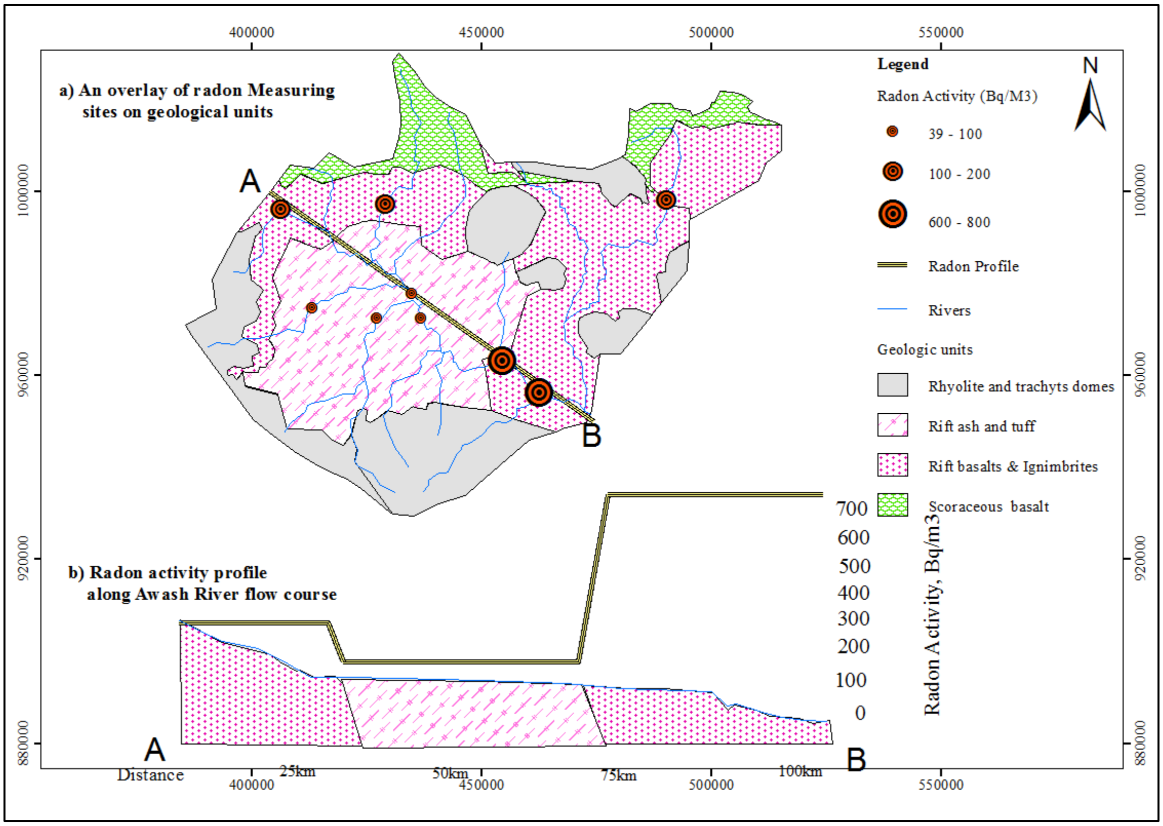

Figure 31.^{222}Rn measuring site (a) ^{222}Rnactivity profile along Awash River course (b)

The result clearly shows that tributary streams that cross the high lineament density zone in YTVL emerging from and flow through highly fractured scoriaceous basalt, rift basalt and ignimbrite units are linked with local groundwater flows in recharge areas. In the downstream reach, as it is flowing through highly fractured basalt and ignimbrite units around its outlet from the study area, the Awash River receives groundwater discharged into its flow system, where it is a gaining river. However; Awash River and its tributary streams flowing through the ash unit are poorly connected to the groundwater system. (Fig. 31).

Chapter Six: Groundwater Flow Modeling

6.1. Introduction

In the study area especially in the Upper Awash basin, due to rapid urbanization and industrialization, groundwater use for domestic and agricultural purposes is rapidly growing. Despite such a voluminous extraction, proper regional-scale groundwater resource evaluation has not been done in the area. This might lead to decrease in the groundwater levels and deterioration of the water quality.

A regional-scale hydrogeological study has been carried out to properly evaluate the groundwater system and to lay a basis for further detail studies. To characterize and determine the aquifer proprieties, all possible investigation methods and available geological, geophysical, hydrodynamic, geochemical and environmental isotopic data were used.

Simple regional groundwater flow model has been conducted for the Upper Awash groundwater basin. This basin has been chosen for this study because data required for the modeling are more available in this basin, and this basin is affected by significant extraction of the groundwater.

The main objective of the groundwater flow modeling is to implement the conceptual model into a numerical groundwater flow model and to help interpret the groundwater system (Anderson and Woessner, 1992).Because of the heterogeneities in geologic materials and structural complexities in the study area (e.g., local-scale variations of aquifer properties, presence of numerous surface water bodies, etc.), due care has been given to consider assumptions, to logically categorize some geologic units, and extrapolate or interpolate values for some parameters based on the few existing data in parts of the study area.

6.2. Conceptual Model

The evidence based conceptual model shows that groundwater localized in volcanic aquifers in the southern part of the Muger sub-basin and the upper Awash basin flows generally to the south, finally discharging into the Awash River flow system defining the Upper Awash groundwater basin(see Fig. 19).

For the flow model, DEM from SRTM of 30m spatial resolution was used as a base map to visualize model area characteristics and boundary conditions (Fig.32).

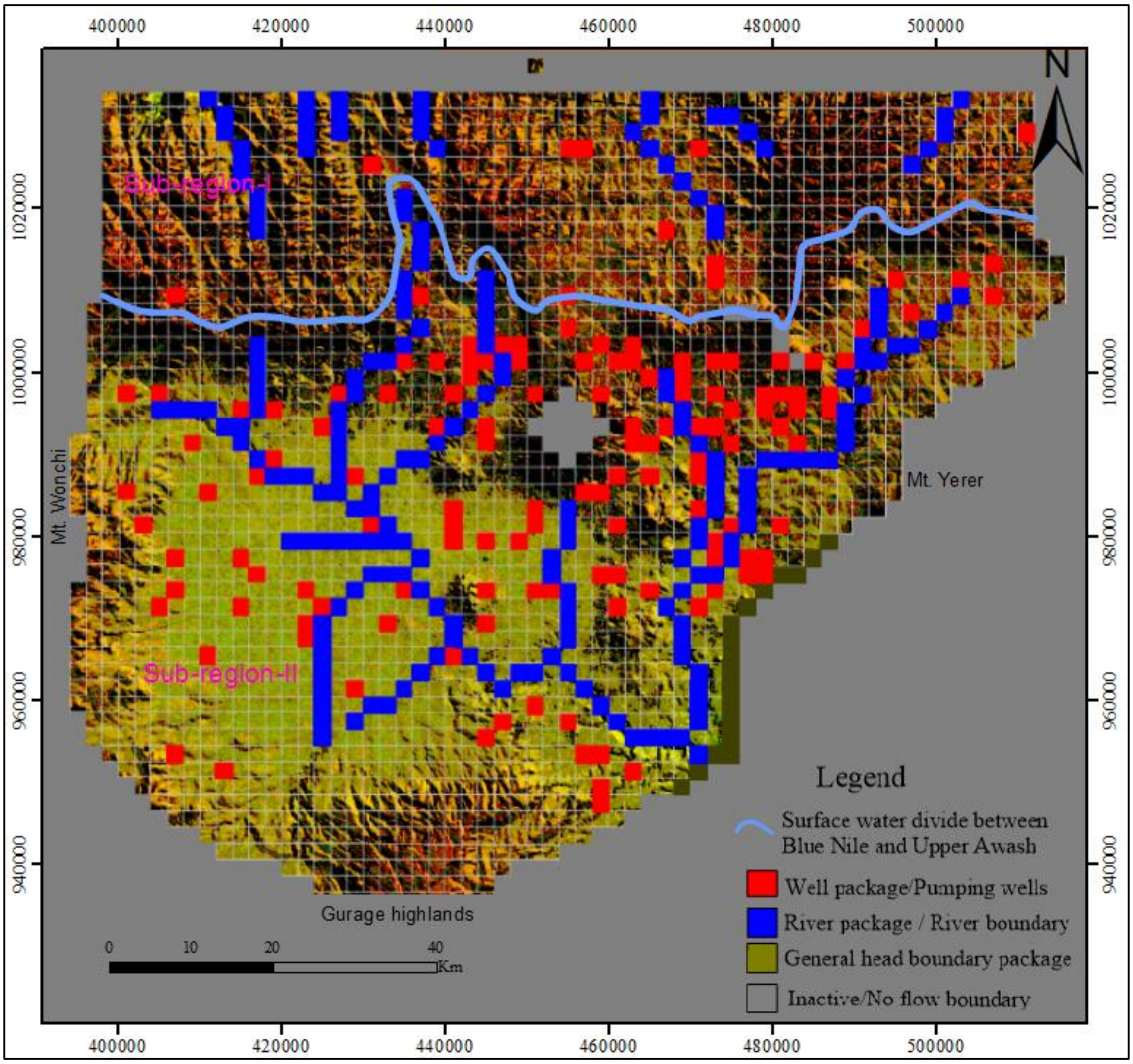

Figure 32.Model grid,boundary conditions and flow packages

6.3. Numerical Model

6.3.1. Model selection

A modular three-dimensional finite-difference groundwater flow model (MODFLOW) was chosen for simulating the 3-D groundwater flow system of the Upper Awash groundwater basin. This deterministic numerical model basedon Darcy's law and mass conservation concept was developed by McDonald and Harbaugh (1988) and Harbaugh etal. (2000).

6.3.2. Spatial model discretization

The numerical model domain is assumed as a rectangle of 130km x120km and an area of 15,600km^2.Itislocatedbetweenthe parallelsof 920000 and 1040000 UTM northand 390000and 520000UTM east.

Themodelinggridconsistsof60 rowsand 65 columns (Fig.32). Eachcellhasadimensionof 2km by 2km. A few cells with rhyolitic domes (acidic volcanic centers) in the model area, are considered to be "inactive". A single layer steady state model of volcanic rock aquifer underlain by regional impermeable mudstone has been assumed in a confined or unconfined condition with variable transmissivity values.

6.3.3. Boundary conditions

Layer top or surface elevations were extracted from DEM of 30m spatial resolution. Layer bottom elevations were obtained by subtracting aquifer thickness from layer top elevations. Aquifer thickness of 900m is considered, as the maximum available drilling depth is 882m. Groundwater head information was derived from water level measurements in the field and pertinent data obtained from drilling companies.

The "no flow boundary" condition in the north has been defined primarily based on geological evidences. It has been set along the loci of points in East-West trending mudstone horst underlying volcanic aquifer in the eastern side and exposed on the surface towards the west. Tuff and ash dominated Mt.Wonchi and Gurage highlands; in the western and southwestern side of the model area respectively forms a no flow boundary due to their poor hydraulic conductivity. Likewise, in the northeastern part of the model area, trachytic Mt. Yerer forms a no flow boundary. The outside part of the model domain is also considered as no flow boundary. Mt. Entotoand Mt. Wochecha from inside the model domain form no flow boundary.

The *General-Head Boundary* package used to simulate head-dependent ﬂow conditions (Cauchy boundary), where groundwater flows into or out of a cell from an external source is provided in proportion to the difference between the head in the cell and the head assigned to the external source. The GHB has been setbased on available measured head information and results from ^{222}Rn measurement in the Upper Awash River and its tributary streams. It has been set in the southeastern part of the model domain.

6.3.4. Input parameters and flow packages

The parameters or flow package inputs into the model include head information, horizontal hydraulic conductivity, recharge, pumping wells, conductance of river bed sediments, and GHB cells. Due to their small sizes (less than model grid) and for the reasons that their bottom part is lined with clay, reservoirs in the area are not included in the simulation. The reservoir package in MODFLOW is designed for cases where reservoirs are much greater in area than the area represented by individual model cells, which is not the case in the study area.

Hydraulic heads

MODFLOW requires initial hydraulic heads at the beginning of a flow simulation. For steady-state flow simulations, the initial headsare used as starting values for the iterative equation solvers. The initial heads introduced arbitrarily into active cells were defined based on depth to water and groundwater flow condition in the area.

Horizontal hydraulic conductivity

The geologic formations in the area significantly vary from massive to highly fractured, over distances as short as a kilometer. Materials exposed on the surface vary fromfresh bedrock to loose pyroclastic deposit. Hence, heterogeneity of lithology, variation in lineament density and geomorphological set up of borehole sites are important factors that affect values of transmisivity calculated from the pumping test data.

Transmissivity values and resultant hydraulic conductivity calculated from pumping test data can also be affected by a number of factors associated to well construction. In this case, screens may be put against impermeable part of the aquifer and the aquifer may be covered with blind casings. It may also be associated with drilling fluids used, inefficient well development and improper gravel pack. In addition, most of the wells are shallow and could not penetrate the whole aquifer thickness. Hence, defining spatial distribution of hydraulic conductivitiesis one of the most challenging aspects of subsurface hydrology.

Therefore, due attention has been given to lithostratigraphy, lineament density and geomorpholoical set up of the area, to assign particular K value or mean of K values to different zones. Geological maps, cross sections, geophysical results and borehole logs together with pumping test data were used to define distribution of hydraulic conductivity (Fig. 33).

In this work an attempt has been made to calculate transmissivity from pumping test data of 145 deep wells. Transmissivity values obtained from drilling reports were also used. The transmisssivity values obtained range between 13m^2/d and17,000 m^2/d. The transmissivity value together with aquifer thickness (screen length in the boreholes) were used to estimate average hydraulic conductivity (K) at a specific site and was found to range between 1.3 m/d and 295 m/d. Model area wide hydraulic conductivity zone map has been produced from the K-values using kriging interpolation tool in ArcGIS. While using the hydraulic conductivity zone map, due attentions were given to lithostratigraphy, lineament density and geomorpholoical set up of the area.

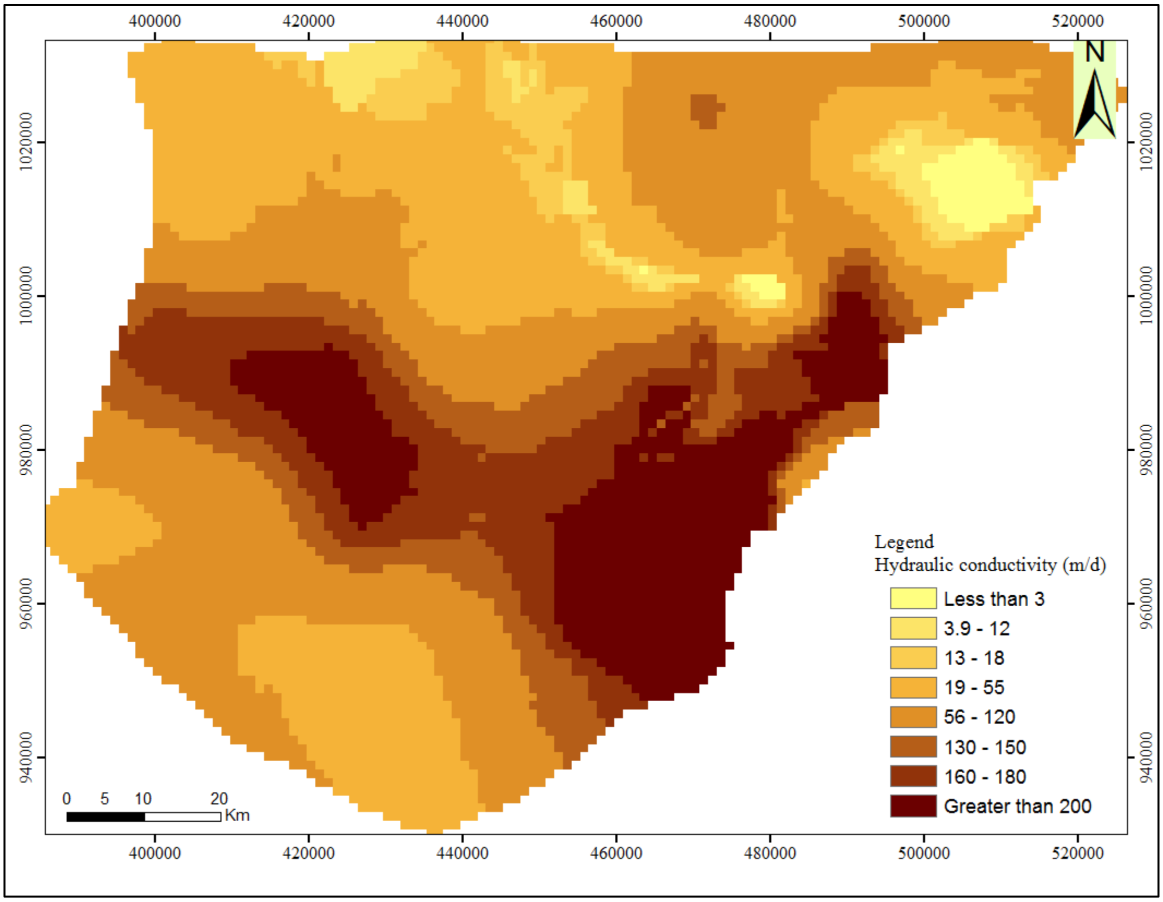

Figure 33.Hydraulic conductivity zones in the model domain.

General head boundary

The GHB, package requires the input of GHB hydraulic conductance and head on the external source. Cells assigned as GHB are chosen based on the groundwater flow direction, depth to the groundwater level in the boreholes and information from ^{222}Rn measurements in Awash River and its tributary streams. The input values of hydraulic conductivity have been obtained from pumping test data analysis from available boreholes in the area. The length of the GHB within a celland head on the external source at active vertices of the external sources were considered in order to calculate hydraulic conductance of the GHB. The hydraulic conductance of the GHB has been calculated using the relation:

$$C_b = K.L$$

Where: C_b is hydraulic conductanceof the GHB (m^2/d)

K is hydraulic conductance of the GHB (m^2/d)

L is length of the GHB (m)

Recharge

The Recharge package is designed to simulate distributed recharge to the groundwater system. Recharge is defined by assigning recharge flux data to each vertical column of cells in the highest active cell in each vertical column. Meteorological, pedological and river discharge data together with chemical tracers were used to characterize recharge in the area.

Rechargeestimates from the BFS better represent recharge distribution in the model domain and were used to produce recharge zone map for the model input. An estimated recharge distribution surface map of seven zones has been generated from a scattered set of base flow values in the model area using kriging tool in ArcGIS (Fig.34). The recharge distribution surface map with minor correction based on the geological, lineament density and topographic set up has been used in the model input.

Correlation has been made to investigate base flow relation with geologic units through which the river flows. Ranges of values were obtained forgiven geologic units. In addition, a given base flow value calculated from river discharge record may represent more than one geologic unit the river crosses. Some geologic units do not have representative gauged river to characterize (Fig. 35).

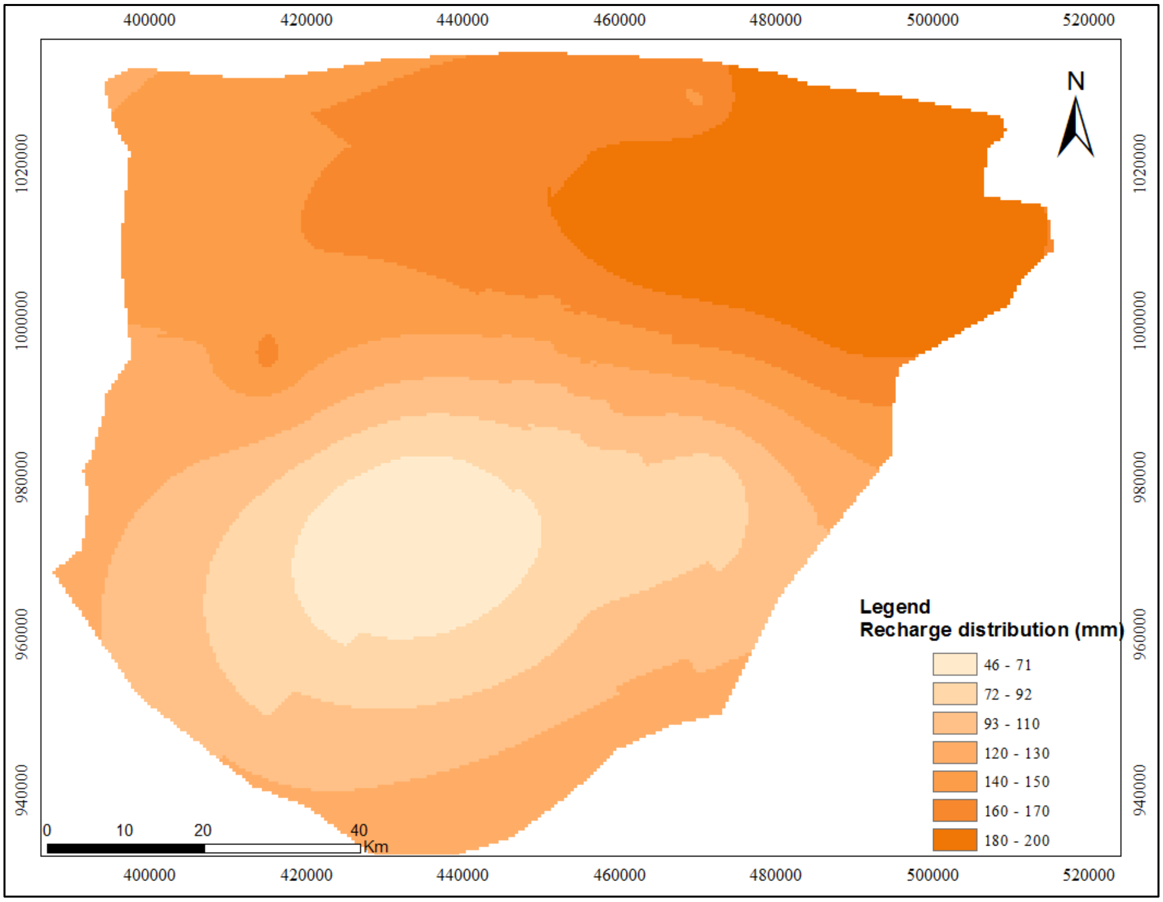

Figure 34. Recharge zone map generated from base flow separation results.

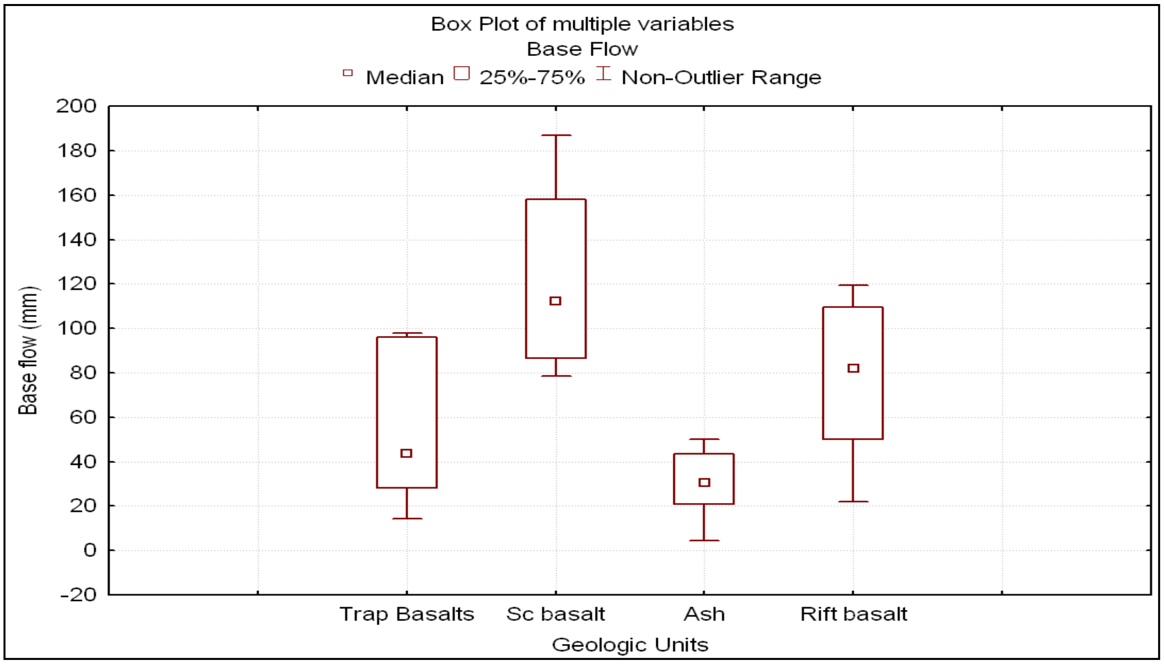

Figure 35.Recharge variations in different geologic units from base flow separation.

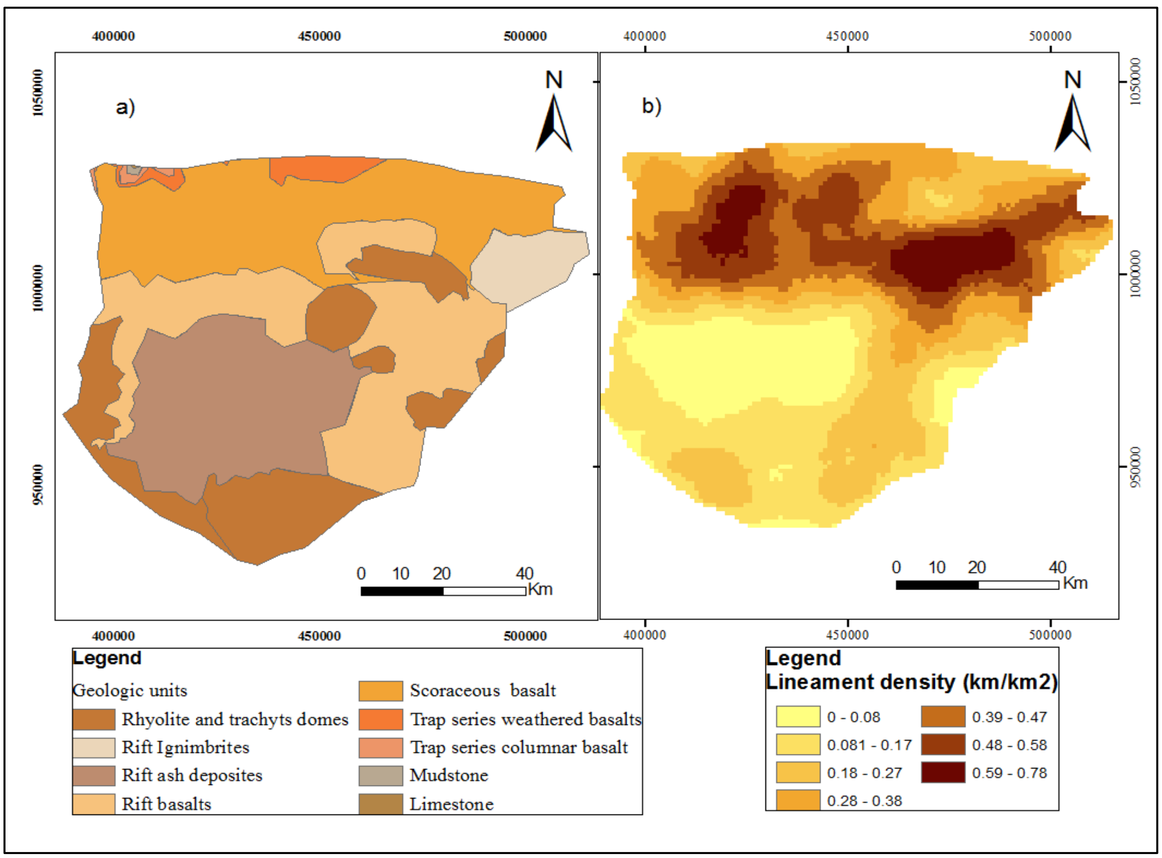

Figure 36.Geologic units (a) and lineament density distribution (b).

Due consideration has been given to the factors that affect base flow values calculated from river discharge data. These factors include proportion of the geologic unit through which the river flows, lineament density, soil, land use/land cover, slope and size of catchment area. Minor corrections have been made on the recharge zone map generated from the base flow results based on geologic unit, lineament density and topography. Highly permeable rock units such as scoriaceous basalt and rift basalts correlate with high base flow. Likewise, high lineament density zones correlate with high base flow (Figs. 35 and 36).

Well package

A pumping well is defined by using the Cell-by-Cell input methods of assigning negative sign to model cells. MODFLOW assumes that a well penetrates the full thickness of the cell.In case more than one pumping wells are located in a given grid cell, the sum of well discharges has been considered for the input (Fig. 33). To characterize and quantify water abstraction from the aquifer system through dug and drilled wells, the estimations and assumptions have been followed for water balance were used.

About 530 wells with water level information were used for head observation anddata from 550 wells were used to quantify daily and annual abstraction from the aquifer. Total annual abstraction from the aquifer of the Upper Awash groundwater basin is roughly about 64.5 Mm^3.

River package

The purpose of the River package is to simulate the effect of exchange between groundwater systems and surface water features. Rivers were defined by using the Cell-by-Cell input method.The input parameters include hydraulic conductance of river bed material, head in the river and elevation of the river bed in a cell (Fig. 33).

Based on some sample site observation and estimation, river bed sediment thickness has been assumed to vary between 0.1 to 0.5m.River widths range from 2 to 50m. River length in a cell has been roughly considered to be equal to the side of the cell size (2000m), since tracing and measuring the river length in a cell is difficult. Hydraulic conductivity of river bed sediments was not characterized and measured in the field, instead the hydraulic conductivity of the underlying formation has been considered. The hydraulic conductance of the river bed sediments has been calculated using the relation:

$$C_{riv} = (K.L.W)/M$$

Where: C_{riv} is hydraulic conductance of river bed material (m^2/d)

K is hydraulic conductivity of the river bed material (m/d)

L is length of the river in the cell (m)

W is width of the river (m)

6.4. Model Simulation and sensitivity analysis

In groundwater flow modeling,equilibrium solution is desired for heads such that inflow and outflow to and from the aquifer are in a perfect match (Andreson and Woessner, 1992). Due to the limitation of MODFLOW pro, sensitivity analysis using single run method by multiplying a single parameter zone by a given multiplication factor has been made to identify the most sensitive parameter among hydraulic conductivity, recharge and river bed conductance. Doing so, hydraulic conductivity has been identified as the most sensitive parameter for model calibration.

6.5. Model Calibration and Results

It refers to a demonstration in finding set of parameters (recharge rates, hydraulic conductivity, specific conductance of river beds), boundary condition and stresses that the model is capable of producing field measured heads and flows (Kresic, 1997).Calibration target is hydraulic head. Hydraulic conductivity values were used as calibration parameters.

Manual inverse trial and error method based on head information has been used for calibration. Field measured water levels or heads at 530 wells were used for head observation duringcalibration. The final simulation result gives head distribution as shown below (Figs. 37 and 38).Calibration results are evaluated by using qualitative and quantitative performance measures. Qualitatively, calibration results are evaluated using pattern matching of raster surfaces of measured and simulated headswhich gives very good match(Fig. 39).

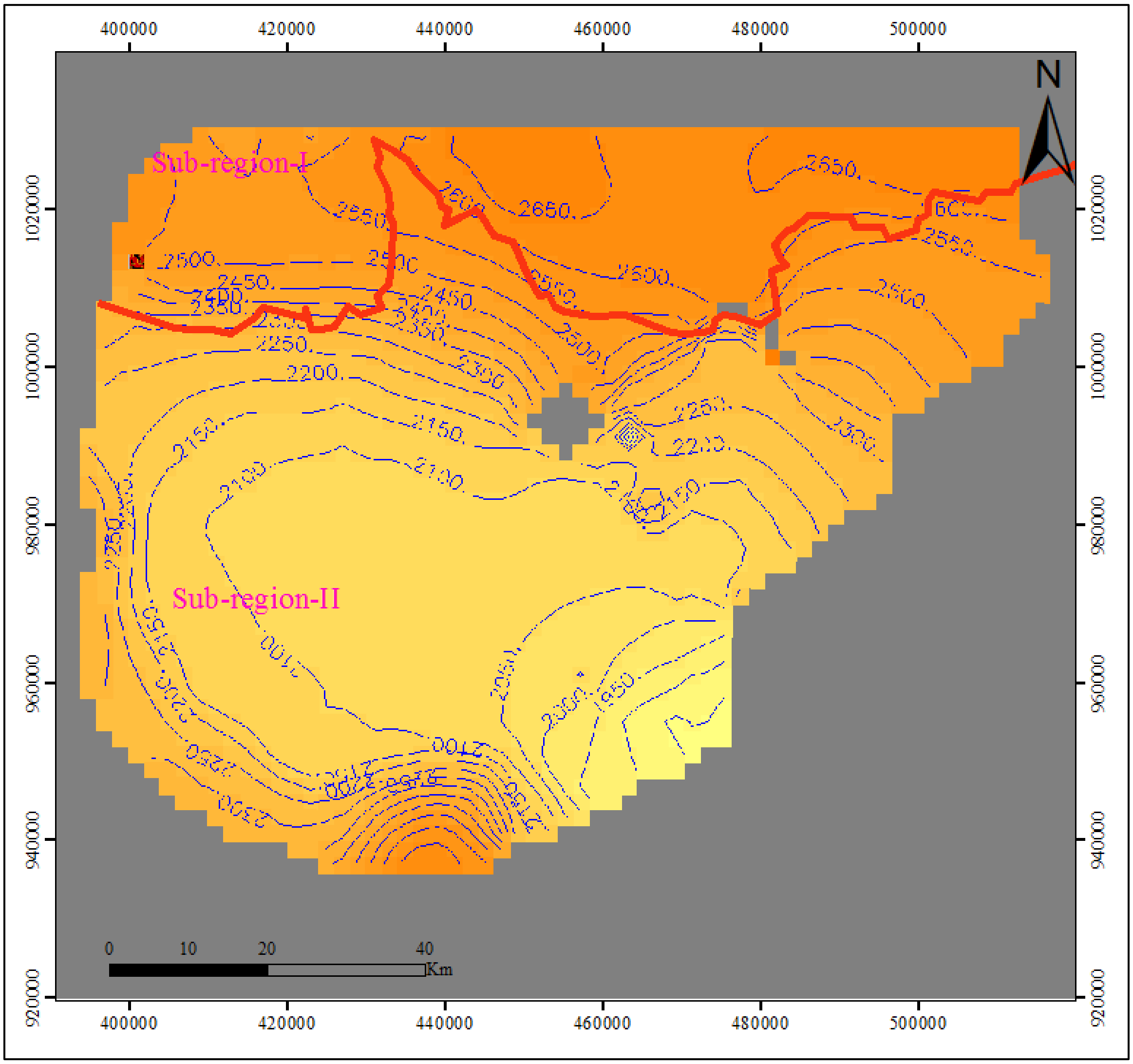

Figure 37. Simulated head distribution in the model domain

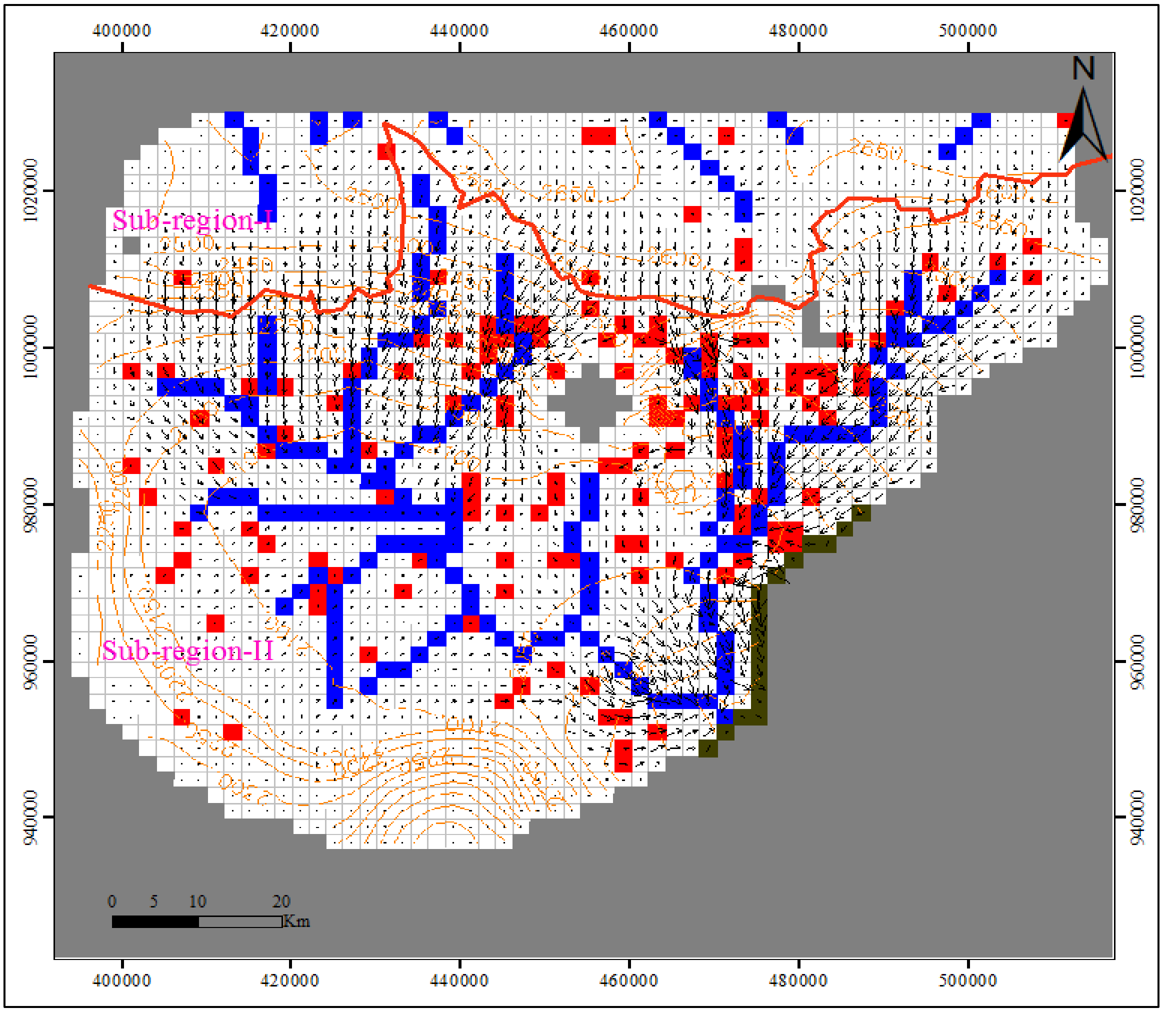

Figure 38.Simulated head distribution with groundwater flow lines.

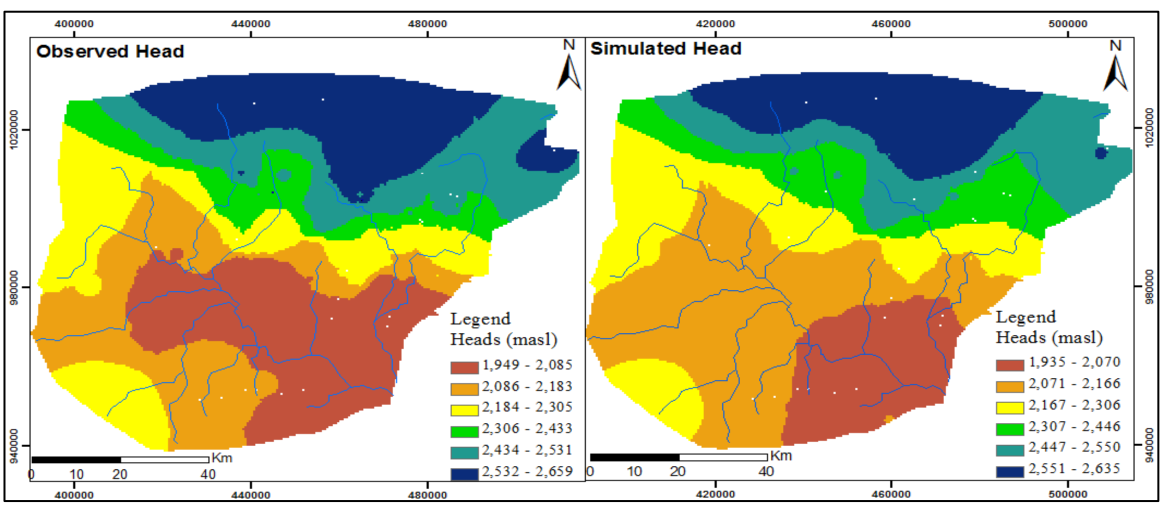

Figure 39.Comparison between observedand model simulated head patterns.

Quantitative calibration measures involve statistical lumped sum description of the average differences of residuals between simulated and measured heads (mean error, mean absolute error, root mean square error and correlation coefficient).

- The mean error is the mean of the differences between measured heads and simulated heads.
- The mean absolute error is the mean of the absolute values of the differences between measured heads and simulated heads.
- The root mean square error is the square root of the averages of the squared differences between measured heads and simulated heads.
- The correlation coefficient between measured heads and simulated heads

The results for the lumped sum statistical calibration show a good calibration level of such a regional model in rugged terrain (Table 25). The correlation coefficient (R^2 = 0.953) between measured heads and simulated headsis also one of good indicator of calibration quality (Fig. 40).

Table 25.Summary of lumped sum calibration errors

No	Statistical parameters	Values, m
1	Mean error	-8
2	Mean absolute error	30
3	Root mean square error	39

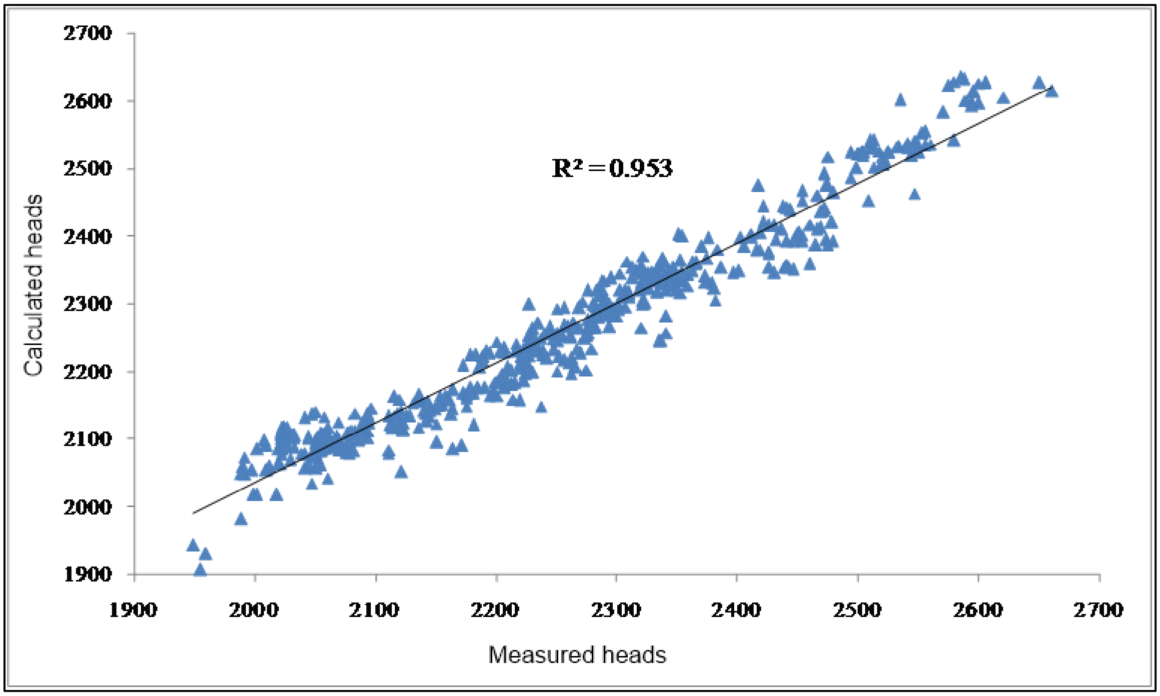

Figure 40. Measured versus model simulatedheads

6.6. Water Budget Results

To check the accuracy, MODFLOW calculates a volumetric water budget for the entire model at the end of each time step. The water budget provides an indication of the overall acceptability of the numerical solution. Change in storage in water balance approach close to zero assures calibration quality, for steady state models (Rushton, 2005). The out flow from and the inflow into the groundwater basin are nearly equal, with percent discrepancy less than 0.01%. This very low calculated water balance error, assures good level of the model calibration (Table 26).

6.7. ModelingResult Summary

The water budget calculation gives inflows to and out flows from the system. It also provides amount of flux between the groundwater basins and relative importance of components to the total budget.

To estimate flux between the Blue Nile and the Upper Awash basins, water budget calculation has been made for two sub-regions and for the entire model domain. Sub-region-I in the model domain is portion of the Blue Nile basin (Muger and Jema sub-basins) and sub-region-II is the Upper Awash basin (Figs.38 and 39).

In sub-region-I, recharges from precipitation and river leakage are major components of inflow to the aquifer system. River leakage contributes smaller proportion. Horizontal exchange (flux to the Upper Awash basin) and river leakageare major components of the out flow. Outflow through groundwater abstraction is negligible in this sub-region of the model domain.

In sub-region-II, recharges from precipitation, horizontal exchange and river leakage in orderof their significance are major components of inflow to the aquifer system. Head dependent flow contributes small amount to the system. The outflow is dominantly through river leakage. Groundwater abstraction by pumping and head dependent flows contributes to the out flow from the sub-region.

For the entire model domain, recharges from precipitation and river leakage are the major inflow components. As river leakage is dominant inflow component, it is also the dominant component of the outflow. Groundwater leaving the aquifer, across the southeastern general head boundary and abstraction by pumping for domestic, industrial and agricultural purpose also contribute some proportions to the outflow from the Upper Awash groundwater basin. The water budget for the two sub-regions and the entire model domain shows that the Blue Nile portion of the model domain receives a total inflow of 186Mm^3 annually. Out of the total, 152Mm^3 is an outflow by horizontal exchange that contributes inflow to the Upper Awash basin and 33Mm^3 is an out flow through river leakage that feeds surface flows of the Muger River through its tributary streams.

A regional groundwater flow model for the Upper Awash groundwater basingives a total volumetric annual inflow of nearly 590Mm^3 into the system of the Upper Awash groundwater basin. Of the total recharge to the Upper Awash groundwater basin, nearly 26% is an inflow from the Blue Nile basin through horizontal exchange(Table 26).

Table 26. Summary of annual water budget results (Mm^3).

Sub Region: 1 (Blue Nile basin Portion)	Inflow	Out flow
Horizontal exchange		151.87
Wells	0	1.26
Recharge	182.82	0
River leakage	0.35	32.89
Sum	186.02	186.02
Flux to the Upper Awash		
Sub Region: 2 (Upper Awash basin)	Inflow	Out flow
Horizontal exchange	151.87	
Wells	0	63.20
Recharge	288.46	0
River leakage	101.95	452
Head dependant boundary	15.39	39.8
Sum	557.67	557.64
Water Budget of the Entirre Model Domain	Inflow	Out flow
Wells	0	64.50
Recharge	471.28	0
River leakage	102.30	482.64
Head dependant boundary	15.39	39.82
Sum	588.97	588.94
Discrepancy		0.001%

Chapter Seven: Conclusions and Recommendations

7.1. Conclusions

Lithostratigraphic set up of the Middle Blue Nile and adjoining Upper Awash basin is so complex that, the inter-relationships of lithological and structural factors, geomorphic setting and hydrostratigraphy are difficult to reasonably evaluate. Converging evidences from geology, geophysics,hydrogeology, hydrogeochemistry, stable and radioisotopeshave been used to conceptualize the aquifer systems. A simple regional groundwater flow model has also been used for the Upper Awash groundwater basin to implement the conceptual model into numerical model and to characterize groundwater dynamics between the basins. The following are the major conclusions of this study:

1) Geological and geophysical investigations have clearly indicated the distinctive geometric architecture of the litho-strata of aquifers and aquicludes in the sub-basins. Such a unique geometry is strongly dependent on the interplay between the tectonic zones defined by the Yere Tulu Wolel Volcanic Lineament zone and the Main Ethiopian Rift margin. The regional fault systems dislocated sedimentary rock units and resulted in fragmentation of sedimentary aquifer systems and forms structural depressions and adjoining highs prior to the formation of the volcanic rock units. The horsts defined by the NW-SE trending fault system together with adjoining highs define the groundwater divide and aquifer distribution within the Middle Blue Nile basin into Guder, Muger and Jema groundwater sub-basins. The E-W trending mudstone caped horst defines aquifer distribution between the Middle Blue Nile and the Upper Awash basins. This impermeable mudstone caped horst located across the middle of the Muger sub-basin and extending to the southern tip of the Jema sub-basin forms a barrier to the regional groundwater flow in volcanic aquifers. The barrier channels the regional groundwater flow in volcanic aquifers to its either side to the north and south. In this manner, significant portion of the Muger sub-basin (1770 km^2) and small part of the Jema sub-basin (304km^2) contribute to recharge the volcanic aquifer of the Upper Awash basin.

2) Wide range of recharge estimates to the four sub-basins was obtained from water balance, chloride mass balance and base flow separation methods. Results from base flow separation method that utilizes records from more adequate river gauges than the sparsely distributed meteorological stations better represent recharge distribution in the area. Due to low analytical precision, together with small number of precipitation and groundwater samples for chloride analysis, recharge estimates from chloride mass balance also look less reliable. The overlay analysis made between base flow values, lineament density and lithology indicated that rock units exposed along the Yere Tulu Wolel Volcanic Lineament zone and the Main Ethiopian Rift margin promote more recharge than the rock units exposed away from these zones.

3) Local geomorphic set up, sub-surface configuration of rock units and the interplay between tectonic structures control depth and pattern of the groundwater movement. Scale of observation was found important for hydrodynamic characterization in the area. The groundwater contours for local groundwater flows give flow patterns that assume surface topography when observed at small catchment or sub-basin level. At a regional scale, a unique groundwater flow pattern indicative of interbasin groundwater flow from the Blue Nile to the Upper Awash basin has been observed. This unique regional groundwater flow pattern, obtained from groundwater level measurement is in general agreement with the evidence based conceptual model from geological and geophysical studies.

4) Groundwater evolves from low TDS, $CaHCO_3$ type and negative residual alkalinity to high TDS, $NaHCO_3$ facies with positive residual alkalinity. However, the unique spatial distribution of hydrochemical signature has been observed where highly evolved waters are found along the surface water divide between the Blue Nile and the Upper Awash basins. The evidence from such evolved waters along the water divide between the two basins and downstream in the Upper Awash basin substantiates conceptual groundwater flow model developed from geological, geophysical and hydrodynamic studies. The high TDS, $NaHCO_3$water types with positive residual alkalinity located very close to the line limiting surface water flows

in the southern part of the Guder River also shows recharge area to the Guder sub-basin aquifer is either from the peripheries within the sub-basin or outside the sub-basin and could be a subject of further study.

5) The $\delta^{18}O$ and δD signature from shallow aquifer systems in all the sub-basins suggest that the aquifer system is locally recharged from modern precipitations. On the other hand, the highly depleted waters from deep wells in the Upper Awash and Guder sub-basins including those located very close to and along the water divide between the Blue Nile and the Upper Awash basin supports the interbasin groundwater flow determined from the evidence-based litho-structural model.

6) The radioactive agesshow that recharges to the aquifer systems is dominated by modern waters. Moreover, ^{14}C modern ages of waters from shallow and deep parts of unconfined aquifers support the dominance of modern recharge favored by high lineament density along the Yerer Tulu Wolel Volcanic Lineament zone and the Main Ethiopian Rift margin. The pre-Holocene waters represent regional aquifers under confined and semi-confined condition in the Upper Awash basin. The oldwaters located very close to the water divide between the Blue Nile and the Upper Awash basin supports the conceptual hydrogeological model which shows groundwater transfer from the Blue Nile basin to the Upper Awash basin.

7) ^{222}Rn values show that tributary streams of the Awash River that cross the high lineament density zone flowing through highly permeable rocks have clear connection with local groundwater flows. In the extreme downstream, the Awash River is strongly connected to the regional groundwater within the highly fractured basalts and ignimbrite aquifers. On the other hand, the Awash River and its tributary streams are poorly connected to the groundwater within poor permeability rocks, at low lineament density zone.

8) A simple regional groundwater flow model for the Upper Awash groundwater basin gives a total volumetric annual inflow of $590Mm^3$ into the system, of which nearly 26% is an inflow from the Blue Nile basin through horizontal exchange (interbasin

groundwater transfer). On the other hand, significant volume of groundwater recharge in the Blue Nile portion of the aquifer domain, from local circulation feeds the Muger River flow through the tributary streams.

In general, the study has provided vital evidence of the complexity of the groundwater dynamics and aquifer distribution in the volcanic and sedimentary terrains. The study defined the groundwater flow pattern, the flow boundary, as well as the interbasin groundwater transfer from the volcanic aquifers of the Blue Nile basin to the Upper Awash basin.

7.2. Recommendations

- A similar approach to that followed in the current study, i.e., detailed lithostructural study coupled with all possible methods of hydrogeological investigation has a paramount importance for better understanding of complex hydrogeological systems, like those at the Main Ethiopian Rift margins.

- More work at a larger scale is required to differentiate local flows from regional flows, confined aquifers from unconfined aquifers in the area and to address water quality issues related to urbanization.

- Hydrogeological characterization of aquifer systems in the rift margin basins and sub-basins (Guder, Jema and others) need to include investigation for hydrodynamic relationship of groundwaters with adjacent basins.

- The simple regional groundwater flow model from this work does not have enough detail to lead decision-making. However, it could serve as a good basis for local and specific site detail groundwater flow model development in different water supply and irrigation fields (currently in use or those planned for future use).

References

Ahimed Wolela, 2008. Sedimentation of the Triassic-Jurassic Sandstone Formation, Blue Nile Basin, Ethiopia. Journal of African Earth Sciences, 52: 30-42.

Ahimed Wolela, 2009. Sedimentation and Deposition Environments of the Barremian-Cenmanian Debre Libanose Sandstone, Blue Nile Basin, Ethiopia. Createaceous Research, 30: 1133-1145.

Andarge Yitbarek, 2009. Hydrogeological and hydrochemical framework of complex volcanic system in the Upper Awash River Basin, Central Ethiopia. University of Poitiers, France, unpublished, Ph.d. Thesis.

Andarge Yitbarek, Moumtaz R., Tenalem Ayenew, Engida Zemedagegnehu, Tilahun Azagegn, 2012. Hydrogeological and hydrochemical framework of Upper Awash River basin, Ethiopia: With special emphasis on interbasin groundwater transfer between Blue Nile and Awash Rivers. Journal of African Earth Sciences, 65:46-60

Anderson, M. P. and Woessner, W. W., 1992.Applied Groundwater Modeling Simulation of Flow and Advective Transport. Academic Press, New York, pp 381.

Andualem Mekonnen, Tsigereda Assefa, Kuribel Tesfaye, Derbu Getahun, 2014. Spatial Distribution of Nitrate in the Drinking Water Sources Found in Ethiopia. Global Journal of Environmental Science and Technology, 075:2360-7955.

Appelo, C. A. J. and Postma, D., 1993. Geochemistry, groundwater and pollution.A.A Balkema/Roterdam/Bookfield, pp 535.

BCEOM, 1997. Blue Nile River Integrated Development Master Plan Project. Ministry of Water Resources, Addis Ababa, Ethiopia, v. II, part 2 Hydrogeology, unpublished report.

BCEOM, 1998. Blue Nile River Integrated Development Master Plan Project. Ministry of Water Resources, Addis Ababa, Ethiopia. V. II, unpublished report.

BCEOM, 2000. Blue Nile River Integrated Development Master Plan Project. Ministry of Water Resources, Addis Ababa, Ethiopia, v. III, part 2 Hydrology, unpublished report.

Beccaluva L., Bianchini G., Natali C., Siena F., 2009. Continental flood basalts and mantle Plumes a case study from Northern Ethiopia Plateau. Journal of Petrology. 1: 1–27.

Birhanu Gizaw, 2002. Hydrochemical and Environmental Investigation of the Addis Ababa Region, Ethiopia.Ludwin Maxmilan University of Munich, Munich, unpublished Ph.D Thesis.

Birhanu Melaku, 1982. Hydrogeology of the Upper Awash Upstream of Koka Dam. Geological Surveys of Ethiopia, unpublished report, Addis Ababa, Ethiopia.

Boccaletti, M., Bonini, M., Mazzuoli, R., Bekele Abebe, Piccardi, L., Tortorici, L., 1998.Quatemary oblique extensional tectonics in the Ethiopian Rift (Horn of Africa). Tectonophysics, 287: 97-116.

Bretzler, A., Osnabruk, K., Gloaguen, R., Ruprech. J. R. Seifu Kebede, Sradler, S., 2011. Groundwater origin and flow dynamics in active rift systems – Amulti-isotope approach in the Main Ethiopian Rift. Journal of Hydrology, 402: 274-289

Bristow, J. W., Saggersom. E. P., 1983. A General Account of Karoo Volcanicity in South Africa. Geologische Rundschau, 72: 1015-1060.

Clark, I. and Fritz, P., 1997. Isotope Hydrology, pp 295

Craig E., Divine, J., McDoneel, 2005. The future of applied tracers in hydrogeology. Hydrogeology Journal, 13: 255-258.

Chorowicz, J., Collet, B., Bonavia, F.F., Mohr, P., Parrot, J.F., Tesfaye Korme, 1998. The Tana basin, Ethiopia: intra-plateau uplift, rifting and subsidence. Tectonophysics, 295: 351–367.

Cook, P.G., 2003. A guide to regional groundwater flow in fractured rock aquifers. CSIRO, Australia, pp 115.

Dafny, E., Burg, A., Gvirtzman, H., 2010. Effects of Karst and geological structure on groundwater flow: The case of Yarqon-Taninim Aquifer, Israel, 389:260-275.

Daniel, C.C., III, 1996, Ground-water recharge to the regolith-fractured crystalline rock aquifer system, Orange County, North Carolina: U.S. Geological Survey Water-Resources Investigations Report, 59: 96-4220.

David P., Genereux, S.J. Wood, C.M. Pringle, 2002. Chemical tracing of interbasin groundwater transfer in the lowlands rainforest of Costa Rica. Jornal of hydrology, 258: 163-178.

Dereje Ayalew, Barbery, F., Marty, B., Reisberg, L., Gezahegn Yirgu, Pik, R., 2002. Source, genesis, and timing of giant ignimbrite deposits associated with Ethiopian continental flood basalts Geochimica et Cosmochimica Acta, V. 66, 8: 1429-1448.

Dereje Ayalew, Gibson, S. A., 2009. Head-to-tail transition of the Afar mantle plume: Geochemical evidence from Miocene bimodal basalt–rhyolite succession in the Ethiopian Large Igneous Province. Lithos, 112: 461–476.

FAO, 1984. Soil and Land use/land cover Map of Africa. Food and Agriculture Organization of the United Nations.

FAO, 2013.Awash River Basin Water Audit Project, Hydro-meteorological Trend Analysis Background Report.Unpublished Report. Addis Ababa, Ethiopia.

Fetter, G.W., 2001.Applied Hydrogeology. University of Wisconsin Oshkesh, USA. pp 598.

Foder, 1989.Age Distribution of Parama Flood Basalts. Journal of South American Earth Sciences, 27: 273-279.

Francesco, S., Dario Z., Marco F., 2013.Development of a deep karst system within a transpressional structure of the Dolomites in north-east Italy. Geomorphology, 184: 51-63.

Freeze, R.A. and Cherry, J.A., 1979, Groundwater. Prentice-Hall, Inc., New Jersssy, pp 604

Gani, N. DS., Abdusalam, M.G., 2006.Remote Sensing Analysis of the Gorge of the Blue Nile, Ethiopia, with Emphasis on Dejen-Gohatsion Region. Journal of African Earth Sciences, 44: 135-150.

Gani, N. DS., Gani, M. Royhan, Abdusalam, M.G.,, 2007. Blue Nile Incision on the Ethiopian Plateau; Pulsed Plateau Growth, Pliocene Uplift, and Hominide Evolution. GSA Today, 9: 4-11.

Gani, N. DS., M. G. Abdelsalam, S. Gera, and M. R. Gani, 2009.Stratigraphy and Structural Evolution of the Blue Nile North Western Ethiopia Plateau. Geological Journal, 44: 30-56.

Gemachu Daniel, 1977. Aspects of Climate and Water Budget in Ethiopia. Addis Ababa University Press: Addis Ababa, Ethiopia.

Genene Mulugeta, Bekele Abebe, Tesfaye Korme, T., Sokoutis, D., 2007. Emplacement mechanisms for Continental Flood Basalts and implications for plume activity during incipient continental breakup. Journal of African Earth Sciences, 48: 137–146.

Getaneh Assefa, 1981. Gohatsion Formation: A New Lithostratigraphic Unit from the Blue Nile River Basin, Ethiopia. Geosciences Journal, 1: 63-88.

Getaneh Assefa, 1991. Lithostratigraphy and Environment of Deposition of the Late Jurassic-Early Cretaceous Sequences of the Central Part of Northern Plateau, Ethiopia. N.Jb. Geol, 182: 255-284.

Hem, J. D., 1985.Research and Interpretation of the Chemical Characteristics of Natural Water (3rd edition), U.S Geological Survey Water Supply Paper 2254: 1- 263.

IAEA, 2000. Environmental Isotopes in Hydrologic Cycle, Principles and applications, V. IV.

IAEA/WMO, 2007.Global Network of Isotopes in Precipitation. The GNIP Database.<http://isohis.iaea.org>.

IWMI, 2009.Characterization and Atlas of the Blue Nile Basin and its Sub Basins.Unpublished Report. Addis Ababa, Ethiopia.

Jr, W. V. and Lewis, G. L., 2003.Introduction to Hydrology, Pearson Education, inc., pp 589.

Kahel, S.C., Olsen, T.D., Morgan, D.S., 2009. Geological Setting and Hydrogeological Units of the Colombia Plateau Regional Aquifer System, US Groundwater Survey Program Report, USA.

Kazmin, V., 1980. Stratigraphy and Correlation of Volcanic Rocks in Ethiopia, Ethiopian Institute of Geological Surveys, unpublished report, Addis Ababa Ethiopia.

Keiffer, B., Ardnt, A.,and Claudin Meugnet, 2004. Flood and Shield basalts from Ethiopia: Magma from the African Super swell. Journal of Petrology, 45: 793-834.

Kirsch, R., 2008. Groundwater Geophysics, A Tool for Hydrogeology, pp 557.

Kovalevsky, V. S., Kruzman, G. P. , Rashton, K. R. , 2004. Groundwater Studies, An International Guide for Hydrogeological Investigations, pp 430.

Kruseman, G.P., 2000. Analysis and Evaluation of Pumping Test Data (2nd edition), International Institute for Land Reclamation and Improvement, the Netherlands, pp 372.

Kulkarni, H., Deolankar, S.B., Anil Lalwani, Bijoy Joseph, Suresh Pawar, 2000. Hydrogeological framework of the Deccan basalt groundwater systems, west-central India, 8: 368-378.

Ma, Z., He, Z., Qi, S., Zhu, G., Zhao, W., Edmunds, W.M., Zhao, Y., 2013. Groundwater recharge and evolution in the Dunhuang Basin, northwestern China.Applied Geochemistry, 28:19-31.

Mege, D., Tesfaye Korme, 2003. Fissure eruption of flood basalts from statistical analysis of dyke fracture length. Journal of Volcanology, 131: 77-92.

Mege, D., Tesfaye Korme, 2004. Dyke swarm emplacement in the Ethiopian Large Igneous, Province. Journal of volcanology and geothermal research, 132: 77-92.

Mengesha Tefera, Tesfaye Cherinet, Workneh Haro, 1996. Explanation of the Geological Map of Ethiopia, 2^{nd} edition, 1:2000000 scale.

Molla Demlie, Stefan, W., Tenalem Ayenew, 2008. Major ion hydrochemistry and environmental isotope signatures as a tool in assessing groundwater occurrence and its dynamics in a fractured volcanic aquifer system located within a heavily urbanized catchment, central Ethiopia. Journal of Hydrology, 353: 175–188.

Nasir, O., Fall, M., Nguyen, T.S., Evgin, E., 2011. Modelling of the hydro-mechanical response of sedimentary rocks of southern Ontario to past glaciations.Engineering Geology, 123: 171-287.

NEERI, 2014. Water Quality Analysis Laboratory Methods, New Delih, India

ODOT, 2005. Hydraulics Manual, Appendix F-Rational Method, Hydrology.

Pierre D. Glynn, L. Niel Plummer, 2005. Geochemistry and the Understanding of Groundwater systems. Hydrogeology Journal, 13: 263-287.

Pik, R., Catherine Deniel, Christian Coulon, Gezahegn Yirgu, Corine Hofmann, Dereje Dereje Ayalew, 1997. The northwestern Ethiopian Plateau Flood Basalts: Classification and Spatial Distribution of Magma Types. Journal of Volcanology and Geothermal Research, 81: 91-111.

Pik, R., Bernard Marty, Jean Carignan, Jerome Lave. 2003. Stability of the Upper Nile drainage network (Ethiopia) deduced from (U-Th)/He Thermochronometry Implications for Uplift and Erosion of the Afar Plume Dome. Earth and Planetary Sciences, 215: 73-88.

Pik, R., Marty, B.,Carignan, J., Yirgu, G., Dereje Ayalew, 2008. Timing of East African Rift development in southern Ethiopia.The Geological Socity of America, 6: 167-170.

Seifu Kebede, Yves Travi, Tamiru Alemayehu, Tenalem Ayenew, 2005. Groundwater recharge, circulation and geochemical evolution in the source region of the Blue Nile River, Ethiopia. Applied Geochemistry, 20: 1658–1676.

Seifu Kebede, Yves Travi, Asfawosen Asrat, Tamiru Alemayehu, Tenalem Ayenew, Zenaw Tesema, 2007. Groundwater Origin and Flow Along Selected Transects in Ethiopia Rift Volcanic Aquifers. Hydrogeology Journal, 10:1007-1040.

Seifu Kebede, Yves Travi, 2012. Origin of the d18O and d2H composition of meteoric waters in Ethiopia. Quaternary International, 257: 4-12.

Sheth, H. C., 2007. Plume-related regional pre-volcanic uplift in the Deccan Traps: Absence of Evidence, Evidence of Absence. Retrieved from WWW.Mantle Plume.org.

Shaw, E. M., 2005. Hydrology in practice.Taylor & Francis e-Library, pp 613.

Sima,. 2009. Water Resources Management and Environmental Protection Studies of the Jema River Basin for Improved Food Security, Unpublished Report, Addis Ababa, Ethiopia.

Singal, B.B.S. and Gupta, R.P., 1999.Applied Hydrogeology of Fractured Rocks.Springer, London, pp 429.

Somaratne and Smettem (2014).Theory of the generalized chloride mass balance method for recharge estimation in groundwater basins characterised by point and diffuse recharge. Hydrology and Earth System Sciences, 11: 307–332.

Stellato. L., Terrasi, F., Marzaioli, F., Belli, M., Sansone,. U., Celico., F., 2013. Is ^{222}Rn a suitable tracer of stream–groundwater interactions? A case study in central Italy.Applied Geochemistry, 32:108-117.

Tamiru Alemayehu, 2001. The Impact of Uncontroled Waste Disposal on Surface water of the Addis Ababa area, Ethiopia. SINET: Ethiopia, J. Sci., 24: 93-104.

Tamiru Alemayehu, Dagnachew Legesse, Tenalem Ayenew, Yirga Tadesse, Solomon Waltenigus, Nuri Mohammed, , 2005. Assessment of pollution Status and groundwater vulnerability mapping of the Addis Ababa water supply aquifers, Ethiopia. Unpublished report.

Tamiru Alemayehu, 2006. Groundwater Occurrence in Ethiopian, Addis Ababa University Press, Addis Ababa.pp 230.

Tenalem Ayenew, Molla Demlie, Wohnillich, S., 2008.Hydrogeological framework and occurrence of groundwater in the Ethiopian aquifers. Journal of African Earth Sciences, 52: 97-113.

Tesfaye Cherinet, YVES TRAVI1 and VINCENT VALLE, 2001.Mechanisms of Degradation of the Quality of Natural Water in the Lakes Region of the Ethiopian Rift Valley.Journal of African Earth Sciences. 1354: 2821-2882

Tesfaye Cherinet, 1997. Hydrogeology of Ethiopia.Addis Ababa, Ethiopia, Ethiopian Institute of Geological Surveys, Addis Ababa, Ethiopia, unpublished Report.

Tesfaye Korme, Acocella, A., Bekele Abebe, 2004. The Role of Pre-existing Structures in the Origin, Propagation and Architecture of Faults in the Main Ethiopian Rift Gondwana Research, 2: 467-479.

Tewodros Rango, Riccardo Petrini, Barbara Stenni, Gianluca Bianchini, Francesca Slejko, Luigi Beccaluva, Tenalem Tenalem Ayenew, 2010. The dynamics of central Main Ethiopian Rift waters: Evidence from dD, d18O and 87Sr/86Sr ratios, Applied Geochemistry, 25:1860–1871.

Tilahun Azagegn, 2008. Hydrochemical Characterization of Aquifer Systems in Upper Awash and Adjacent Blue Nile Plateau using Geochemical Modeling and Isotope Hydrology. Unpublished M.Sc. thesis, Addis Ababa University, Addis Ababa, Ethiopia.

Todd, D.K., 1976. Groundwater Hydrology (2nd edition), John Willey and Sons, New York, pp 535.

Tsegaye Abebe, 1995. The Yerer-Tulu Wellel Extentional Structures Evidences from Remote Sensing, Petrologic and Geochronological Data, Central Ethiopian.

Ethiopian Institute of Geological Surveys, unpublished report, Addis Ababa, Ethiopia.

Tsegaye Abebe, F. Mazarini, F. Innocenti and P. manneti, 1998. The Yerer – Tulu Wellel Volcano-Tectonic Lineameent: a Transitional structure in Central Ethiopia and the Associated Magmatic Activity. Journal of African Earth Sciences, 1: 135-1150.

Visentin, E.J., Micoletti, L. Tolomeo and Zanettin, B., 1974. Miocene and Pliocene Rocks of the Addis Ababa – Debra Berhan Area (Ethiopia) Geo-Petrographic and Radiometric Studies, Geological Surveys of Ethiopia, unpublished report, Addis Ababa, Ethiopia.

Wakgari Furi, 2011. Hydrogeological System Analysis of the Middle Awash Basin, Ethiopia. University of Poitiers, France unpublished Ph.d. Thesis.

Ward E. Sanford, Werner Aeschbach-Herg, 2011.Insights from Environmental Tracers in Groundwater Systems.Hydrogeology Journal. 19: 1-3.

WHO, 2003.Drinking Water Guidelines.New Publications, Web-sites and Multi-media on Water, Sanitation and Hygiene (WASH).

WWDSE, 2008.Adaa-Becho Groundwater Resource Evaluation for Irrigation.Unpublished report, Addis Ababa, Ethiopia.

Zanettin, B., Justin, E., Viesntin, E. Piccirillo, M., 1974.Geological and Petrological Researches on the Volcanics of Central Ethiopia. Geological Surveys of Ethiopia, Addis Ababa, unpublished report.

Zanettin, B., Gragnain, A., Justin, E., Viesntin, B., Nicoletti, M., Piccirillo, E.M., 1974. Migration of Oligocene-Miocene ignimbritic volcanism in the Central Ethipia Plateau. N. Jb. Geol., 9: 567-574.

Zanettin, B., Justin Viesntin, E.,. Piccirillo, E.M., 1978. Volcanic Succession, Tectonics and Magmatology in Central Ethiopia. Geological Surveys of Ethiopia, Addis Ababa, unpublished report.

Appendices

Appendix 1.Borehole data data

Appendix 2.Spring data

Appendix 3.Water quality data

Appendix 4.Stable isotope data

Appendix 5.Geophysical survey data

Appendix 6. Published article